NERC Scientific Facilities and Technology
Ion Microprobe Facility

University Of Edinburgh
NERC Ion Microprobe Facility

2006 Annual Science Report

Ion Microprobe Facility
School of Geosciences
Kings Buildings
West Mains Road
Edinburgh
EH9 3FE

https://www.edweb.ed.ac.uk/geosciences/facilities/ionprobe

Contents

Ion Microprobe Projects

	activity at Volcán de Colima, Mexico: insight from trace element, H_2O and CO_2 contents of melt inclusions.
L. Robinet, C. Hall, K. Eremin & S. Fearn	The role of organic pollutants in the alteration of historic soda silicate glasses
D. N. Schmidt	Biology of boron isotopes in planktic foraminifers: new understanding based on in-situ analysis (SIMS)
J.A. Small & C.J. Hawkesworth	CO_2 contents of phonolitic melt inclusions from the 472 AD 'Pollena' subplinian eruption of Mt Somma-Vesuvius
V.C. Smith, J. Blundy & J.L. Arce	Trace element and volatile compositions of melt inclusions from the 10.5 ka Upper Toluca Pumice, Nevado de Toluca, Mexico: insights into magmatic processes
F.M. Stuart & S. Basu	Li isotope composition of primitive mantle-derived olivine
F. M. Stuart & K. J. Dobson	U and Th zonation in Fish Canyon Tuff zircon: Applicability as a (U-Th)/He standard
R.J.M. Taylor, S.L. Harley, R.W. Hinton & S. Elphick	Distribution of trace elements between zircon, garnet and melt: a key to understanding crustal events and processes II
M. Tichomirowa & EIMF	Mantle $\delta^{18}O$ values in zircons from high pressure granulites
M. Tichomirowa & EIMF	Rare earth element concentrations in zircons from carbonatites
G. Turner, J. Gilmour, A. Busfield & S. Crowther	Extinct $^{24}4Pu$ in Hadean zircons
M. J. Walter	Partitioning of trace elements among Mg-perovskite, Majorite-garnet, and silicate melt
M. J. Walter & G. Bulanova	Trace element abundances in Majorite-garnet and Ca,Ti-perovskite inclusions in natural diamond
H. Wickens & T. Elliott	Investigating diffusive fractionation of Li in olivine phenocrysts

Lithium isotopes in foraminferal hosted calcite

R. Abell & T. Elliott

Department of Earth Sciences, University of Bristol, Bristol BS8 IRJ, UK

Overview

Our work on Li isotopic variations in the foraminiferal calcite of bulk specimens highlights an apparent control of ambient carbonate ion composition on the isotopic composition on δ^7Li. This is potentially a valuable proxy of carbonate equilibrium in palaeo-oceanographic studies. Yet recently a wide range of elemental abundances in foraminiferal tests (e.g. Mg, U and Li) have been shown to have an apparent dependence on the carbonate concentration of seawater from which they grew. However, elemental distributions within foraminiferal tests have been shown to be complex and it is not necessarily simple to reconstruct palaeo information from their measurement. We wished to similarly investigate the *in situ* variability of Li isotopes to assess its robustness as a palaeo-carbonate ion proxy and determine if the additional complexity in its measurement was worthwhile compared to analytically simpler elemental proxies, not least Li/Ca.

Rationale

In order to obtain sufficient precision to potentially resolve the small differences implied by modest variability in bulk analyses, we used 12nA primary beams which restricted our work to thicker shelled foraminifera. Here we used *G.tumida*,and *G.truncatulinoides*. The latter species in particular shows migration to greater water column depths in its life cycle and as a consequence will likely enhance any variability seen in a single test, due to decreasing temperature as it drops through the thermocline. Unfortunately we do not currently have bulk Li isotope data on these species as we had originally concentrated on surface dwelling forams.

Results

We made isotopic transects along different chambers of two large individuals (Fig. 1). Unfortunately analytical precision is large compared to expected variability. Thus we have averaged different analyses of the same chamber and report this with its (2 sigma) standard error. There is a decrease in ^{7}Li/^{6}Li with chamber number in *G.truncatulinoides* whilst any possible variation in *G.tumida* is too small to discern.

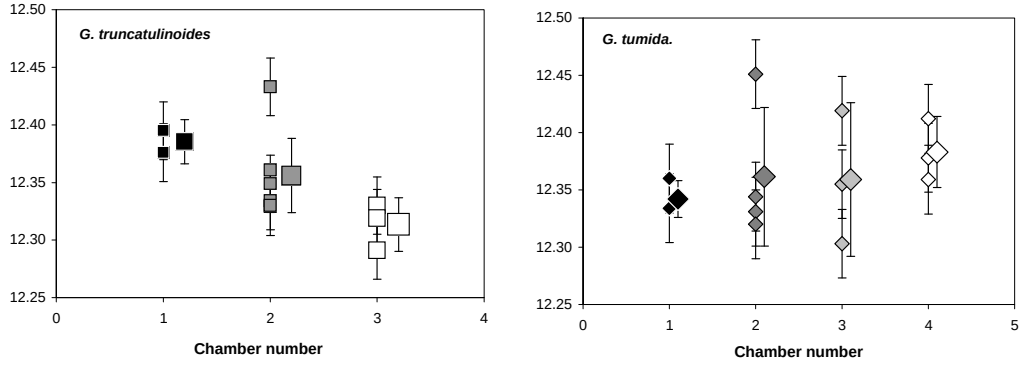

Figure 1. Inter-chamber Li isotope variability in large specimens of *G.truncatulinoides* and *G.tumida*. Individual analyses with 1 sigma measurement errors are shown as small symbols and chambers means with 2 sigma standard errors are shown as larger symbols.

The variability of different chambers within *G.truncatulinoides* is not unexpected given its life cycle and its accompanying trace element variability. In particular we contrast Li and Mg abundances. Both elements show increasing abundance with chamber number (Fig. 2). This is ostensibly makes sense for Mg, given lower values represent colder temperatures, since the later grown chambers (lower numbers) form as the foram dwells at greater depths. The magnitude of the change in Mg abundances is large and corresponds to change of some 5°C or more. Such a temperature change should have an opposite effect on the Li abundances, but

this does not appear to be the case. However, we have already noted that carbonate ion concentration is proposed to influence Li abundances in formanifera. The younger chambers (lower numbers) formed at greater depth will have grown in a more acidic environment and this should decrease the Li abundance. This is at least qualitatively consistent with the observations. Moreoever, the large increases of Li/Ca in glacial species suggest that the carbonate ion influence can out-weigh temperature.

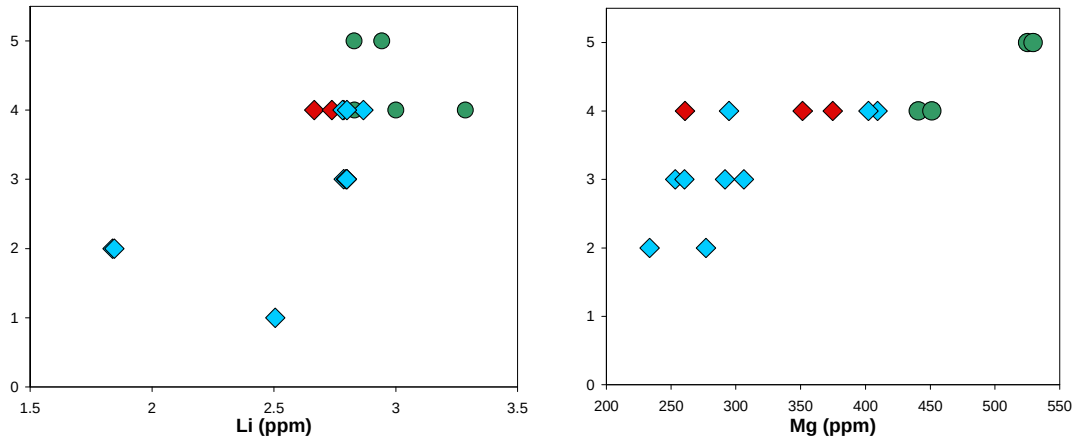

Figure 2. Li and Mg abundances in different chambers of three *G.truncatulinoides* tests (different tests in different colours).

Given the consistent picture yielded by the elemental data, the isotopic measurements are puzzling. Our bulk analyses suggest that $^{7}Li/^{6}Li$ of forams become heavier with increasing carbonate ion concentration. Thus we would have anticipated a decrease in $^{7}Li/^{6}Li$ with decreasing chamber number, especially given the changes in Li abundances. Admittedly the changes in $^{7}Li/^{6}Li$ are subtle but apparently significant. There remains the possibility that test structure might exert an influence on the measured isotopic ratio. Notably the old chambers have a larger number of calcite overgrowths. It is thus critical to undertake a detailed SEM examination of our large *G.truncatulinoides*. Indeed the role of test structure in influencing the chemistry is evident in cross-sectional elemental transects taken across the final chamber of our *G.truncatulinoides* (Fig. 3). The minimum corresponds to the primary organic membrane and it can be seen that both elements, although Mg in particular, increase away from this surface. It would be extremely interesting to similarly profile Li isotope ratios, but the necessary spot size is unfortunately too large.

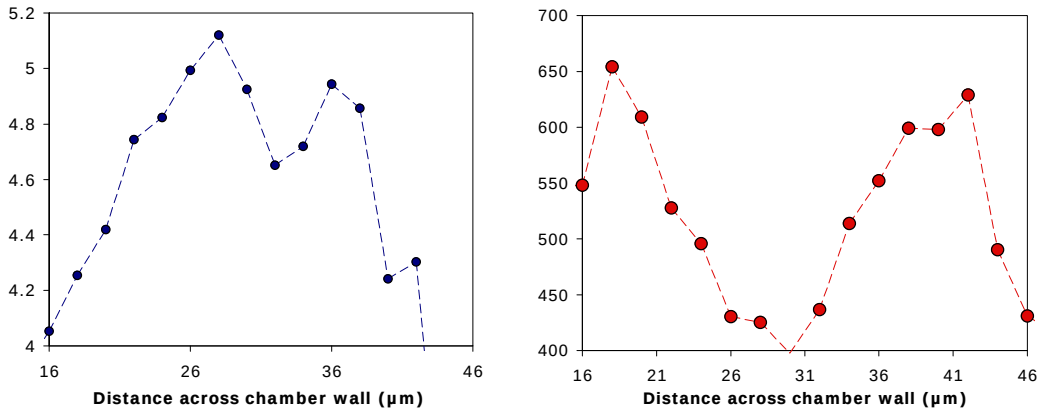

Figure 3. Elemental profiles across final *G.truncatulinoides* chamber.

Predicting sea surface temperatures from fossil coral skeletons

N. Allison & A. A. Finch

School of Geography and Geosciences, University of St. Andrews, St. Andrews KY16 9AL, UK

Introduction

The geochemistry of coral skeletons may reflect the environmental conditions at the time of skeletal deposition and the analysis of fossil skeletons offers a method to reconstruct past climates. In particular skeletal Sr/Ca has been used as an indicator of past sea surface temperatures (SSTs). However fossil corals are susceptible to diagenetic alteration which may modify skeletal geochemistry and subsequent climate estimates (e.g.1). The high spatial resolution of SIMS allows the selective analysis of the original skeleton independent of any cements and offers a potential route to the reconstruction of past SSTs from significantly altered fossil specimens.

Results and discussion

We are using SIMS measurements of trace element geochemistry from unaltered sections of fossil *Porites spp*. corals collected from submerged reefs around Hawaii to estimate seawater temperatures at the times when the corals were deposited. To validate this analytical approach we present data from a 15.8 ka coral sampled from a 150 m depth reef at Mahukona, Hawaii (Figure 1). Sr/Ca exhibits a clear seasonal signal. The mean Sr/Ca of the fossil coral indicates a SST of ~-2˚C compared to the present day (assuming a Sr/Ca temperature dependence of 0.080 mmol mol^{-1} ˚C^{-1} for Hawaiian corals [2,3]). These predictions are in good agreement with other estimates of SST changes in this region, at that time [4].

Figure 1. A: Sr/Ca (determined by SIMS) across a 2 year transect of a fossil *Porites* coral. B: Mean annual Sr/Ca of the fossil compared to a modern coral of similar growth rate collected from Lanikai, Oahu (also analysed by SIMS), with estimates of SST. Typical 95% ci ± 0.04 mmol mol^{-1} for microprobe Sr/Ca (equivalent to ~0.5˚C).

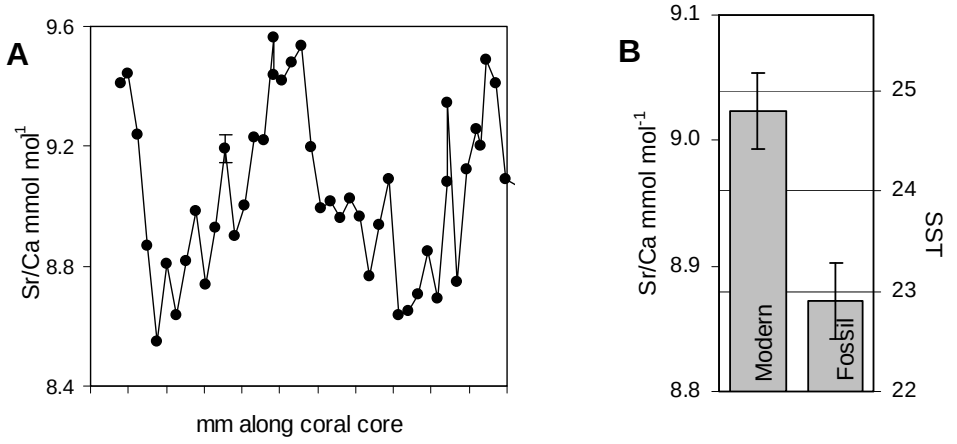

Conclusions

SIMS estimates of Sr/Ca of pristine coral aragonite in diagenetically altered fossil specimens are in good agreement with climate estimates from other proxies. The 95% confidence limits of multiple (>100) Sr/Ca SIMS analyses across an annual growth band are typically <±0.04 mmol mol^{-1}, equivalent to a temperature precision of ~±0.5ºC [2].

References

[1] N. Allison, A.A. Finch, A.W. Tudhope, M. Newville, S.R. Sutton & R. Ellam, Geophysical Research Letters 32 (2005) doi: 10.1029/2005GL02.
[2] S. De Villiers, G.T. Shen & B.K. Nelson, Geochim. Cosmochim. Ac. 58 (1994) 197-208.
[3] N. Allison& A.A. Finch, Geochem. Geophys. Geosyst. 5 (2004) doi 10.1029/2004GC000696.
[4] K.E. Lee, N.C. Slowey & T.D. Herbert, Paleoceanography 16 (2001), 268-279, 2001.

An integrated SIMS trace element / REE, U-Pb and oxygen isotope study to unravel the petrogenetic evolution of granites

S.K. Appleby[1], C.M. Graham[1], M.R. Gillespie[2], R.W. Hinton[1] & G.J.H Oliver[3]

[1]School of GeoSciences, University of Edinburgh, Edinburgh EH9 3JW, UK
[2]British Geological Survey, Murchison House, West Mains Road, Edinburgh, EH9 3LA, UK
[3]School of Geography & Geosciences, University of St. Andrews, St. Andrews, KY16 9AL, UK

Introduction

Previous studies have shown that zircon, which is a common accessory mineral in igneous rocks, preserves its elemental and isotopic composition from the time of crystallisation and may remain essentially unaffected by subsequent thermal events or hydrot hermal alteration. Zoning patterns observed in CL and BSE images of zircon grains are interpreted to reflect changes in trace element and REE abundances. By carrying out a combination of *in-situ* SIMS trace element / REE and oxygen isotope analyses and U-Th-Pb age dating of these individual zones (e.g. core to rim, usually all on the same ~20µm spot) it is possible to retrieve information about the magma that the zircon grains crystallised from. Thus, the sources and petrogenetic evolution of plutonic rocks, not accessible by conventional whole-rock data, are now resolvable.

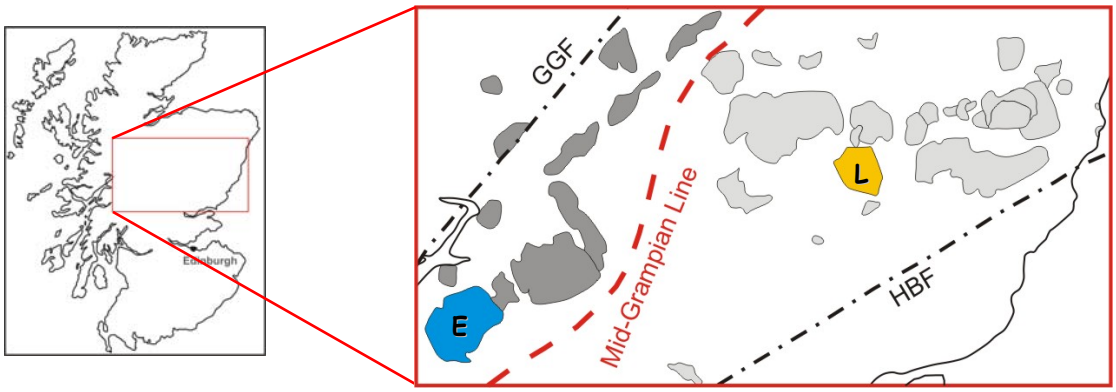

Figure 1. Map showing the location of the Lochnagar and Etive plutons and the Mid-Grampian Line

Two 'I-type' plutons, Lochnagar and Etive, which belong to the classic suite of late-Caledonian granite intrusions, were selected for detailed study. Both are located in the Scottish Grampian Highlands (Fig. 1) and represent the Cairngorm and Argyll granite suites respectively. Previous whole-rock geochemical and isotopic studies indicated that both plutons were emplaced into Dalradian metasediments approximately at the same time (430-400 Ma), but have contrasting geochemical compositions suggesting that the granitic magmas had different deep crustal or mantle sources. Therefore the existence of the Mid-Grampian Line, a boundary between basement blocks of differing age and composition was postulated. Despite numerous whole-rock studies late Caledonian magmatism and the nature of the deep Scottish basement are still controversial. Thus, a detailed *in-situ* SIMS study on zircon has been carried out with the following objectives:

1. To determine the U-Pb crystallisation ages, oxygen and trace element compositions of zircons from the Lochnagar and Etive intrusions.
2. To use *in-situ* microbeam analysis of zircon as a direct comparison to previous whole-rock isotopic studies of late Caledonian granites.
3. To constrain potential magma sources and obtain information about the deep Scottish basement that underlies the Grampian.

This report provides an overview of the results of ion microprobe studies to date, including those undertaken in 2006-07.

Results

U-Th-Pb geochronology

Age dating of the Lochnagar pluton, which consists of three main granite facies (L1, L2, L3) and associated diorite intrusions (d1, d2), showed that all parts of the pluton were emplaced approximately contemporaneously at 420±4 Ma. Based on field relationships L1 is the oldest intrusion followed by L2, L3 and the diorites. However, these minor age differences were not resolvable with this technique. Inherited zircon cores display $^{207}Pb/^{206}Pb$ ages of 1050 Ma to 1400±13 Ma within L2 and are thought to represent assimilated Dalradian metasediments.

The Etive pluton comprises four main facies (Meall Odhar, Cruachan, Quarry Intrusion, Starav) and was emplaced over a period of 20-25 Ma (Meall Odhar: 424±4 Ma; Cruachan: 420-412±7 Ma; Quarry Intrusion: 406-399±6 Ma; Starav: 407±6 Ma). Field relationships previously suggested that the Quarry Intrusion, being located along the outer edge of the pluton, is the oldest part of Etive. However, this study shows that it represents the youngest facies. Inherited zircons were found within some samples of the Cruachan facies displaying $^{207}Pb/^{206}Pb$ ages of 1000 Ma to 1650±16 Ma similar to those found in the Lochnagar pluton. Again these inherited components may reflect assimilated Dalradian material.

REE / trace elements

Zircon grains from the Lochnagar and Etive plutons show very similar steeply positive chondrite-normalised REE patterns typical for granitic zircons with a clear enrichment of the heavy over light REE (Fig. 2). All samples display a positive Ce anomaly and a negative Eu anomaly. In comparison to Etive, Lochnagar is enriched in the REEs and displays a stronger negative Eu anomaly (Lochnagar: Eu/Eu* = 0.33-0.77; Etive: Eu/Eu* = 0.15-0.59), which suggests geochemical differences in the magma sources.

Within each pluton minor variations in Ce anomalies and light REE abundances were observed between the granite facies. Differences between the granitic and dioritic facies in each pluton were mainly reflected in their varying Eu anomalies, i.e. Eu/Eu* of the diorites is much weaker, which may reflect the less feldspar-rich nature of the magma they crystallised from. Comparison of core and rim compositions showed that a decrease in Th/U ratios from the core to the rim can be identified, but this trend is not obvious from other REE and trace elements.

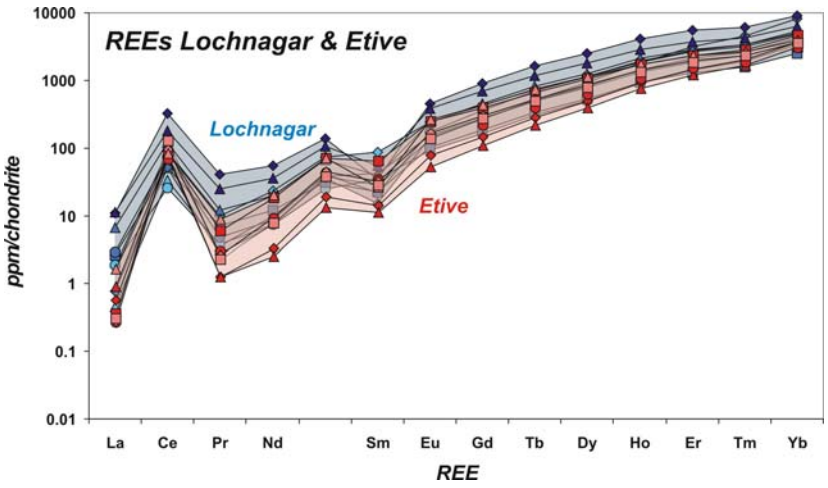

Figure 2. Chondrite normalised REE patterns for Lochnagar and Etive.

Oxygen isotopes

$\delta^{18}O$ values of zircons from Lochnagar and Etive display an almost identical range of compositions between 4.6‰ and 8.4‰ with an average of c. 6.6‰ (precision based on reproducibility of standard 91500 = 0.3‰ (1SD)). However, a statistical analysis of the spread of $\delta^{18}O$ values within each sample has revealed that some samples are normally distributed and therefore represent only one single zircon population (e.g. Lochnagar d1) (Fig. 3a) whereas others comprise two or more distinct zircon

populations (e.g. Lochnagar d2) (Fig. 3b). Variations were also recognised within individual grains (Fig. 4) with the core usually displaying lower $\delta^{18}O$ values than the rim. As oxygen isotope variations of these magnitudes in zircon are insensitive to fractional crystallisation this pattern can only be explained by mixing with - and / or assimilation of - material with an elevated $\delta^{18}O$ composition during magma evolution. A preliminary conclusion is that the observed oxygen isotope variations represent melting / mixing / assimilation events involving two or more sources, which were not identified using conventional techniques. As the samples mentioned above were often analysed in the same sessions, it can be ruled out that this variation is caused by instrumental artifacts. The $\delta^{18}O$ values preclude both unmodified mantle source contributions (5.3± 0.3‰) and major assimilation of ^{18}O-enriched metasedimentary crustal material.

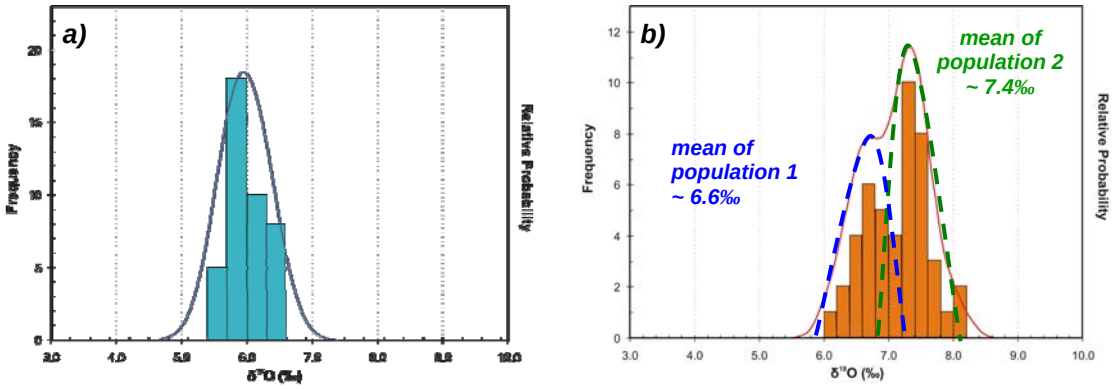

Figures 3a & b. $\delta^{18}O$ probability plots of Lochnagar diorites d1 and d2.
a) d1 displays a normal distribution, thus consists of only one zircon population.
b) d2 shows a bimodal distribution; statistical analysis indicates at least two zircon populations.

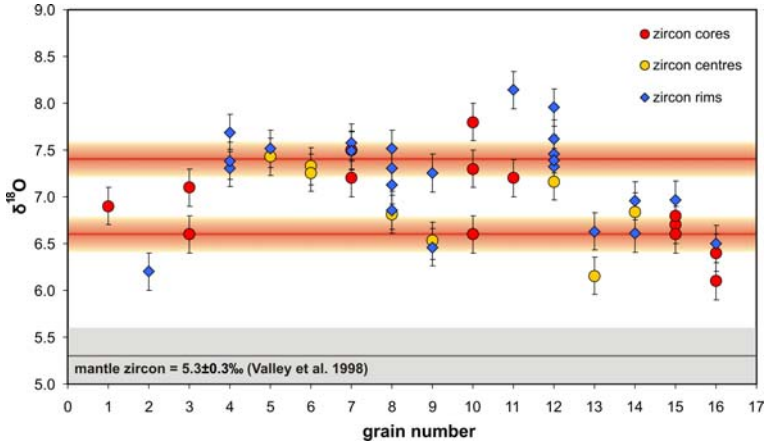

Figure 4. $\delta^{18}O$ variation observed within the Lochnagar d1 sample. Note the variation at intra- (e.g. grains 8 & 12) and inter-grain level (e.g. 12 & 13). Variation interpreted as mixing or assimilation of two or more sources. Orange bars represent the means of populations 1 & 2, error bars are 1SD.

Summary

This study has proven that combining *in-situ* SIMS U-Pb dating and REE and oxygen isotope analyses of zircon is a successful approach to examine the petrogenetic evolution of granites in much greater detail. Not only is it possible to identify inherited or hydrothermally altered material, which will modify the results obtained by conventional methods (TIMS and laser fluorination), but more importantly to characterise magma sources and to detect mixing / assimilation events. High-precision oxygen isotope data seems particularly powerful in uncovering these events. Subsequently combining the SIMS data with *in-situ* Lu-Hf LA-ICP-MS should deliver information about the nature of these different magma sources and therefore the basement beneath the Grampian Highlands.

Investigating the role of recycled crust in generating radiogenic Pb isotope signatures in the mantle

R. Avanzinelli & T. Elliott

Department of Earth Sciences, University of Bristol, Bristol BS8 IRJ, UK

Overview

The objective of this study was to exploit the observation of large variability of Pb isotopic ratios in melt inclusions [1] and couple this with trace element analyses. In this manner we hoped to characterise the endmembers that go to make bulk lava samples and understand their origins. Specifically we wished to test if radiogenic Pb isotope ratios in some oceanic basalts were plausibly explained by recycled oceanic crust by linking Pb isotopic signatures with key incompatible trace element ratios (e.g. Ba/Nb).

Background

The samples for our study came from La Palma, Canaries. We have a large collection of La Palma samples, characterised petrographically, chemically and isotopically. Moreover, in collaboration with Dr. I. Nikogosian (University of Utrecht), the melt inclusions (dominantly hosted in mafic, Fo>80, olivines) of a number of these samples have been investigated in some detail. La Palma provides an interesting location, as its whole rocks have radiogenic Pb isotopic compositions that show a greater relative variation ($^{206}Pb/^{204}Pb$ 19.2-20.0) than the somewhat more extreme island of Mangaia ($^{206}Pb/^{204}Pb$ 21.5-21.9). The latter has been the previous focus of *in situ* Pb isotope work. We thus anticipated at least comparable isotopic variability to the considerable range evident in Mangaia melt inclusions.

The analyses were undertaken in two one week sessions. Initially Pb isotope ratios were measured on as many potentially suitable inclusions using the Cameca 1270. Pb contents were not sufficiently high to allow ^{204}Pb measurements, in keeping with previous studies and so isotopic ratios are reported in a less familiar form, normalised to ^{206}Pb. Subsequently the same inclusions were reanalysed for a suite of incompatible trace elements (Ti, Rb, Sr, Y, Zr, Nb, Ba, La, Ce, Nd, Pb, Th, U) using the Cameca 4f. In all 32 silicate melt inclusions were analysed together with 5 sulphide inclusions.

Results

The most striking feature of our results are the modest variations observed. The *in situ* analyses slightly extend the observed range of Pb isotopic compositions, but this is barely significant given the greater errors of the SIMS measurements (Fig. 1a).

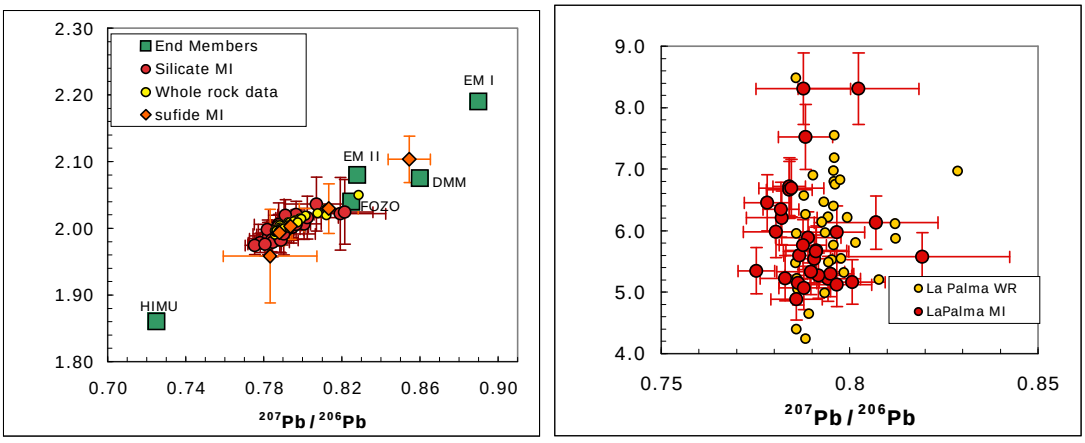

Figure 1. $^{207}Pb/^{206}Pb$ vs a) $^{208}Pb/^{206}Pb$ for silicate and sulphide inclusions, contrasted with whole rock compsotions (yellow circles) and mantle endmember compositions (green squares) b) Ba/Nb with silicate melt inclusions compared to whole rock analyses (yellow circles).

The single exception is the analysis of a sulphide inclusion hosted within a clinopyroxene inclusion. Likewise the trace element analyses show little variability beyond that encountered in the whole rocks (Fig. 1b). We had hoped to examine covariations of Ba/Nb with Pb isotopic ratios, but any possible correlation within such minor variation is difficult to discern.

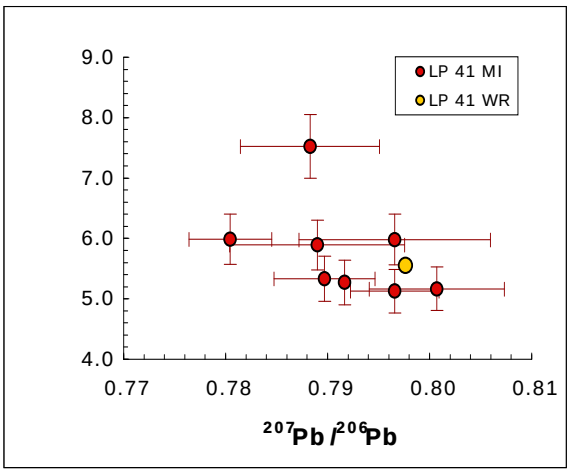

We additionally illustrate the range in compositions exhibited by a single sample in Fig. 2. For one sample (LP41) we obtained analyses of 8 different melt inclusions. There is (reassuring) overlap between whole rock and melt inclusion compositions but the bulk composition is towards the less radiogenic (high $^{207}Pb/^{206}Pb$ end of the inclusion array). There is a vague trend to more radiogenic compositions and higher Ba/Nb.

Figure 2. Data for melt inclusion (red circles) and whole rock (yellow circle) analyses of sample LP41.

Discussion

The uniformity of the La Palma melt inclusions is in striking contrast to the variability of Mangaia [1]. Interestingly, other localities recently analysed have also failed to demonstrate such marked ranges in Pb isotopic composition [2]. Thus Mangaia appears to be a special case and the presence of carbonatite inclusions in these samples maybe significant. Plausibly samples have interacted with a carbonatite metasomatised lithosphere. That the La Palma samples show little Pb isotopic variability may then suggest that these lavas have interacted little with the lithopshere through which they pass. This is perhaps surprising, given the thickness of the lithosphere beneath La Palma and petrological evidence for extensive mantle differentiation of the lavas. Yet, given the low incompatible element abundances expected of oceanic lithopshere, it likely requires an additional re-enirchment event to be able to influence the incompatible element composition of magmas that transit the lithopshere. Within LP41 there is a poorly defined trend of lower Ba/Nb in higher $^{207}Pb/^{206}Pb$ inclusions (i.e. less radiogenic), which is consistent with minor lithospheric contamination. This is not compatible with a model of source variability in which the most radiogenic compositions contain a larger proportion of recycled crust and thus would be anticipated to have lower Ba/Nb. Likewise, the anomalous Pb isotopic composition of the clinopyroxene hosted sulphide is also possibly suggestive of lithospheric interaction.

Concluding Remark

Although the modest variability in compositional variability is a disappointment in terms of the original aims of the study, it is an important finding. Any source variability has been efficiently mixed before melts start crystallising mafic olivines and this is in contrast to work on mid-ocean ridge and arc environments.

References

[1] A. Saal et al., Earth Planet. Sci. Lett. 240 (2005) 605-620.
[2] A. Saal et al., Science 282 (1998) 1481-1484.

The role of rutile during melting of ancient subducted oceanic crust

G.D. Bromiley and S.A.T. Redfern

Department of Earth Sciences, University of Cambridge, Cambridge CB23EQ, UK

Introduction

Beyond the depths of sub-arc magmatism, the fate of subducting oceanic crust remains poorly constrained. A paradigm of mantle geochemistry is that HIMU, one of the end-member compositions of ocean island basalts (OIB), represents melt derived from ancient (subducted) oceanic crust[1]. This could represent large-scale melting of crust accumulated in the lower mantle, melting of entrained nodules in upwelling mantle plumes, or shallower melting of oceanic crust recycled into the upper mantle. The presence of substantial quantities of ancient crust in the mantle could also be important in balancing the trace element chemistry of the bulk silicate earth (BSE). It has been suggested that rutile could act as a sink for Nb in ancient crust, balancing the BSE's apparently subchondritic Nb/Ta ratio[2]. If rutile is present in ancient crust during melting, it should leave a characteristic signature on HIMU chemistry. For example, at lower pressures, the presence of rutile in melt residues results in characteristic Nb and Ta (and to a lesser extent Zr and Hf) depleted melts.

In this study, we have determined partition coefficients ($D_{min/melt}$) for Nb, Ta, Zr and Hf between rutile and its high-pressure polymorph TiO_2(II), and basaltic melt from samples synthesised at 2 to 10 GPa. The aims of this study are to determine how pressure and the rutile/TiO_2(II) transition affect trace element partitioning, whether HIMU compositions are consistent with the presence of TiO_2 phases in melt residues, and whether rutile/TiO_2(II) in ancient subducted crust could act as a hidden reservoir for Nb in the mantle.

Results

Effects of pressure and the rutile/TiO_2(II) transition on trace element partitioning are shown in Figure 1. Trends in D^{Nb} and D^{Ta} with increasing pressure can be correlated with an increase in the amount of $Si^{[6]}$ present in high-pressure melts, implying that both Nb and Ta behave as network modifiers rather than forming isolated complexes with non-bridging oxygens. Similarly, melt structure affects Zr and Hf partitioning, although lattice strain has a greater influence due to the large difference in ionic radii between Zr/Hf^{4+} and Ti^{4+}.

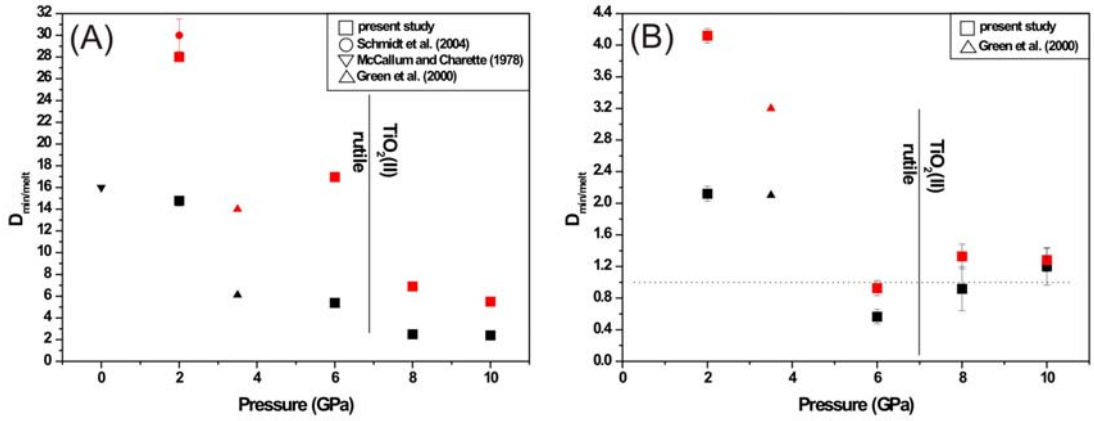

Figure 1. Rutile/TiO_2(II)-basaltic melt partition coefficients for (A) Nb (black) and Ta (red) and (B) Zr (black) and Hf (red) as a function of pressure. Additional data are from studies by Schmidt et al (2004)[3], McCallum and Charette (1978)[4] and Green et al. (2000)[5]. ^{Nb}D and ^{Ta}D from Green et al. (2000) are lower because experiments were water-saturated.

Zr/Hf, Nb/Ta and Zr/Nb partition ratios are shown in Figure 2. Extrapolation of trends to higher pressure demonstrates that D^{Ta} is always greater than D^{Nb}. Therefore, slab-derived melts will always have higher Nb/Ta than their source. OIB generally have subchondritic Nb/Ta, which implies that rutile/TiO_2(II) present in ancient subducted slabs cannot act as a 'hidden' superchondritic Nb/Ta reservoir.

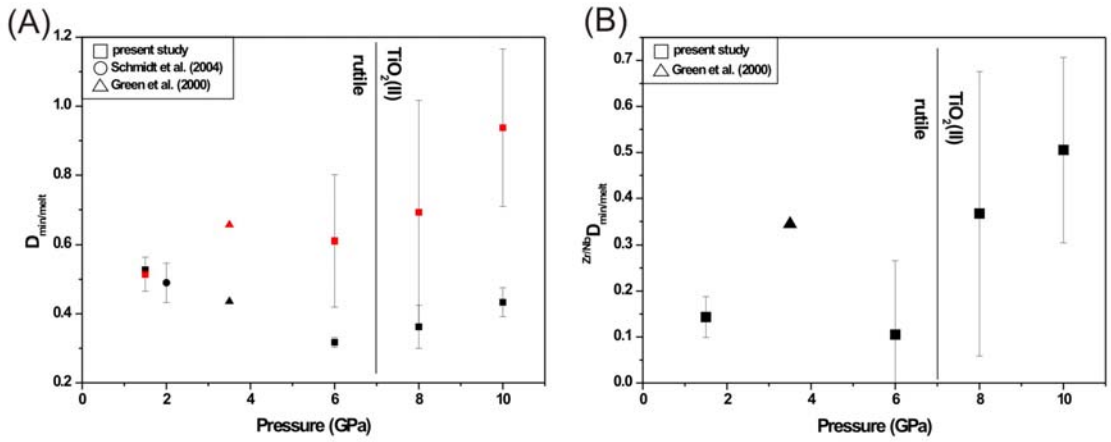

Figure 2. Partition coefficients for (A) Nb/Ta (black) and Zr/Hf (red) and (B) Zr/Nb.

At pressures above 10 GPa (>300 km), Zr is no longer partitioned relative to Hf. A similar trend is noted in garnet-melt partition data[5], implying that high-pressure slab-derived melts should have the same Zr/Hf as their source (subduction modified crust). Although we find that TiO_2 phases are not important in terms of balancing the BSE Nb budget, partition data are consistent with the presence of TiO_2(II) in melt residues during partial melting of ancient crust. At high pressures, partitioning of Nb and Ta by TiO_2(II) is markedly reduced, a trend that should extend up to at least 30 GPa due to a steady increase in the proportion of $Si^{[6]}$ in silicate melts. HIMU compositions typically contain much higher Nb and Ta than melts hypothesised to have resulted from direct melting of subducting crust at shallower depths[1, 6]. This can be explained by shallow vs deep partial melting of oceanic crust. In fact, partitioning of Nb and Ta by TiO_2(II) at high pressure would provide a means for balancing Nb and Ta contents in calculations of the trace element chemistry of model HIMU-type melts formed by partial melting of altered, garnet-rich subducted crust[7]. The presence of TiO_2(II) during very high-pressure melting of ancient crust can also explain the remarkably strong correlation of Zr and Nb concentrations in global surveys of OIB geochemistry[8], without invoking complex binary mixing. Zr is no longer partitioned by rutile/TiO_2(II) above 6 GPa, and D^{Nb} and D^{Ta} continue to fall, implying that with increasing pressure, Zr/Nb will approach unity. As such, Nb and Ta contents, and Nb/Zr ratios of slab-derived melts could provide an important indicator of depth of partial melting. Data from OIB arrays are consistent with deep (>300 km) rather than shallow melting of subduction-modified oceanic crust.

References

[1] A. Hofmann, Nature 385 (1997) 219-229.
[2] R. Rudnick, M. Barth, I. Horn, & W. McDonough, Science 287, (2000) 278-281.
[3] M. Schmidt, A. Dardon, G. Chazot, R. Vannucci, EPSL 226 (2004) 415-432.
[4] I. McCallum, & M. Charette, Geochim. et Cosmochim. Acta 42 (1978) 859-869.
[5] T. Green, J. Blundy, J. Adam, G Yaxley, Lithos 53 (2000) 165-187.
[6] M. Drummond, M. Defant, P. Kepezhinskas, Trans. Roy. Soc. Edin 87 (1996) 25-215.
[7] A. Stracke, M. Bizimis, and J.M. Salters, Geochem. Geophys. Geosys 4(3) (2003) 1-33.
[8] B. Kamber, & K. Collerson, J. Pet. 41 (2000) 1007-1021.

Hydrogen contents of Biotite in HT anatectic metapelites

B. Cesare[1,2], G. Cruciani[3] & M. Satish-Kumar[4]

[1]Dipartimento di Geoscienze, Università di Padova, Via Giotto 1, Padova, 35137, Italy
[2]C.N.R., I.G.G., Sezione di Padova, Corso Garibaldi 37, Padova, 35137, Italy
[3]Dipartimento di Scienze della Terra, Universita' di Ferrara, Via Saragat 1, Ferrara, 44100, Italy
[4]Institute of Geosciences, University of Shizuoka, Shizuoka, 422-8529, Japan

Scientific Report

In a previous study of partially melted metapelites [1], also based on SIMS data from this Ion Microprobe Facility, it has been shown that deprotonation, by way of the Ti-oxy exchange ($Ti^{4+} + 2O^{2-} = Mg^{2+} + 2OH^-$) is the main exchange vector for the entrance of Ti in biotite equilibrated at 850±50°C, and outlined the implications of Ti-oxy on HT petrologic processes. The results of Cesare et al. (2003) were obtained on F- and Cl-free biotites from xenoliths in lavas, therefore they are not entirely satisfactory to represent the behaviour of biotite in far more common HT metapelites such as those regionally metamorphosed, and in melted granulites and migmatites. In these rocks biotite often shows high contents of F and Cl. To extend our investigation to halogen-rich biotites, we have conducted the present study on micas from the metapelitic granulites of the Kerala Khondalite Belt (KKB) of S India, one of the best exposed and studied examples of HT metasedimentary lower crust. After selection and detailed petrography of two lithologies (pegmatite and host granulite) from the same quarry, we have performed the same multidisciplinary approach adopted by [1] for the full chemical characterisation of biotite, including EMP, SIMS, C-H-N analysis, Mössbauer spectroscopy and single-crystal XRD.

The analyses obained were normalized on the basis of $[O_{12-(x+y+z)}(OH)_xCl_yF_z]$. Biotite in the pegmatite is Ti-, F- and Cl-rich (0.33, 0.46 and 0.16 a.p.f.u., respectively), H_2O-poor (OH = 0.86 p.f.u.), has X_{Mg}=0.49 and $Fe^{3+}/Fe_{tot} \leq 3\%$. The low octahedral vacancies (0.06 p.f.u.) and the large oxygen content in the hydroxyl site (OH+F+Cl = 1.49 p.f.u., Figure 1) confirm the role of the Ti-oxy substitution as a major exchange vector in these high-T biotites.

In the host granulite, fine-grained biotite is Fe^{3+}-free, has low Cl (0.03 a.p.f.u) and more variable in composition, with Ti, F, and X_{Mg} in the ranges 0.26-0.36, 0.52-0.67, and 0.67-0.77, respectively. The amount of octahedral vacancies is relatively large (0.10-0.18 p.f.u.) and the sum of volatiles is variable (OH+F+Cl = 1.71-2.06 p.f.u., Figure 1). Systematic variations of X_{Mg} are a function of the microstructural position: biotite included in or in contact with garnet has the maximum values, whereas crystals in the matrix have the minima. Such variations are induced by retrograde Fe-Mg exchange with garnet. Titanium displays systematic negative correlations with F, X_{Mg} and (OH+F+Cl). On the contrary, Al and octahedral vacancies are virtually constant.

These trends indicate that: a) the Ti-vacancy, along with substitutions involving Al, cannot explain the observed short scale variations; b) conversely, the Ti-oxy exchange appears to be active, resulting from combination of two vectors: the more conventional hydroxylation $Ti^{4+} + 2O^{2-} = (Fe,Mg)^{2+} + 2OH^-$ and the "fluorination" $Ti^{4+} + 2O^{2-} = (Fe,Mg)^{2+} + 2F^-$. The latter appears to play a relevant role, probably in relation to the Fe-F avoidance.

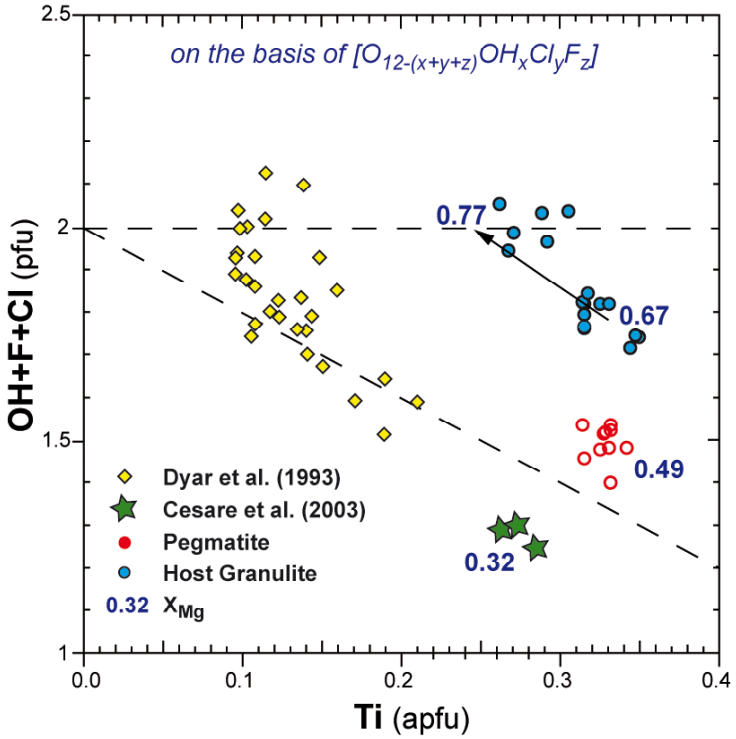

Figure 1. Ti vs (OH+F+Cl) diagram with data from this study, from partially melted metapelitic xenoliths [1] and from greenschist- to amphibolite-facies graphitic metapelites [2]. All datapoints refer to crystals in which H was analysed. Also reported are the X_{Mg} values of biotite in the HT, granulitic rocks. The arrow represents the re-equilibration trend observed in the biotites from the host granulite in this study.

References

[1] Cesare, B., Cruciani, G. and Russo U. (2003) American Mineralogist, 88, 583-595.
[2] Dyar, M.D., Colucci, M.T. and Guidotti, C.V. (1991) Geology, 19, 1029-1032.

Pb Isotopes in Detrital K-Feldspar Grains Support Oligocene-Miocene Drainage Capture from the Red River

P.D. Clift

School of Geosciences, University of Aberdeen, Aberdeen, AB24 3UE, UK

Constraining the history of surface uplift in eastern Tibet and surrounding regions of southwest China is important to understanding the overall history of surface uplift and strain accommodation following India-Asia collision. The evolution of drainage patterns can be used to understand how topography has evolved because rivers are sensitive to changes in the regional gradient. It has been suggested that the unusual, non-dendritic drainage patterns recognized in some river systems in eastern Tibet, southwest China and parts of Indochina represent remnants of an ancestral Red River system that dominated the area prior to Tibetan uplift [1] (Fig. 1). In this project I analyzed a series of detrital K-feldspar grains taken from sandstones and modern river sediments in the Red River delta to investigate how the composition of the river has evolved since the Eocene. The method is based on the contrasting evolution and thus isotopic geochemistry of the different terrains that comprise eastern Asia. Rivers eroding these various blocks transfer the contrasting Pb isotope characteristics from the bedrock to their sediments, so that the populations of grains found in the delta should change as the headwaters of the Red River were progressively lost to adjacent river systems. Earlier TIMS analysis has established the Pb isotope character of the modern river for ready comparison [2]. Borehole samples from the region of the delta have been analyzed by bulk sediment Nd isotopes and suggest major drainage capture, including loss of the flux from the Yangtze Block prior to 24 Ma [3]. An earlier pilot study of Pb isotopes suggested that the Yangtze Block was supplying sediment to the South China Sea in the Eocene, but the precise timing of the drainage loss was unknown [4].

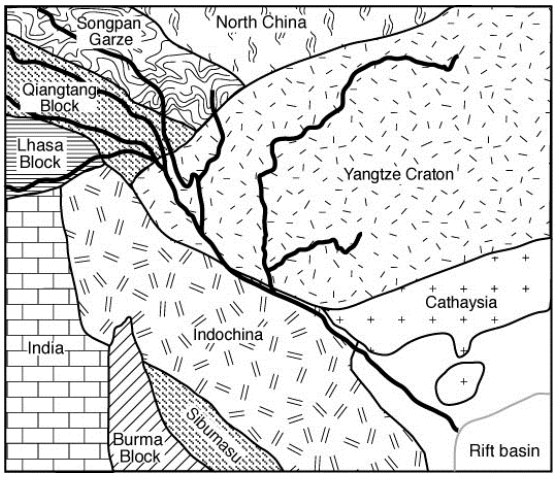

Figure 1. Map showing proposed original drainage pattern for the palaeo-Red River, with the middle Yangtze draining to the southwest into the South China Sea.

In September 2006 I analyzed 226 grains of K-feldspar from a series of sands and sandstones in the Red River system for Pb isotopes. A minority of the grains contained less Pb than anticipated and yielded poor analyses, yet the vast majority were of good quality and allow the provenance evolution of the Red River to be assessed. Fig. 2 shows the range of values seen in the Eocene Gulf of Tonkin. The range of grains overlaps the known composition of the modern river indicating that the two share some sources that are isotopically identical. These are likely some of the rocks now exposed in the modern drainage. The new data confirm that the Red River was receiving sediment from the Yangtze Block in the Eocene, implying a reverse flow in the middle Yangtze compared to that seen today. In turn this suggests a reversed regional gradient of downslope to the SW. These data require that topographic growth postdated the Eocene. Many of the grains seen in the Eocene plot at lower 207/204 values than both the modern river and the few terrains from SE Tibet and Yunnan whose Pb isotope composition is known [5]. In an attempt to identify the source of these low 207/204 grains I analyzed a sand from the “first bend” of the Yangtze River (Fig. 3), the location where the Yangtze now changes from flowing to the SE to the NE, and presumed to be

a place of capture [1]. This sample characterizes the sediment sources in eastern central Tibet which are otherwise unknown. Fig. 3 shows that grains from that region plot below the modern Red River. This result raises the possibility that the Eocene Red River was being supplied by sediment eroded from rocks now located in the headwaters of the Yangtze and again implying major drainage loss since that time. Additional analyses of sediment from the Red River tributary, the Song Da, raises an alternative hypothesis. This river also shows grains of this isotope character, but this river drains into the Red River from the SW, i.e. eroding Indochina. The river does not appear to be important today but may have contributed a greater proportion of the Red River clastic load in the past. The new analyses provide further constraints on the timing of drainage capture.

Figure 2. Pb isotope discrimination diagram showing the different isotope ranges of basement units and mantle arrays. Data are shown from Eocene Red River sediments. These show partial overlap with the modern Red River, as well as with the Yangtze Craton.

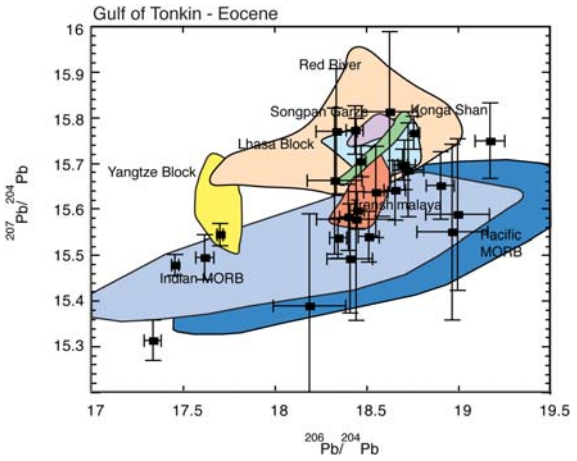

Fig. 4 shows that the sand in the Middle Miocene Red River is clearly different from the modern river in plotting consistently at lower 207/204 ratios [2]. Grains with higher 207/204 ratios seen in the Eocene (Fig. 2) have been lost by this stage, and the contribution from low 206/204 grains, associated with erosion of the Yangtze Block is also reduced. Comparison with the upper Yangtze range (Fig. 3) suggests that the Red River was still connected to drainage in eastern Tibet during the Middle Miocene (12 Ma), as there are many grains that match that composition. A similar pattern in the Late Miocene (9 Ma) indicates that final loss of these headwaters is more recent. The Pb isotope data here support a long history of ongoing capture away from the Red River since the Oligocene, with the drainage from the Yangtze Block being lost relatively early, pre-24 Ma, but with further capture events during the Miocene. There is no proof of an original connection to the Tsangpo as previously suggested [1]. The timing is broadly consistent with recent palaeo-altimetry work on the plateau suggesting Mid Miocene and older uplift of the central and southern plateau [6], but with uplift propagating to the SE [7].

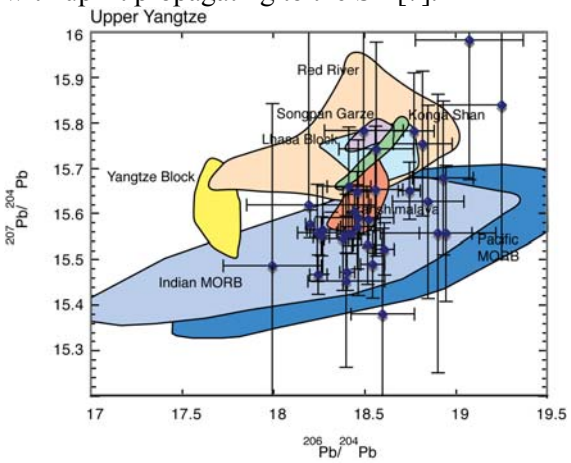

Figure 3. Pb isotope discrimination diagram showing detrital Pb compositions from the first bend

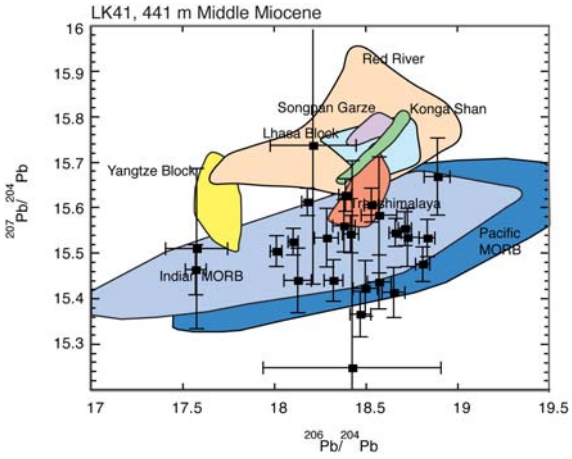

Figure 4. Pb isotope discrimination diagram for sand grains from the Middle Miocene (12 Ma)

of the Yangtze River immediately upstream from the Red River. This sediment samples unknown terrains in eastern Tibet, mostly plotting at lower 207/204 values than grains now found in the modern river.

showing that even at this time the river was eroding quite different sources than seen at present. Sediment flu from the Yangtze Block appears to have ceased by this time.

References

[1] M.K. Clark, L.M Schoenbohm,., L.H. Royden, et al., Tectonics, 23 (2004) doi:10.1029/2002TC001402.

[2] F. Bodet, and U. Schärer, Chem. Geol., 177 (2001) 265–285.

[3] P.D. Clift, J. Blusztajn, and D.A. Nguyen, D.A., Geophys. Res. Lett., 33 (2006) doi:10.1029/2006GL027772.

[4] P.D. Clift, G.D. Layne, and J. Blusztajn, in *Continent-Ocean Interactions in the East Asian Marginal Seas*, Am. Geophys. U. mono., 149 (2004) 255–282.

[5] F. Roger,., S. Calassou, J. Lancelot, et al., Earth Planet. Sci. Lett., 130 (1995), 201–216.

[6] D.B. Rowley and B.S Currie, Nature, 439 (2006) 677–681.

[7] L.M. Schoenbohm, B.C. Burchfiel, and L. Chen, Geology, 34 (2006), 813–816.

Trace elements variations across walls of planktonic foraminiferal tests: potential tracers of ocean vertical thermal and nutrient structure?

J.K. Darling & M. Elliot

School of GeoSciences, University of Edinburgh, Edinburgh EH9 3JW, UK

Background

Planktonic Foraminifera are commonly used in paleoclimate studies as recorders of past hydrographic conditions and oceanic circulation. Each species grows by sequentially adding chambers and also adds new layers of calcite over existing chambers. A transect across a foraminifera test thus reveals successive layers of calcite deposited sequentially throughout the lifespan of the specimen. A final layer is often added at the time of reproduction at greater water depth. The shell calcite is imprinted at each growth stage with a chemical record of the environment in which it was precipitated and can potentially provide information on the range of habitats in which the foraminifera grew. Although geochemists have exploited this paleo-environmental archive, the conventional techniques of averaging many specimens for bulk measurements obliterate the high resolution signals within the calcite layers. Laser Ablation ICP-MS techniques approaches illustrate that profiles of trace elements can be obtained across the foraminifera walls. However, the ion probe can derive similar profiles of trace element composition without destruction with potentially increased resolution due to smaller beam size.

Sediment traps collect planktonic forams before they reach the sediments so that they can be isolated from sedimentary contamination. Forams can then be recovered on a regular cycle accompanied by simultaneous measurement of the environmental conditions prevailing at the time they grew in the water column. It this way it should be possible to directly link the shell calcite signatures with water column chemistry. Bulk Mg/Ca has been analysed on sediment trap samples of surface dwelling *G. bulloides* and *G. ruber* which have shown that they faithfully record the seasonal range of temperature variations at that location [1]. Their study illustrated that that there were species specific relationships between sea surface temperature and Mg/Ca in shell calcite which were most probably related to the differences in range of depth habitat and physiology between *G. bulloides* and *G. ruber*. Our proposal was to investigate these species specific relationships further on the same sample set by obtaining high resolution measurements of trace elements across the walls of individual test of *G. bulloides* and *G. ruber* using the ion microprobe. Since these two species have different habitat preferences there should be detectable differences in the geochemical signatures of their test calcite.

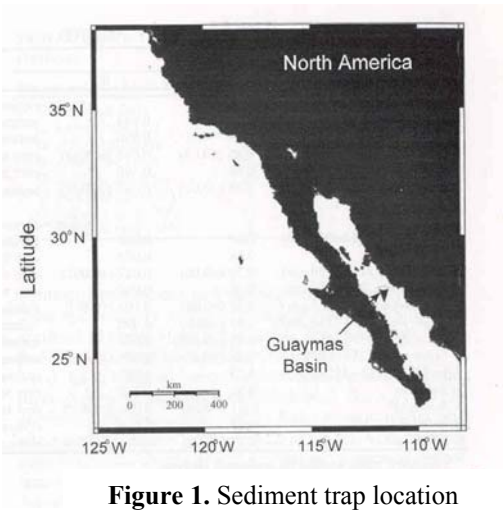

Figure 1. Sediment trap location

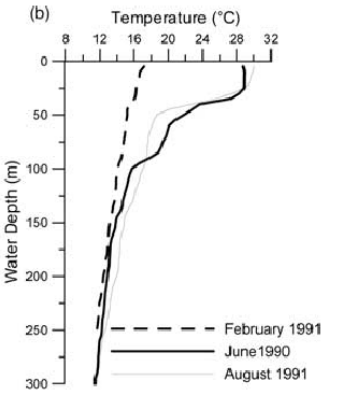

Figure 2. Seasonal temperature profile Guaymas Basin

Progress to date

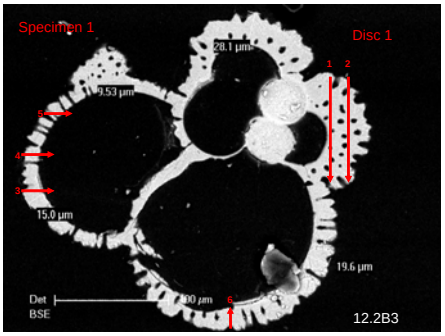

Figure 3. *G. bulloides* ion microprobe profiles (2 µm steps)

The *G. bulloides* and *G. ruber* samples obtained from collaborating colleagues in the USA were unfortunately very tiny and had much smaller walls than had been envisaged for this project. However, specimens were successfully mounted in resin disks by Mike Hall and polished to expose the full cross sections of the shells. SEM images were taken of each test prior to sampling with the Cameca ims-4f. Extensive profile sampling was carried out over a period of 5 days on both *G. bulloides* and *G. ruber* specimens. Sample I (Figure 3) shows the cross section of a *G. bulloides* and indicates where test wall profiles were taken for elemental measurements. Profiles of Mg, Ca, Sr, and Ba were carried out in 2µm steps across 6 regions of the walls of this specimen. The walls varied up to 15 µm in width which corresponds to the maximal test wall size found in any of the *G. bulloides* specimens provided. This created consi-derable difficulty in finding suitable sampling sites for profiling. No signi-ficant differences were recorded in 5 different specimens of *G. bulloides* in the elemental profiles. The same problems were experienced in the 3 *G. ruber* specimens used for profiling where shell walls were again too small for high resolution sampling. Electron microprobe evidence carried out in the Electron Microprobe Facility at Edinburgh does however show that Mg layers are present in the wall calcite of *G. ruber* specimens (Figure 4) but it is clear that there is not sufficient resolution to detect these minute bands using the ion microprobe. Having carried out sufficient profiles to determine that there was no benefit to be gained using this approach, discrete spot sampling was started on single specimens to determine whether differences could be detected between the different chambers which would have been precipitated at different levels within the water column. This approach proved much more successful and a single specimen of *G. ruber* was sampled using the Cameca ims-4f (beam focus 1.8 µm). The positions of the sampling points are shown in Figure 5. The Mg/Ca ratio values show that there are differences in the Mg/Ca ratios between chambers which reflect the temperature of the water in which they were precipitated

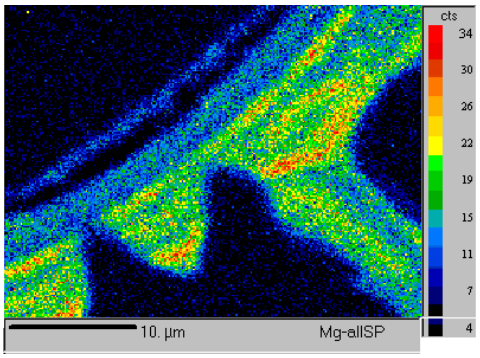

Figure 4. Electron microprobe map *G. ruber* Test wall showing Mg and Ca layers

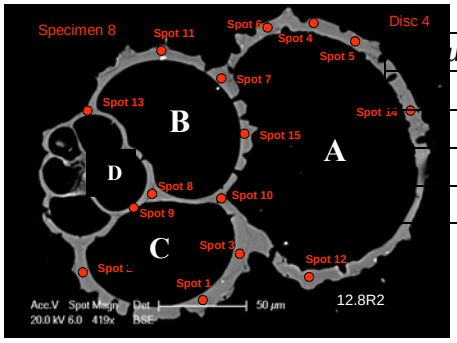

Figure 5. Trace element ion microprobe point positions sampled in *G. ruber* specimen

uber	Chamber	Mg/Ca ratio	Uncertainty
	A	4.5	+/- 0.5
	B	4.1	+/- 0.5
	C	5.2	+/- 0.5
	D	7.6	+/- 0.5

The low Mg/Ca ratios values shown above for the last 3 chambers (A, B and C) in the specimen shown in Figure 5 indicates that they were precipitated at lower temperature than the earlier chamber D. This is highly consistent with the known behaviour of planktonic forams in the water column. Juvenile planktonic foraminifers are known to frequent the near surface and therefore their temperature signatures will correspond to the sea surface

temperature. As the forams grow they sink towards the thermocline and the water temperatures in which they precipitate their later chambers will be lower depending on how deep they sink. This successful approach will now be utilized for the second week of measurements when much more progress should be made to address the questions raised in the proposal.

References

[1] McConnell, M. C., and R. C. Thunell (2005), Calibration of the planktonic foraminiferal Mg/Ca paleothermometer: sediment trap results from the Guaymas Basin, Gulf of California, *Paleoceanography*, *20*, art. no.-PA2016.

Mg/Ca ratios in sequential chambers of the foraminifera Streptochilus from the Arabian Sea

K. Darling & S. Kasemann

School of GeoSciences, University of Edinburgh, Edinburgh EH9 3JW, UK

Background

Several Mio- and Pliocene biserial *Streptochilus* species (Figure 1) were originally described as belonging to the benthic genus *Bolivina*, until isotope and distributional data were interpreted as indicating a possible planktonic mode of life [1]. Early investigators thought *Streptochilus* was extinct when the genus was first described but it has since been found to be locally common, often up to 15% of the living assemblage in plankton tows south of India, where upwelling causes highly variable conditions close to the shelf edge [2]. The spatial and temporal distribution of living *Streptochilus* are poorly known because they are minute and the size fraction in which they occur is rarely studied in the sediments. It is surprisingly difficult to ascertain whether biserial foraminifera are planktonic or benthic based on morphology only. Most biserial planktonics are thought to have more inflated chambers than benthics, and a wide, arched aperture without an internal tooth-plate. The genus *Streptochilus,* however, is characterized by an aperture bordered by a collar (Figure 2), with a connecting internal plate superficially resembling the bolivinid toothplate, although it does not extend freely outside the aperture. The exact nature of the toothplate, however, is not easily observed in a light microscope, especially since *Streptochilus* species are small. In some specimens the toothplate is missing, and many published figures do not show this feature.

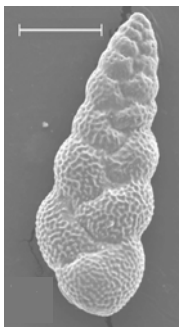

Figure 1. *Streptochilus* species

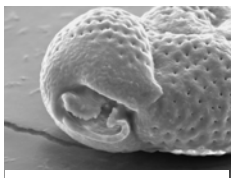

Figure 2. *Streptochilus* Aperture

Streptochilus species could become a useful palaeoceanographic palaeoproxy if they are truly planktonic and specifically associated with upwelling systems. However, the lack of a robust taxonomy and the associated morphological confusion, questions their planktonic habit. To answer this specific question, Kate Darling collected living specimens of *Streptochilus* species in the Arabian Sea on NERC cruise CD148 in 2003 (Figure 3). The aim was to genetically characterize them to determine their true affinity to the benthic foraminifer *Bolivina variabilis* which looks very similar. *Bolivina variabilis* was genetically characterized by Ertan *et al* [3]. Kate Darling found that the DNA sequences amplified from the *Streptochilus* in the plankton 540 miles offshore Kenya were genetically identical to the *Bolivina variabilis* from the Kenyan inter-tidal coastal region. This indicated that they were expatriated from the Kenyan shelf. The prevailing wind at this time was the summer monsoon blowing offshore Africa which would be consistent with this scenario. It was unknown at what stage of growth this expatriation occurred and it was decided to probe individual chambers and measure the Mg/Ca ratios to provide an indication of the comparative sea temperatures in which they had been precipitated. Change in calcification temperature between chambers would indicate whether they were just surviving in the plankton following expatriation from the continental shelf or slope and or whether they had calcified in the open ocean and were living and growing in the plankton.

Figure 3. Arabian Sea cruise track

Probing at the limit of possibility

Streptochilus is tiny, being only 250 µm in length when fully grown. The wall thickness is often no more than 5-6 µm. Mike Hall successfully mounted these tiny specimens in resin and polishing them to expose the chambers of each specimen in full cross sections. Without his skill and patience in the preparation of these specimens, this project would not have been possible. Using the Cameca ims-4f, highly discrete (beam focus 1.8 µm) trace element point analyses were taken for Mg/Ca ratio measurements. The SIMS probe pits and shown on the embedded *Streptochilus* specimen in Figure 4. The full exposure of all chambers in the same specimen allowed us to probe all of the chambers individually. The results from this specimen (sample 5) and from three other specimens (Samples 7, 8 and 12) are shown in Figure 5. These measurements were made in a single day using the SIMS and are highly exciting. They show that *Streptochilus* clearly precipitated the early chambers of its shell at a different temperature than the later ones. This was consistent in all four specimens and indicates that they were alive and growing in the plankton. This data was shown as a poster at the FORAMS 2006 Symposium in Brazil [4] where it attracted considerable interest. It is intended to probe further specimens to increase sample numbers for publication. As yet we are not sure whether the Ca/Mg values can be calibrated successfully and transformed into sea temperatures. It is clear from the genetic and SIMS results that the *Streptochilus* specimens were expatriated from the shelf and are growing in the plankton. It shows that they grew their small chambers at a higher temperature than their larger ones. There are two scenarios that could explain this. First, the higher temperature of the small chambers reflect the shelf inter-tidal zone temperatures and following expatriation they precipitated their large chambers in the lower temperatures of the thermocline at 200m where they are mostly found (ref). Secondly, they may be expatriated as propagules which may be only the first single chambers. If they then followed the pattern of most planktonic forams, the juvenile stages would live in the upper levels of the water column and then progressively sink as they grew. Here they would also precipitate their small chambers in the warmest water similar to the temperature of the inter-tidal zone.

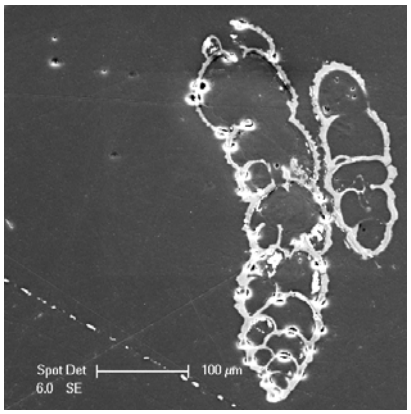

Figure 4. Trace element analysis of *Streptochilus* chambers (Sample 5) showing SIMS probe pits where discrete trace element point measurements (beam focus 1.8µm) were taken for Mg/Ca ratio measurements.

What the future holds

Following a successful second day of measurements on the second sample set, there will be sufficient data to publish. It is then our intension to obtain samples of *Bolivina variabilis* from the Kenyan shelf region to make comparative measurements against the ones that are sedentary and should have precipitated their shells in a constant temperature environment. We also would like to include Electron Microprobe scans to determine whether the Mg layering observed in healthy foram shell walls is also found in the chamber calcite of the ones precipitated in the plankton. This may tell us whether they are stressed or whether this is their normal habit and that they have both a benthic and a planktonic habit involving a reproductive strategy. This conclusion would have considerable implications for our understanding of the evolution

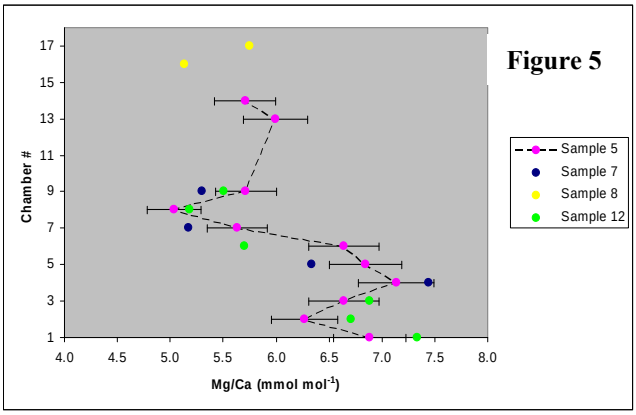

Figure 5

of planktonic forams from the benthos and also for the way they disperse around the oceans. More importantly, if we can start to understand their ecology we could realise their potential for use as palaeoceanographic indicators and use their geochemical signatures as palaeoproxies of shelf temperatures, sea surface temperatures or thermocline temperatures in the same shell.

References

[1] P. Brönnimann & J. Resig *in* Winterer, E Riedel, W *et al* Initial reports of the Deep Sea Drilling Project 7 (1971) 1235-1469
[2] D. Kroon & A. J. Nederbragt, Marine Micropaleontology 16 (1990) 25-38
[3] K.T Ertan., V. Hemleben & C Hemleben. *Marine Micropaleontology* 53 (2004) 367-388
[4] K.F. Darling *et al*, Anuario do Instituto de Geociencias 29(1) (2006) 187. FORAM 2006 Conference abstracts

The cause and consequences of extreme Li isotope variation in mantle peridotites II

T. Elliott[1], H. Wickens[1,2] & M. Regelous[1,3]

[1]Department of Earth Sciences, University of Bristol, Bristol BS8 IRJ, UK
Now at: Shell UK, Aberdeen[2] and Royal Holloway, University of London, Egham[3]

Overview

This report describes our further attempts to understand Li isotopic zoning within mantle peridotites. We initially discovered isotopic zoning during the PhD thesis of Alistair Jeffcoate and attributed it in general to differential diffusion of the two Li isotopes. This work is now published [1] but it was unclear as to the ultimate processes that drove diffusion. By more detailed investigation of the same peridotites we hoped to address this issue. The work summarised here completes the project for which the first set of data were documented in a report last year. In a final one week session in May 2006 we measured 117 Li isotope ratios in three different peridotite samples.

Influence of metasomatism

Having established in the previous year that zoning was muted in our 'baseline' unmetasomatised samples, we concentrated on the influence of melt veining and modal metasomatism on two key samples 8520-5g and 4320-16 respectively. We have reconfirmed the isotopically light compositions (-9‰) of melt pools in sieved relict clinopyroxenes, believed to be product of the ingress of a carbonatitic melt [2]. Likewise we have bolstered our observations of a trend to heavier rims in opx (Δ^7Li ~+2‰) but lighter rims in ol (Δ^7Li ~-2‰) adjacent to the melt pools. This is inconsistent with our original suggestion that the interstitial melt is light as a result of diffusive Li isotope fractionation along melt pathways into the xenolith as this should lead to lighter rims in both phases. These effects can possibly be explained by an on-going decarbonation reaction during decompression, as suggested by Wiechert et al [2]:

$$\text{carbonate melt} + \text{opx} \wedge \text{cpx} + \text{ol} + CO_2$$

It is plausible that Li diffuses from reactant opx into the product melt and growing olivine. Thus the isotopic disequilibrium is driven by on-going local reaction, accounting for the preservation of the isotopic disequilibrium and restricted extent of anomalous values to the melt pools. Moreover, melt films that more commonly rim minerals have more normal isotopic compositions (δ^7Li ~ 5‰), implying that melt is not ubiquitously light.
We also examined more extensively the phlogopites in 4230-16 (Fig. 1).

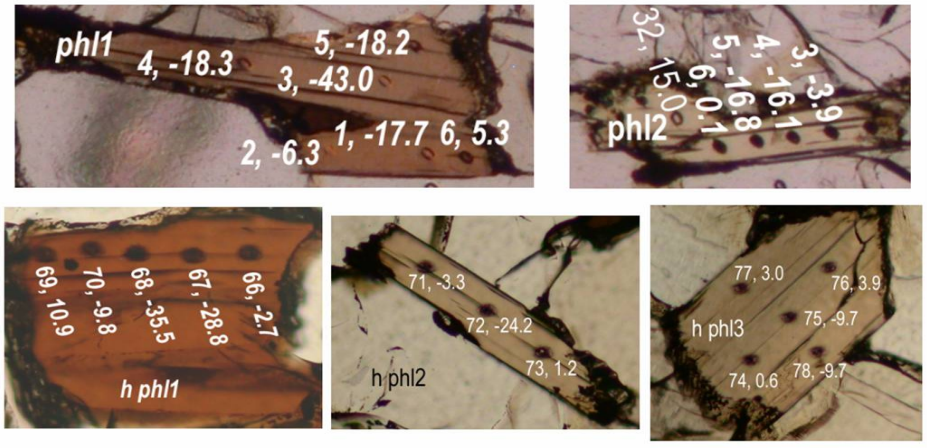

Figure 1. Analysed phlogopites, with individual analysis pits marked with analysis number followed by Li isotopic composition (in ‰).

These were also puzzling as textural and radiogenic isotope evidence suggested that they had formed hundreds of thousands to millions of years prior to eruption, yet they showed extreme isotopic zoning. It would be expected any initial isotopic disequilibrium present in the metasomatic mineral would have long since diffusively equilibrated. We were concerned that these features might be an analytical artifact, potentially related to the strong anisotropy in the mica structure. Thus we analysed three additional phlogopites in different orientations. These all show the same form of zonation from heavier rims to extremely light interiors (as low as –40‰). Such strong zonation must be a result of recent processes, given the likely high diffusivity of Li in mica and the very small length scales. This evidence suggests that disequilibrium is also a result of local changing equilibrium conditions during decompression and cooling. If the partition coefficient of Li between phlogopite and an adjacent phase changes with temperature, then as the xenolith cools Li will be diffusively redistributed in an attempt to maintain equilibrium. The effect on phlogopite should be marked, as they are small crystals with large amount of grain boundary relative to volume. In contrast diffusion of Li from the major phases into phlogopite will have a less important influence on their mass balance and so be less evident. However, we did explore how the Li isotopic composition of the other major phases changed in response to their location next to grain boundaries of different minerals.

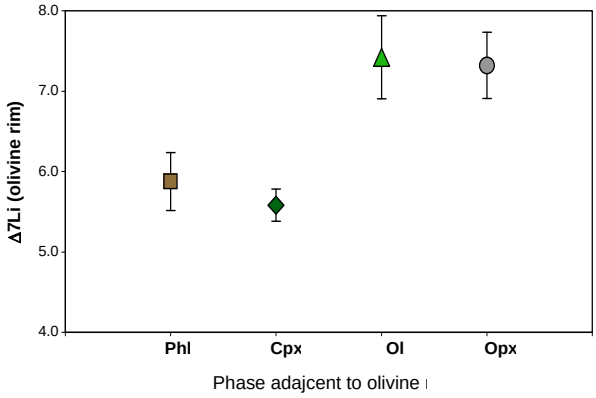

Figure 2. The Li isotopic compositions of the rims of different olivine grains in 4320-16 according to varying adjacent phase.

In Fig. 2 we compare the changes in olivine rim compositions with the nature of co-existing phase. Although the differences are subtle, there appear to be some consistent features. Notably olivine rims next to clinopyroxene and phlogopite appear to be lighter than those next to orthopyroxene or other olivine. This implies that $K^{ol/cpx}_{Li}$ increases with decreasing temperature, which is surprising given the tendency of clinopyroxenes to have isotopically light compositions. That $K^{ol/phl}_{Li}$ is also inferred to increase with decreasing temperature from out data is also unexpected and would imply that addition of Li to phlogopite to promote its light isotopic signature is either derived from clinopyroxene or else occurs in the initial heating of the xenoliths and is not fully undone during cooling. Such relationships clearly need experimental investigation.

Concluding remarks

The spatial relationships investigated in this work strongly implicate the importance of redistribution of Li during cooling rather than the introduction of a melt phase with light Li as a cause of Li isotope zoning in xenoliths. A range in complexities can be expected from the thermal histories of the xenoliths. Additional experimental work to define diffusivities and changes in partition coefficients would allow such information to be used more qualitatively, which would in turn create a need for further detailed studies. A remaining puzzle is that the olivines within a particular polished section define fairly constant isotopic compositions but that these vary from sample to sample in a manner uncorrelated to the bulk composition of olivine determined by MC-ICP-MS. This is likely an analytical effect, potentially related to different olivine Fo contents (Fo 86-90) but needs more work to resolve.

References

[1] A.B. Jeffcoate, T. Elliott, S.A. Kasemann, D. Ionov, K. Cooper & R. Brooker, *Geochim. Cosmochim. Acta* 71(2007) 202-218.
[2] U. Wiechert, D. Ionov & K.H. Wedepohl, Contrib. Mineral. Petrol., 126 (1997) 345-346.

Distribution of trace elements between zircon, garnet and melt: a key to understanding crustal events and processes (NERC grant NE/B504157/1)

S.L. Harley, R.W. Hinton, N.M. Kelly and R. Taylor

School of GeoSciences, University of Edinburgh, Edinburgh EH9 3JW, UK

Background

The interpretation of zircon age data in multiply-deformed and polymetamorphosed high grade terrains presents a significant problem in geochronology because the response of zircon to metamorphism is highly variable even on the microscale. The reliable interpretation of zircon age data must be founded upon detailed textural analysis coupled with in-situ microanalysis that yields independent chemical criteria for constraining the processes that have affected or controlled zircon behaviour. The distribution of REE and other trace elements between zircon and garnet in high-temperature crustal processes is being determined in this project, using both an empirical approach, based on in-situ analysis of zircon, garnet and co-existing phases in natural granulites and migmatites, and high-PT trace element doped experiments that yield zircon-granitic melt, garnet-melt and zircon-garnet-melt products. Coupled with Cameca 1270 U-Pb age dating of chemically and texturally constrained zircons, the distribution data are applied to evaluate the event significance of zircon ages in HT and UHT terranes, the responsiveness of zircon to post-peak mineral-melt reactions, and the relative importance of zircon recrystallisation versus new growth in metamorphism. Examples of such applications are provided in this report; experimental results are presented in a separate but parallel report (Taylor et al., this volume).

Results

1. Empirical Equilibrium Zircon-Garnet REE Distribution Coefficients (*D*REE(zir/grt))

The equilibrium distribution of REE between zircon and Fe-Mg garnet (X_{Mg} = 0.30-0.65) at temperatures of 850-1100°C has been empirically defined using the compositions of multifacetted and fir-tree to sector zoned zircons and inclusion-free garnets analysed in-situ in several migmatites from five different metamorphic belts that have distinct P-T histories. The results are largely in accord with our previous D_{REE}(zir/grt) values obtained from two garnet-mesoperthite-quartz UHT leucosomes (D_{Gd} = 0.9; D_{Ho} = 0.8; D_{Yb} = 0.6-0.7). The larger data set now available suggests that equilibrium D_{REE}(zir/grt) values are within the ranges 0.9-2 at Gd and 0.7-2 at Yb, and most critically that the equilibrium D_{REE}(zir/grt) values for HREE are all similar, and near unity, across the range of HREE and notwithstanding the absolute abundances (in ppm) of the REE in zircon and garnet.

2. Post-peak zircon modification and its bearing on the geochronology of UHT metamorphism

The insights provided by integrating REE chemistry with in-situ geochronology are demonstrated here by the application of zircon-garnet REE distribution data (D_{REE}) to the Napier Complex, East Antarctica. Metamorphic zircon formation / recrystallisation in a garnet-bearing Napier Complex gneiss, *Cronus*, has been evaluated using the HREE D_{REE}(zir/grt) criteria described above. This gneiss is characterised by early porphyroblastic garnet and orthopyroxene, both overgrown or rimmed by secondary, post-fabric, garnet and garnet-quartz symplectites, and in the case of orthopyroxene decorated with garnet lamellae (Fig. 1).

Abundant zircons display variably disturbed oscillatory-zoned cores (Fig. 2) that have moderately steep HREE patterns (Yb(n)/Gd(n) = 10-12). These yield U-Pb ages of c. 2700-2750 Ma, interpreted to be those of the protolith. Homogeneous to weakly planar-zoned and curviplanar zoned rims and grain terminations against coronal and lamellar garnet preserve a range of HREE patterns, from core-like to flat (Yb(n)/Gd(n) = 1-2) (Fig. 3). The outermost

zircon rims adjacent to late garnet preserve flat HREE patterns, and record near-concordant U-Pb ages that spread between 2520 Ma and 2200 Ma (Fig. 4). Coronal and lamellar garnets in the same microtextural domains also have flat HREE patterns (Yb(n)/Gd(n) = 1-1.5) at c.

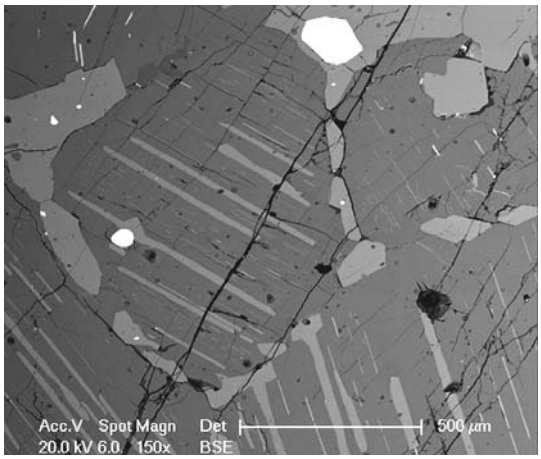

Figure 1. *Cronus* Grt-Opx-Plag granulite, showing late (post-peak, IBC related) lamellar and grain boundary garnet in exsolved orthopyroxene. Bright BEI phases are zircon and ilmenite. Zircon Ti contents are generally < 22 ppm, irrespective of the zircon internal textural type.

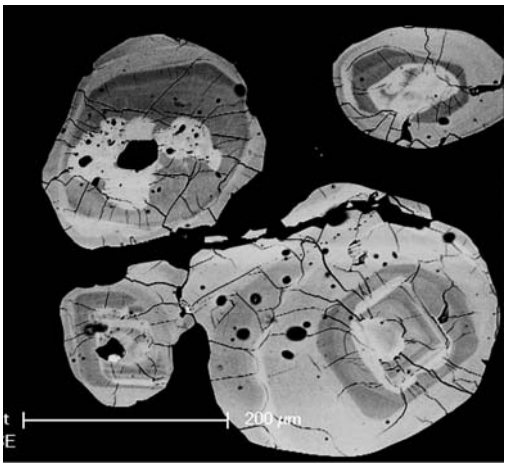

Figure 2. Zircons in *Cronus* sample, Napier Complex, showing oscillatory zoned original detrital cores, often modified, and weakly zoned highly modified rims and local overgrowths. These zircons are hosted in orthopyroxene and coronal garnet.

D_{HREE} (zir/grt) calculated from the weakly zoned zircon rim and coronal garnet REE compositions are near unity, similar to the equilibrium zircon-garnet D_{HREE} values as defined from our parallel leucosome study (Fig. 5). On the other hand, D_{HREE} (zir/grt) calculated using any modified zircon composition coupled with initial, higher HREE, porphyroblastic garnet fall well below the preferred equilibrium values. The chemistry of the >2520 Ma old 'metamorphic' zircon in this case does not, therefore, reflect zircon-garnet equilibrium under UHT conditions. Instead, these zircon rims and weakly zoned domains reflect extensive zircon recrystallisation and re-equilibration concomitant with the *post-peak* formation of garnet during prolonged near-isobaric cooling through the temperature range (as calculated from Zr-in-rutile and Ti-in-zircon thermometry of other samples) 775-705°C, some 50-80 Ma after UHT. The spread in zircon U-Pb ages (Fig. 4) downwards from a cluster at c. 2480 Ma may reflect continued re-equilibration following garnet corona formation initiated at c. 775ºC through fluid activated or mediated reactions.

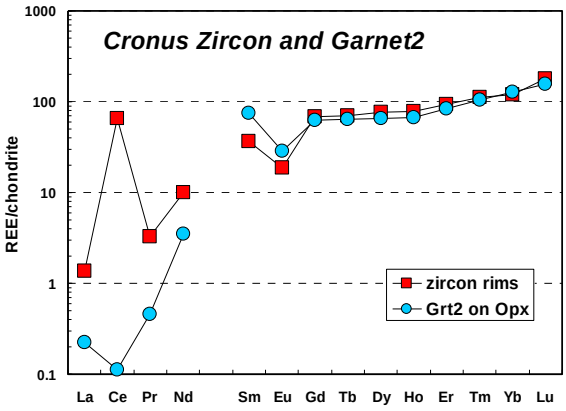

Figure 3. Edinburgh IMS-4f REE data for zircon rims / recrystallised domains and adjacent garnet coronas and lamallae analysed in-situ in the *Cronus* sample. Each pattern is the average of 8 –

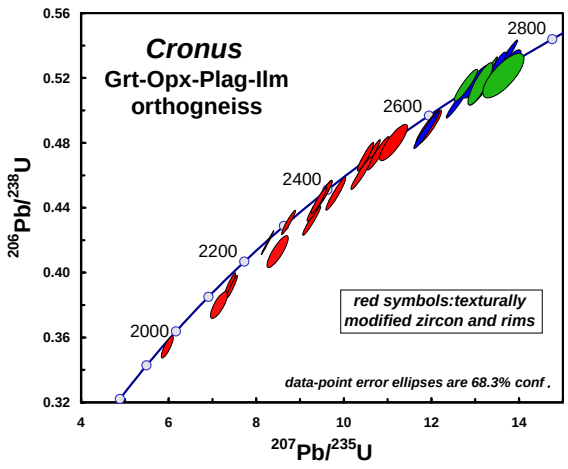

Figure 4. Edinburgh IMS-1270 U-Pb age data for zircons analysed in-situ in the *Cronus* sample. Red data points include those obtained from the zircon rims and outer zones shown in Fig. 2. The

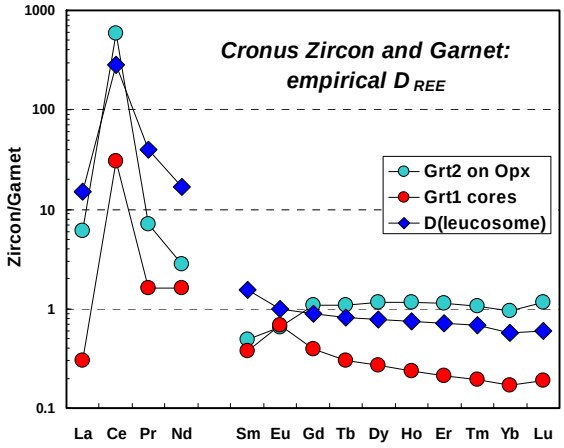

Figure 5. Distribution of REE between zircon and garnet in *Cronus*, compared with the empirically determined equilibrium D values from UHT leucosomes and with the disequilibrium apparent D values calculated from zircon rims and UHT garnet in *Cronus*.

Significance for Crustal Evolution Studies

The examples briefly described here illustrate the importance of integrating in-situ trace element accessory mineral analysis with both internal microtexture characterisation and petrology in order to interpret zircon U-Pb geochronological data. In the case of *Cronus*, and indeed several other on-going case studies from the Napier Complex and elsewhere, it is apparent from this approach that zircon is sensitive to garnet-forming reactions that have progressed during cooling and so preferentially records the ages of events that have occurred after peak metamorphism. In the case of slowly cooled high grade terranes the ages recorded by such 'metamorphic' zircons may be significantly younger – by several tens of million years to greater than a hundred million years in extreme cases – than the main tectonothermal events responsible for the observed gneisses. This has major consequences for reconstructing crustal histories and correlating between crustal units, as well as for the validity of terrane amalgamation scenarios based largely on zircon U-Pb age data.

H_2O diffusion in melt inclusions: a geospeedometer for explosive volcanic eruptions

M.C.S. Humphreys[1], T.Menand[2], J.D. Blundy[2] & K. Klimm [2]

[1]Department of Earth Sciences, University of Cambridge, Downing Street, Cambridge, CB2 3EQ
[2] Department of Earth Sciences, University of Bristol, Wills Memorial Building, Queen's Road, Bristol, BS8 1RJ, UK

Confidential

The link between granulite formation, silicic magma generation and crustal growth in arcs: insights from the Hidaka Metamorphic Belt, Japan

A.I.S. Kemp & C.J. Hawkesworth

Department of Earth Sciences, University of Bristol, Bristol BS8 1RJ, UK

Objectives

This project involved (U-Th)-Pb isotope microanalysis of zircon to determine the crystallisation age of key tonalite, granite and gabbro samples, and the age of granulite facies metamorphism, in the Hidaka Metamorphic Belt, Hokkaido, Japan. The terrane exposes the roots of an island arc, exhumed by a Tertiary collision between the Kuril and Japan arcs, and is one of the few places on Earth where a near complete lithospheric section can be observed in outcrop. The igneous samples derive from different emplacement levels in this sequence. The specific aims of the study were to (1) constrain the formation of granulites, in particular to establish the tectonic controls, and (2) to understand the generation and differentiation of silicic magmas in convergent margin environments. The project is an integral part of a wider investigation into crustal evolutionary processes in arcs.

Methods

The research utilised the Cameca ims 1270 ion microprobe operating in single collector mode. The samples were prepared as polished grain mounts using Epofix resin, which were pre-cleaned with 2% HNO_3. Each analysis was about 28 minutes in duration (including a preliminary 2 minute, 15 μm raster across the analysis site) and employed a 4 nA primary O_2- ion beam current and Kohler illumination to produce a spot approximately 20 μm in diameter on the sample (Figure 1). Isotope ratios were measured over 20 cycles, the first five being rejected to minimize surficial lead contamination. The Pb/U calibration was performed relative to the Geostandards zircon 91500, which was also used as the U-Th-Pb concentration standard and was analysed after 3-4 analyses of sample zircons. Fifty analyses of 91500 yielded a $^{207}Pb/^{206}Pb$ age of 1061 ± 24 Ma (1 standard deviation, MSWD = 1.7, a common lead correction based on the measured abundance of ^{204}Pb was applied), identical to the TIMS age [1]. Repeat analyses of standard zircons Temora 2 (TIMS Pb/U age 416.8 ± 0.3 Ma [2]) and FC1 (TIMS Pb/U age 1099 Ma [3]) were also interspersed throughout each session to monitor data quality. Thirty-seven analyses of Temora 2 returned a common lead corrected $^{206}Pb/^{238}U$ age of 418.2 ± 6 Ma (1 std. dev) the corresponding figure being 1100.6 ± 14.4 Ma for FC1 (n = 6). Isotope ratios were corrected for common Pb according to the ^{204}Pb method or, where the inferred ^{207}Pb concentration was below 0.15 ppm, the ^{208}Pb correction.

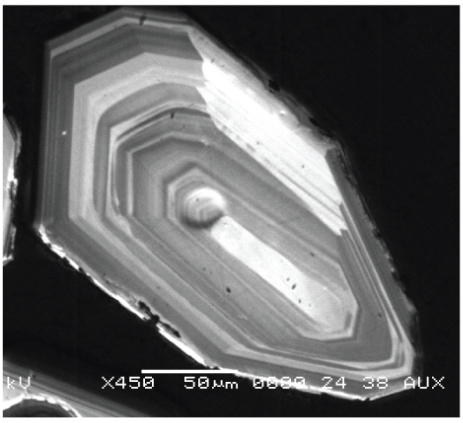

Figure 1. Cathodoluminescence image of a zircon from a Hidaka tonalite. Ion probe analysis in the centre of the crystal yielded a crystallisation age of 37.1 Ma.

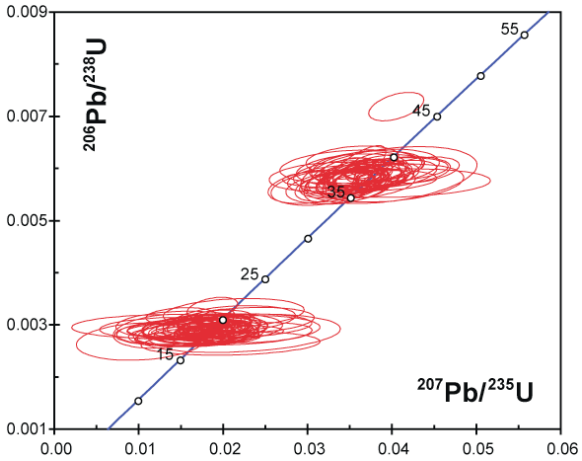

Figure 2. Concordia diagram plotting analyses of melt-precipitated zircons and granulite zircon rims from the Hidaka samples. Two discrete episodes of zircon growth are apparent.

R

Results

Table 1 and Figure 2 summarise the U-Pb ages determined from the sample zircons. Analysis of zircon crystals separated from the hornblende tonalite (granulite facies) and granite (biotite zone) revealed a single age population at ca. 37 Ma that represents the time of magmatic crystallisation. The Pb/U ages of oscillatory-zoned zircon rims from the cordierite tonalites (amphibolite facies) also cluster around 37 Ma, although these grains enclose older cores entrained from the metasedimentary protolith.

In contrast, granulite zircon rims, and zircons from the amphibolite, define a precise age group that is interpreted to denote zircon growth during granulite facies metamorphism and incipient anatexis at 19 Ma. The Hidaka granulites are thus amongst the youngest exposed on Earth. Identical ages were obtained from the rims of the garnet tonalite zircons. The cores of the granulite and garnet tonalite zircons yielded a spectrum of pre-magmatic ages extending to 2.7 Ga that reflect the sedimentary provenance of the precursors. A single age population from zircons of the gabbro at 18.5 ± 0.3 Ma supports the notion that heat input from mafic liquids promoted granulite and garnet tonalite generation.

These data provide compelling evidence that the Hidaka sequence was constructed in two remarkably discrete thermal pulses in the Eocene (37 Ma) and early Miocene (19 Ma) (Figure 2), the latter coinciding with the onset of back-arc spreading in the nascent Japan Sea. The widely accepted model that the Hidaka granulites formed from a ridge-trench interaction at 55 Ma is therefore no longer tenable. Instead, we correlate the two-stage evolution of this terrane with episodes of supra-subduction zone magmatism (late Eocene) and back-arc extension (early Miocene), as the Hidaka Belt evolved from a continental arc to oceanic back-arc realm with the opening of the Japan Sea. Our results emphasise the importance of coupled lithosphere thinning and mafic magma underaccretion in the formation of granulites, and imply that granulite-facies metamorphism may be a hallmark of tectonically driven mantle differentiation and continental growth.

Rock type	Sample	No. of	Weighted average $^{206}Pb/^{238}U$ age (Ma)	
		analyses	*melt-precipitated*	*older cores (age range)*
Grt-opx tonalite	HD23	20	18.8 ± 0.4 (n = 12)	50 to 75
	HD19	28	18.7 ± 0.5 (n = 11)	39 to 178
Granulite	HD19e	29	19.8 ± 0.5 (n = 4)	43 to 2744
	4HB29	12	19.4 ± 0.6 (n = 8)	33 to 723
	HB1	9	18.9 ± 0.3 (n = 6)	38 to 60
Amphibolite	HB2	11	18.7 ± 0.5	-
Gabbro	P2	11	18.5 ± 0.3	-
Hbl-opx tonalite	HD22	17	37.4 ± 0.3	-
	HD14	8	37.4 ± 0.5	-
Crd-bt tonalite	HD13	17	37.8 ± 0.5 (n = 10)	42 to 171
	HD21	18	37.8 ± 0.9 (n = 6)	42 to 73

Table 1. Summary of the weighted average $^{206}Pb/^{238}U$ ages (at 95% confidence error limits) computed for individual samples of this study (all ages are common lead corrected).

References

[1] M. Weidenbeck, P. Alle, F. Corfu, W.L. Griffin, M. Meier, F. Oberli, A. von Quadt, J.C. Roddick & W.

Spiegel, Geostandards Newsletter 19 (2005) 1-23.
[2] L.P. Black, S. Kamo, C.M. Allen, D.W. Davis, J.N. Aleinikoff, J.W. Valley, R. Mundil, I.H. Campbell, R. Korsch, I.S. Williams & C. Foudoulis, Chem. Geol. 205 (2004) 115-140.
[3] J.B. Paces & J.D. Miller, J. Geophys. Res. 98B (1989) 13997–14013.

Sediment recycling in the Taiwan active orogenic setting

Linda A. Kirstein

School of Geosciences, University of Edinburgh, West Mains Road, Edinburgh EH9 3JW

The aim of this one day ion microprobe study was to examine whether large scale recycling of orogenic sediments due to thrust sheet activity or smaller scale sediment dissolution and re-precipitation could be quantified using oxygen isotope ratios from detrital quartz grains and their overgrowth textures.

Average $\delta^{18}O$ of quartz in igneous rocks is around 9 ‰, in metamorphic rocks <20 ‰ and in sandstones around 11 ‰ [1]. Therefore assuming all grains are detrital, the expected $\delta^{18}O$ range is 11 ± 2‰. If the quartz overgrowths are authigenic and formed in situ from either percolating meteoritic fluid or ^{18}O enriched fluids then higher $\delta^{18}O$ are anticipated. Modern meteoric water in Taiwan has a value of -5.4‰ which at temperatures of ~ 110° C would generate $\delta^{18}O$ values of ~15‰ (using the equation of Matsuhisa et al. [2]). Holocene oxygen isotope values of 1‰ were recently measured in Central Taiwan generating $\delta^{18}O$ values of ~20‰ in authigenic quartz at a similar temperature.

In this preliminary study we selected one sample from the Plio-Pleistocene sediments of the Coastal Range, eastern Taiwan to investigate the variation in oxygen isotope ratios. The sample (S1) from Shiulien is composed of quartz and feldspar with minor amounts of mica. Petrographically the quartz grains vary in shape from angular to (sub) rounded. Cathodoluminescence (CL) imaging was used to identify grains for analyses. CL microscopy revealed a large range in CL intensity among different detrital grain populations not previously discernible using a petrographic microscope, and was used to categorise detrital grains according to colour (white - grey).

The oxygen isotope ratios of the detrital cores vary from 10.13 to 17.51 ‰, while $\delta^{18}O$ of the overgrowths ranges from 16.29 to 20.67 ‰. The range in $\delta^{18}O$ of the overgrowth textures is typical for authigenic quartz (e.g Hervig et al., [3]) and is within the range expected to have precipitated from meteoritic water in this region since the Holocene (15-20 ‰). Where a significant change in CL intensity occurred that also corresponds to a variable degree of roundness, a significant change in $\delta^{18}O$ was noted. For example, in grains that are grey and rounded $\delta^{18}O$ varied from 13.17 to 16.60 ‰ while $\delta^{18}O$ varied from 10.13 to 10.93 in those that were white and angular.

The range in $\delta^{18}O$ in detrital quartz suggests a variety of source materials. The majority of the analyses are higher than the average for plutonic igneous rocks (~9 ‰; [1]) but are within the reported range for metamorphic rocks (<20 ‰; [1]). The $\delta^{18}O$ subdivision of grains particularly in terms of degree of rounding and colour is extremely interesting. Are these grains rounded during the recycling process and hence can the proportion of these grains be used to quantitatively estimate the proportion of sediment that is recycled? The data at present are limited so it is too early to draw any conclusions. However this preliminary study has raised the intriguing possibility that using this approach we may be able to quantify the amount of recycled sediment. A future proposal to NERC is planned to investigate this further.

Referenc

[1] H. Blatt, J. Sedimentary Pet. 57 (1987) 373-377.
[2] Y. Matsuhisa et al., Geochim. Cosmochim. Acta 43 (1997) 1131-1140.
[3] R.L. Hervig et al., Geochim. Cosmochim. Acta 59 (1995) 2537-2543.

Melt Mixing and Crystallisation in the Plumbing System of the 1783 Laki Eruption

J. Maclennan[1], E. Passmore[2] & J.G. Fitton[2]

[1]Department of Earth Sciences, University of Cambridge, Cambridge CB2 3EQ, UK
[2]School of GeoSciences, University of Edinburgh, Edinburgh EH9 3JW, UK

Justification: Understanding the causes and consequences of large basaltic eruptions

The link between basaltic volcanism and variations in climate has been recognised for over 200 years. Shortly after the 1783 AD eruption of the Laki fissure row in southern Iceland, Benjamin Franklin suggested that the dry fog that enveloped much of Europe in the following years was a result of the eruption. He linked Laki to a string of unusual environmental events in the mid-1780s, including cold winters and crop failures. While these events made life difficult over large parts of the northern hemisphere, the effects of the Laki eruption were most disastrous in areas adjacent to the eruption. The Cl and F rich haze generated by the eruption lead to famine, disease and the death of 25% of Iceland's population. Laki was a very large basaltic eruption, producing approximately 15 km^3 of lava and tephra over a period of 8 months. However, Laki is by no means unique in Iceland, with the neighbouring Eldgja fissure eruption having produced almost 20 km^3 of lava and tephra in 934 AD.

It is therefore important that a better understanding of the causes and consequences of such eruptions is acquired. Recent studies of Laki have focussed on the volcanology of the eruption and on petrological estimates of the total flux of volcanic gases to the atmosphere[1]. We therefore chose to focus our investigation on processes that occur in chambers that store magma before its eruption. In particular, we sought to define the relationship between melt mixing, crystallisation and deep degassing. The resulting observations can be used to better understand the fluid dynamics of magma stored in the crust and may improve models of the processes that trigger large eruptions. In addition, the results of our study will lead to improvements in the estimate of the total gas flux and expected environmental impact of the eruption.

Results: Variation in trace element content of olivine-hosted melt inclusions

The concentrations of 20 trace elements, including the Rare Earth Elements (REEs), Zr, Y, Nb and Sr, were obtained for 90 olivine-hosted melt inclusions from Laki using the Cameca 4f at Edinburgh during October 2006.

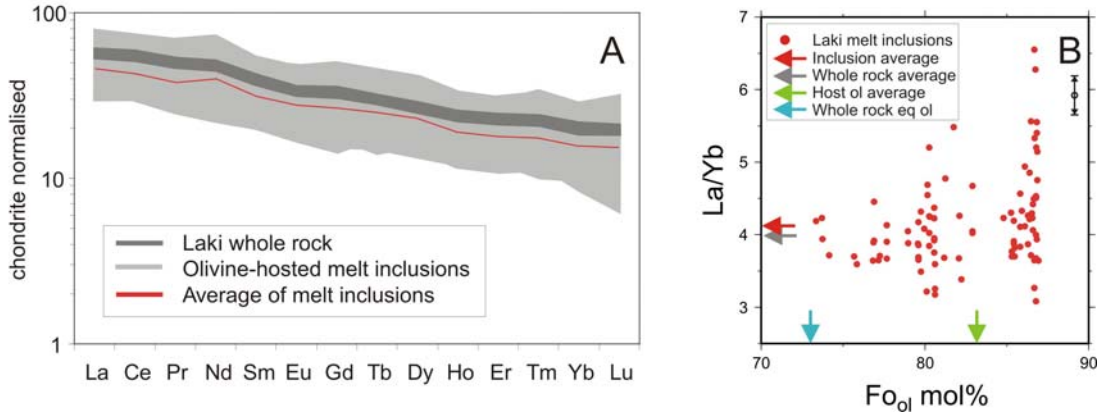

Figure 1. Summary of Laki melt inclusion, host olivine and whole-rock data. A) Chondrite normalised REE plot showing the field of melt inclusion compositions, the melt inclusion average, and the range of whole rock compositions. B) La/Yb of melt inclusions plotted against the forsterite content of their host olivines. The average La/Yb of the melt inclusions (n=90) and the whole rock samples (n=40) are

shown with arrows on the La/Yb axis. The average forsterite content of the olivines that host the analysed inclusions, and the composition of olivine in equilibrium with the Laki whole-rock samples are also marked with arrows. Error bars shown in the top-right corner show ±1σ precision for La/Yb

Volatile data, which can be used to study the degassing history of the Laki magma, will be acquired in early May 2007, so only the trace element results are presented herein. The composition of the olivine crystals that host the melt inclusions was determined before SIMS analysis. The compositions of 40 lava samples from Laki have also been acquired. Figure 1A shows the relationship between the REE contents of the melt inclusions and those of the lava samples. The range of melt inclusion compositions is much greater than that observed for the lava samples. For example, melt inclusion La concentrations vary by a factor of 2, while the whole rock samples of lava only vary in La content by ~10%. Another important observation is that the slope of the REEs on Figure 1A is similar for the average of the melt inclusions and the average of the whole rock samples. The REE concentration in the average whole rock samples is ~30% higher than that in the average of the melt inclusions. Figure 1B shows that olivine crystals with forsterite contents over 85 mol% contain melt inclusions with extremely variable La/Yb. However, olivines with lower forsterite contents show a small range of inclusion compositions, with the lowest fosterite olivines containing inclusions with compositions similar to those of the whole-rock samples. The standard deviation of La/Yb in melt inclusions in olivines with Fo>85 mol% is 0.75 (n=40). In contrast, olivines with Fo<78 mol% contain inclusions with a La/Yb standard deviation of 0.25 (n=16), which is close to the estimated precision of the measurements. This relationship between concentration ratios and forsterite contents is generally applicable to incompatible trace elements in the melt inclusions. The average forsterite content of the olivines that host the inclusions is significantly higher than that of olivines in equilibrium with the erupted lava.

Interpretation: Coupled melt mixing and crystallisation before the Laki eruption

The forsterite content of olivine is controlled by the temperature and extent of crystallisation of melt. Olivines with fosterite contents of ~90 mol% are commonly thought to have crystallised from mantle melts. As the temperature drops, and crystallisation proceeds, the composition of the crystallising olivine becomes less forsteritic. The variation in La/Yb reflects variation in the composition of mantle melts fed into the crust beneath the SE Iceland. This ratio is little changed by modest extents of fractional crystallisation, and can therefore be used as a passive tracer of mixing of these variable mantle melts. Melt inclusions are trapped as olivine crystals grow and they reflect the diversity of melt compositions at depth within the volcanic plumbing system. The observation that the lava samples have a more limited range of compositions than the melt inclusions indicates that mixing has destroyed compositional variation between entrapment of the inclusions and the eruption of the melt. The coupled decrease in variation of La/Yb and forsterite content of the host olivine can be accounted for by concurrent mixing, cooling and crystallisation of the Laki melt. The temperature drop corresponding to the range in host olivine compositions is ~50°C. The concurrent cooling and mixing may be generated by convection within the magma chamber, and the relative rates of mixing and cooling can be used to constrain the fluid dynamics within the Laki magma chamber. A similar relationship between mixing and cooling has been found in a much smaller, more primitive lava flow from northern Iceland[2]. The observations from Laki indicate that coupled mixing and crystallisation is widespread in the plumbing systems of Icelandic volcanoes.

It is commonly assumed that olivines found in lava samples with compositions that are not in equilibrium with the host lava are xenocrysts (i.e. that they have been picked up from fully solidified rock in the wall of the magma chamber or on ascent to the surface). However, the relationship between the average melt inclusion composition and the average whole rock composition indicates that the olivines grew from compositionally distinct batches of melt than then went on to mix and provide the magma for the Laki eruption. The presence of forsteritic olivines in Laki is caused by incomplete separation of olivines from melt.

References

[1] T. Thordarson, S. Self, N. Óskarsson, & T. Hulsebosch, Bull. Volcanol. 58 (1996) 205-225.
[2] J. Maclennan, D. McKenzie, K. Gronvöld, N. Shimizu, J.M. Eiler, & N. Kitchen, Geochem. Geophys. Geosyst., 4 (2003), doi:10.1029/2003GC000558.

Lithium isotopes in high-pressure metamorphic rocks from Syros, Greece

H. R. Marschall

Dep. Earth Sciences, University of Bristol, Bristol BS8 1RJ, UK

Background to the project

Li isotopes have attracted increasing attention from geochemists working on metamorphic, igneous and sedimentary rocks. The strong isotopic fractionation of Li at low temperatures provides a robust tool for tracing hydrous alteration processes at the Earth's surface, and has great potential as a tracer of low-temperature alteration material in subduction zone-related fluids, magmas and metamorphic rocks, in mantle xenoliths and ocean island basalts. Li fractionates during low-temperature (<400 °C) fluid/rock interaction with the heavier isotope entering the fluid. The geochemical cycle of Li and its isotopic fractionation during major processes like slab dehydration and metasomatism remain uncertain, and so investigation of the Li isotopic compositions of samples with a well-constrained geological history is necessary to understand the geochemical cycle of this exciting new tracer of crustal recycling.

High-pressure metamorphic (HPM) rocks can provide a record of various stages of the subduction process rather than just one final product, provided the history can be disentangled. An important example is the Aegean island of Syros (Greece), which displays a mélange composed of rigid HPM blocks within a schistose mafic-ultramafic matrix. Most of the blocks preserved their peak-metamorphic mineral and chemical compositions, while contacts between blocks and matrix display reaction zones (blackwalls) formed by fluid influx during exhumation. Most blackwalls show strong enrichments in Li, manifest by abundant Li-rich omphacite, glaucophane and chlorite.

Recently, some of the Syros samples were analysed for their whole-rock Li isotopic compositions. The results are very encouraging and show that the HPM blocks (δ^7Li ≈ -4.8 to +3.6 ‰, Marschall et al., in prep.) are lower than MORB and overlap with compositions of Alpine eclogites reported by Zack et al. (2003, EPSL 208: 279-290), whilst enrichment of Li in the blackwalls (up to 80 µg/g) is accompanied by a strong increase in δ^7Li to values between +4.4 and +11.2 ‰. However, many samples display evidence of partial rehydration, making the interpretation of whole-rock data ambiguous.

Objectives of the research and tested hypothesis

The low δ^7Li values in the HPM blocks are probably a result of various subsequent processes, such as Li isotopic fractionation during prograde dehydration, diffusive re-enrichment of Li and influx of Li-rich fluids during exhumation. The release of isotopically heavy fluids from the slab into the mélange at shallower depths are probably recorded in the high-δ^7Li rehydrated zones.

It was to be tested, (i) if the minerals omphacite, chlorite and glaucophane, which are the major hosts for Li in the samples, reflect the Li isotopic composition of the respective whole rocks, (ii) whether or not intra-mineral and inter-mineral variations in Li isotope compositions allow a meaningful calculation of whole-rock δ^7Li values from SIMS analyses of minerals.

Results

The results of this preliminary study show that Li isotopic compositions determined by SIMS on the major host minerals of Li in the rocks are in good agreement with the whole-rock compositions determined by multi-collector ICP-MS. This result is highly encouraging, as it allows us to investigate Li isotopic composition of rocks that show limited alteration and formation of Li-rich secondary mineral phases. The number of samples available for Li isotope studies is therefore greatly increased. Results of this study were presented at the Goldschmidt Conference in Melbourne, Australia in August 2007 [1].

Figures and Tables

Sample	Mineral	n	δ7Li mean (‰)	2σ mean (± ‰)	[Li] (µg/g)	2σ mean
SY309B	tourmaline	4	+13.7	±0.9	2.10	0.33
	omphacite	7	+10.8	±0.5	27.2	3.9
	glaucophane	4	+10.5	±0.7	41.0	3.1
	phengite	4	+13.1	±1.1	5.85	1.04
	chlorite	4	+13.1	±0.6	34.7	2.5
	WR		+11.2	±0.2	31.7	0.6
SY431	garnet	15	-6.0	±1.1	3.0*	1.0*
	omphacite	7	-6.6	±0.9	75*	15*
	paragonite	5	-6.0	±1.2	14*	4*
	WR		-4.3	±0.3	22.7	3.3

*estimated from 7Li count rates. All other concentrations from [2]. WR = whole rock data determined by multi-collector ICP-MS at Bristol (Marschall et al., in prep.).

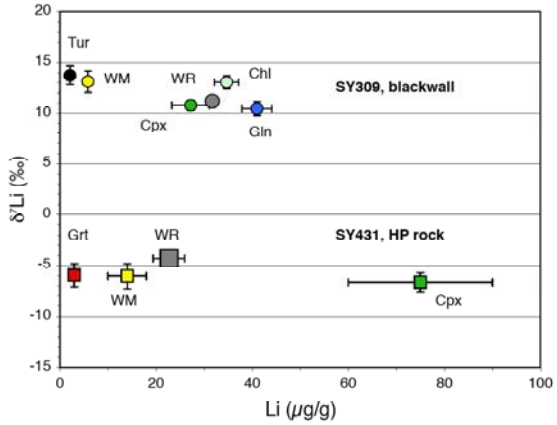

Figure 1. Li isotopic composition versus Li concentrations of Li host minerals of investigated high-pressure metamorphic block (SY431) and blackwall schist (SY309B). Whole rock (WR, grey) MC-ICP-MS analyses are in good agreement with the isotopic composition of the minerals determined by SIMS.

References

[1] H.R. Marschall, T. Elliott & R. Abell, Suppl Iss Geochim. Cosmochim. Acta (2006) A16.

[2] H.R. Marschall, R. Altherr, T. Ludwig, A. Kalt, K. Gméling, Kasztovszky, Geochim. Cosmochim. Acta (2006) 70: 4750

4769

Importance of burial diagenesis in carbonates and causes of carbonate diagenesis: Evidence from stable oxygen isotope composition of Upper Silurian carbonates, Palaeozoic Baltic Basin, Lithuania

N. Molenaar[1], G. Bičkauskas[2] & J. Craven[3]

[1]Institute of Environment & Resources, Technical University of Denmark Bygningstorvet, Building 115, DK-2800 Kgs. Lyngby, Denmark
[2]Department of Geology and Mineralogy, Vilnius University K.M. Čiurlionio 21/27, LT-03101 Vilnius, Lithuania
[3]Ion Microprobe Unit, School of Geosciences, Edinburgh University, Edinburgh EH9 3JW, UK

The use of stable oxygen isotope compositional data in sedimentary geology is very common in particular in diagenetic studies of carbonates. In fact, such data are considered as essential for understanding environmental conditions during cementation. Usually analyses are done by standard mass spectrometry on whole rock samples or samples of more specific portions of the rock obtained by microdrilling. This study uses the SIMS technique to measure the stable oxygen isotope composition of a number of specified components in Silurian ramp carbonates from the Palaeozoic Baltic Basin. Components measured are skeletal material (including brachiopod and ostracod shells that are composed of stable low-Mg calcite; trilobite carapaces and stromatoporoidal remains both of uncertain original mineralogy) and diagenetic material (replaced early cements and late low-Mg calcite cement). The numerical results are used to support the hypothesis that carbonate diagenetic systems are essentially closed, and used as evidence for the importance of burial diagenesis as opposite to surface related diagenesis in carbonates. The Upper Silurian was chosen for detailed analyses because it is a ramp carbonate system unaffected by larger scale tectonic activity causing deformation of uplifted terrains that could form hydraulic head during some stage of the geological history. Moreover a good stratigraphic control was established, and based upon the availability of organic matter maturation data a reliable burial history model could be constructed during the study.

Despite of the belief that such data is essential, the interpretation of oxygen isotope compositions is difficult and often equivocal. This is partly the result of the unspecific nature of most of the sample material used for analyses, merely representing a combination of a multitude of depositional and diagenetic components and their successive environments of origin, and partly because oxygen isotope fractionation is temperature dependent. Both the isotopic composition of the pore water from which diagenetic components precipitated and the temperature are unknown parameters or only know with considerable uncertainty. Although meteoric water influx or mixing of meteoric and marine pore water are still considered as the main triggers and causes of carbonate diagenesis, it has become evident that much of the diagenesis takes place under burial conditions out of reach in infiltrating surface water. The mechanisms for such infiltration are often inadequately explained in existing studies. The conditions during formation of the diagenetic carbonate components are basically unknown and need to be understood before the controls on main diagenetic processes influencing important petrophysical properties such as porosity and permeability can become clear.

A further complication is that seawater composition is known to have varied during the Phanerozoic. This secular change is still under debate. For instance some mass calculations based upon seawater circulation and submarine weathering of fresh basalt suggest equilibrium conditions. Since short evidence is amounting that the rate of sea floor spreading (plate tectonic activity) is indeed variable (e.g., Conrad and Lithgow-Bertelli, 2007) and there is no bases for supposing equilibrium oxygen isotope sea water composition. Base upon several types of evidence, sea water composition in the Palaeozoic had a negative $\delta 18O$. Many studies on carbonate diagenesis do not consider these secular changes and therefore still

suggest meteoric water as trigger for diagenesis in carbonates based upon negative $\delta^{18}O$ (PDB) of carbonate cements. This would suggest that diagenesis in carbonates is taking place in essentially open systems with unknown mass import or export. This would be devastating for any attempt to predict porosity of carbonate reservoirs based upon basin history and development of reservoir conditions. If the system is merely open and related to largely unpredictable meteoric water influx no prediction could be made.

The Silurian carbonates used in the present study are a good target for critical assessment of the paradigms of carbonate diagenesis. The carbonate is a ramp system, as probably most early Palaeozoic carbonate systems since fauna capable of forming frameworks and thus reef barriers and platforms do not exist at that time. The carbonate contains a number of skeletal components, mainly of crinoids, bryozoans and stromatoporoids that formed the main non-photic carbonate factory. It is cemented in two phases by calcite and minor dolomite cement. Brachiopod and ostracod shells, both originally composed of stable low-Mg calcite and thus considered to be stable even during extended burial diagenesis, could be a good indicator of original seawater composition, if biological fractionation (the vital effect) is known. Thin section studies showed that most brachiopod shells indeed appear pristine and still showing original two layer shells and their internal textures. Additional CL studies showed that most brachiopod shells are non luminescent that is a criterion for having retained the original mineralogy. However, outer parts of the shells are often replaced or include luminescent laminae that cannot be avoided when analyzing whole shells or by microdrilling sampling methods. Only SIMS microspot analyses can avoid such diagenetic contaminations. Extensive electron microprobe work with analyses of main element contents of shells, showed low Fe and Mn contents that fall well within the ranges of unaltered, non-replaced original mineralogy. This confirms the CL and textural observations.

The aim of this part of the study is to use detailed oxygen isotope analyses of specifically targeted cement phases and bioclastic material that negative oxygen isotope values do not necessary indicate meteoric water. The original seawater composition was negative during most of the Palaeozoic. Measured $\delta^{18}O$ values of brachiopods and ostracod shells indeed confirm this: Brachiopod $\delta^{18}O$ (SMOW) 23.73‰ ± 1.36 (range = 20.86-26.04; N=58); Ostracod $\delta^{18}O$ (SMOW) 23.78‰ ± 0.55 (range = 22.94-24.79; N=23). The brachiopod data clearly point to an oxygen isotopic composition of ocean water several per mille more negative than the present day. The spread in the date also suggest appreciable vital effects.

Late calcite cement has average $\delta^{18}O$ (SMOW) 23.21‰ ± 1.06 (range = 18.77 – 25.26; N=122).These SIMS analyses results would according to standard practices be explained as indicating precipitation of calcite cement from meteoric water. However, taking the secular changes into account, the comparison between the brachiopod oxygen isotope composition, that is a proxy for the original Silurian seawater composition albeit lightly modified through vital effects, and the cement compositions indicate that calcite cement precipitated during burial under slightly elevated temperatures from buried marine water. This is confirmed by burial history modelling of the succession and the paragenetic succession of textural relationships between the various primary and diagenetic components. For instance, intergranular volumes indicate that mechanical compaction did reduce the primary intergranular porosity before late calcite cement was introduced.

Volatiles in magmas inferred from Ion-Probe analysis of glass inclusions in equilibrium phases.

N. Oskarsson

Institute of Earth Sciences, University of Iceland, Sturlugata 7, 101 Reykjavik. Iceland.

Significance of silicate inclusions

Silicate inclusions in rock-forming minerals of volcanic rocks are of different origin ranging from segregated impurities in phenocrysts or xenocrysts to pristine volcanic glasses occluded during rapid growth of equilibrium phases. During slow cooling, pristine magmatic inclusions may crystallize on the surface of the confining host minerals leaving residual glasses that are more evolved that the original magma. In order to eliminate corrections for post-eruptive crystallization, the present study is focused on rapidly cooled glass inclusions in minerals from volcanic ash and pillow rims.

Silicate glass inclusions in equilibrium minerals of volcanic rocks are assumed to be the only available samples where the pre-eruptive volatile-content of magmas is preserved.

Importance of magmatic volatiles

Four large disciplines of volatile studies can be resolved:

1) Effects of volatiles on magmatic equilibria. Petrochemical modelling has reached an advanced state where the effects of dissolved water on liqudus temperatures and viscosity can be accounted for. Equilibrium modelling based on analysed water content of magma gives the most realistic outline of magmatic properties during evolution and ascent.

2) Effects of volcanic gases on eruption mechanism. Viscosity of silica saturated magmas largely depends on their water content. Dissolved water that dissociates in solution has a depolymerization effect on the silica chains of the magma. Eruption behaviour, both in explosive and effusive volcanism that can be related to viscosity therefore also depends on the pre-eruptive water content and the degassing behaviour of water.

3) Contribution of volcanic gases on the composition of the atmosphere. Quantification of volcanic gas-flux to the atmosphere can only be made based on inclusion analysis and remote sensing of volcanic plumes. Considering the recent invention of remote sensing of volcanic gases it will take at least few centuries to yield sensible long term averages of volcanic pollution by remote sensing. It has to be concluded that potential atmospheric pollution from all known kinds of volcanic eruption can only be predicted by analysing the volatiles preserved in glass inclusions.

4) Origin of volcanic hazard imposed by toxic gases and condensed material. Fluorosis in grazing animals and acid damages on vegetation is a persistent threat in many volcanic areas. Understanding of the degassing behaviour of the halogens and sulphur during solidification of different magmas is essential for estimation of potential pollution disasters in volcanic areas.

It is evident that although considerable understanding of these processes and phenomena has been achieved by classical geochemical and volcanological methods, the quantification of fluorine in magmatic systems can only be made by volatile analysis of un-degassed glass inclusions.

The role of the Ion-Probe

Analysis of chemical components of glass inclusions in minerals are made with various micro-beam techniques. The Ion-Probe method is unique in this context since there is no other analytical technique that permits simultaneous quantification of water, carbon dioxide and fluorine that can be directly normalized to silicate composition by simultaneous analysis of a lithophile component such as titanium. Other techniques such as electron microprobe analysis

can be used for analysis of heavier elements such a chlorine and sulphur. The present project uses this approach; Electron-microprobe analysis of glass inclusions are used for screening of target material that subsequently is analysed with both techniques.

During three sessions at the Ion-Probe facility in Edinburgh a considerable set of data has been acquired. These data are being used for addressing research questions within the following themes: 1) Water content of basaltic andesite magmas that forms the basis for equilibrium modelling (temperature, pressure) and sets constraints on the viscosity relations of magmas before and during degassing in the eruptive vent. Results based on one of these studies are already published [1] and Papers on the volatile content of subalkaline rhyolite and tholeiitic basalts are in preparation. 2) Degassing mechanism of fluorine from baslatic andesite as exemplified by the 2000 Hekla (S-Iceland) eruption. Soluble fluorides adhering to the volcanic ash from this volcano cause severe toxic effects (fluorosis) in grazing animals. Preliminary results based on Ion-Probe analysis of fluorine and water indicate that the anomalous fluorine-degassing of the basaltic andesite is caused by the instantaneous, almost complete, crystallization of the magma upon water loss that favours supersaturation of the rock-forming minerals. 3) Fractionation of volatiles during degassing of alkali-olivine basalt. Analysis of volcanic gas that was collected during the Surtsey 1963-1967 eruption (S-Iceland) is compared with the volatile content of glass inclusions form the volcanic ash produced in the eruption. Preliminary results, based on water and carbon dioxide Ion-Probe analysis, indicate that the volcanic gas was significantly enriched in water and the carbon gases. These results impose serious doubts on the use of volcanic gas analysis for estimating the juvenile gas composition of magmas.

References

[1] Höskuldsson, A., Oskarsson N., Pedersen, R., Grönvold, K., Vogfjord, K., and Ólafsdottir, R., The millennium eruption of Hekla in February 2000, Bull. Volc. 2007 (In Press).

Control of magmatic and degassing dynamics on the volcanic activity at Volcán de Colima, Mexico: insight from trace element, H_2O and CO_2 contents of melt inclusions.

O. Reubi & J. Blundy

Earth Sciences, University of Bristol, Bristol, BS81RJ, UK

Linking the magmatic processes occurring in the upper crust below active volcanoes and surface monitoring data, such as ground deformation, seismicity and gas flux recoded prior to eruptions is fundamental to understand the behaviour of volcanoes. Establishing this link is a major step toward quantitatively interpreting the monitoring record and ultimately creating models capable of predicting the style and intensity of future eruptions. In order to address this elusive link, the petrology of the products of the current eruption (1998-2005) at Volcán de Colima, Mexico are investigated in detail and compared with the surface monitoring data for the same period. Melt inclusions hosted in phenocrysts play a central role in this study, as they provide a mean to constrain the evolution of magmas and the exsolution of volatiles during ascent in the subvolcanic magmatic system and may therefore be correlated with changes observed at the surface prior and during the eruption. Melt inclusions have been analysed by EMPA (@University of Bristol) for major elements and SIMS (@NERC, Edinburgh) for H_2O, CO_2 and trace elements. Preliminary results show that:

(I) A key finding of this work is that melt inclusions are significantly more silicic (65 to 74 wt% SiO_2), than any of the whole rock compositions of historical magmas analysed to date (59 to 61 wt% SiO_2) (Fig. 1A). The chemistry of melt inclusions and of phenocrysts show that despite the andesitic bulk composition, the magma crystallising in the feeding system is a dacitic melt that contains entrained gabbroic fragments. This paradoxal absence of andesitic melt has been observed for several other arc volcanoes and is likely to represent a fundamental characteristic of arc magmatism.

(II) On the basis of their K_2O and trace elements at a given SiO_2 content, melt inclusions can be divided in two groups (Fig. 1A, B). Inclusions from the high-K group are also characterized by higher Rb, Cs, Cl and to some extent Ba and lower Sr and H_2O compared to the low-K group. Both groups have similar contents of all other incompatible elements. Glass inclusions from the low-K group show a trend consistent with crystallization of the phenocryst assemblage observed in the magmas. H_2O (<2.5 wt%) and CO_2 (<360 ppm) contents indicate crystallization at P_{total} between 900 and 0 bars (<7 km in depth) (Fig. 1C). Groundmass glasses form the linear prolongation of this trend, indicating that they represent the ultimate products of this low pressure fractionation. The high-K melt inclusions have exotic compositions compared to the whole rock and groundmass glasses compositions. Their compositions are best explained by grain boundary melting of phenocryst assemblage comprising biotite, a process also supported by textural evidences. These low-K melt inclusions consequently provide evidences for significant melting and remobilisation of highly crystallized portion of the magmatic system, a process easily overlooked on the basis of phenocrysts compositions and textures.

(III) Seismic swarms prior to the 1998 eruption were evenly distributed between 0 and 7 km in depth and became shallower with time [1]. Volatiles in the melt inclusions (low-K group) of the 1998 lava flow indicate crystallization in a volatile saturated system over a range of pressure corresponding to 0-7 km in depth. The strong correlation between the seismic and melt inclusion records suggests that the former record the ascent, degassing and crystallisation of a partially crystallized magma column that initially extend to the pressure of volatile saturation of the melt.

(IV) Preliminary investigations of temporal variations of the petrology and monitoring data since 1998 suggests a correlation between melt inclusion volatile content, the SO_2 flux recorded by COSPEC at the surface [2], and depth of seismic swarms [1]. Overall, this suggests that the

eruption is fed by a ≤7 km deep column of volatile saturated, crystallising dacitic magma. The maximum depth of tapping varies throughout the eruption. It reached a minimum in 2001, when degassed and viscous magmas formed an unusual (for Colima) spine. Major vulcanian explosive events correspond to periods of maximum depth of tapping but do not exceed the depth of preceding effusive events, indicating that ascent rate is a more important parameter than maximum volatile content in controlling the transition between explosive and effusive activity.

In conclusion, the work undertaken on Volcán de Colima melt inclusions at the NERC ionprobe facility has provided extremely valuable information regarding the magmatic evolution and the degassing path of the magmas prior and during the eruption, hence greatly improving our understanding of the behaviour of the feeding system of this threatening volcano. Most importantly this work shows that there is a correlation between the data monitored at the surface of active volcanoes and the subsurface record provided by melt inclusions, which as great implications in terms of understanding the behaviour of arc magmatic system and improving the monitoring strategy. We are currently investigating, in collaboration with Dr. N. Varley (University of Colima, Mexico), this link in more detail, with a particular emphasis on the correlation between the degassing path recorded by the melt inclusions and the chemistry of fumaroles.

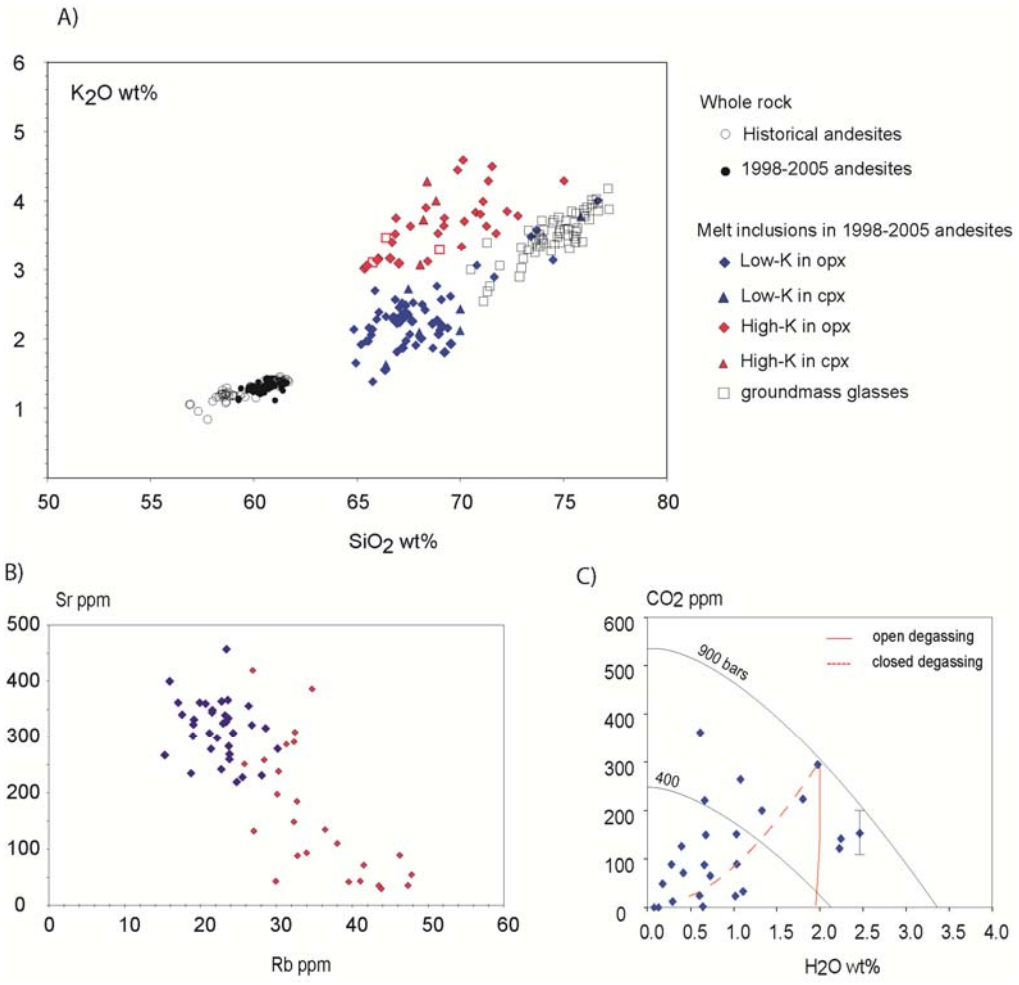

Figure 1. Chemical variations in melt inclusions, groundmass glasses and whole rocks. Colour coding is the same in all plots. The high-K melt inclusions have very low volatile contents and are not plotted

in C). Note that H_2O and CO_2 of melt inclusions are not consistent with simple degassing trends and indicate fluxing by CO_2 rich gas.

References

[1] Zobin et al., 2002, . Volcanol. Geotherm. Res., 117, 47-60.
[2] Varley & Taran, 2003, Geol. Soc. Lond. Spec. Publ. 213, 263-280.

The role of organic pollutants in the alteration of historic soda silicate glasses

L. Robinet1, 2, C. Hall[1], K. Eremin[3], S. Fearn[4]

[1]The University of Edinburgh, Centre for Materials Science and Engineering, Edinburgh, EH9 3JL, UK
[2]Laboratoire de Dynamique Interactions et Réactivité, CNRS, 94320 Thiais, France
[3]Harvard University Art Museums, 32 Quincy Street, Cambridge, MA 02138, USA
[4]Department of Materials, Imperial College, London, SW7 2AZ, UK

The glass collections in the National Museums of Scotland (NMS) were affected by the organic pollutants (acetic acid, formic acid and formaldehyde) emitted by the materials of the showcase and storage cupboards in which they were stored. The alteration resulted in the formation of crystalline deposits at the surface and modification of the chemical structure of the glass. A PhD project investigated the role of these pollutants in the alteration of these historic soda silicate glasses. Secondary Ion Mass Spectrometry (SIMS) was used to follow the elemental variations as a function of depth on replica glasses aged in ambient conditions.

Bouteille à décanter
britannique (copyright NMS)

The previous SIMS analyses indicated that volatile organic acids greatly enhance the alteration compared to a non-polluted atmopshere. The analyses carried out in 2006 were the final ones and were used to determine the kinetics of the alteration in polluted and non polluted atmospheres. The PhD research was completed in July 2006 and can be accessed online at http://hdl.handle.net/1842/1475

Experimental

Replicas of historic soda silicate glass were aged in ambient conditions within two series of experiments carried out in parallel over 13 months :

- A first series of fragments was exposed in glass desiccators to atmospheres polluted with either formic acid or formaldehyde and to non-polluted atmospheres with either N_2 or ambient air. The temperature was regulated to 19 ºC and the RH to 48 %.
- A second series of fragments was exposed to the polluted atmosphere of two storage cupboards in the NMS (cellars 3 and 12) which emitted high concentration of pollutants. The conditions in cellar 3 were around 23 ºC and 40-45 % RH compared to 20-22 ºC and 43-53 % RH in cellar 12.

For each series, a glass fragment was taken out approximately every 4 weeks in the first 7 months, then at longer time intervals in the following 6 months and were then analysed by SIMS.

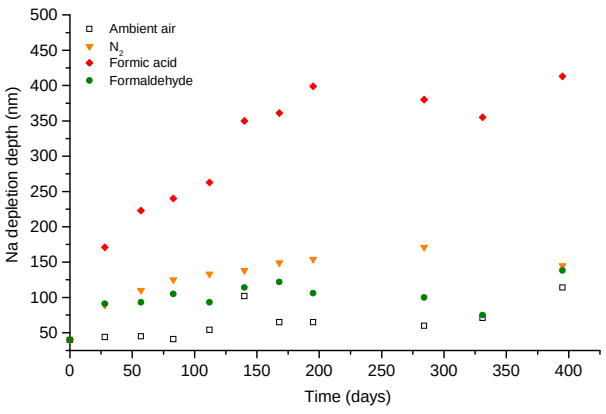

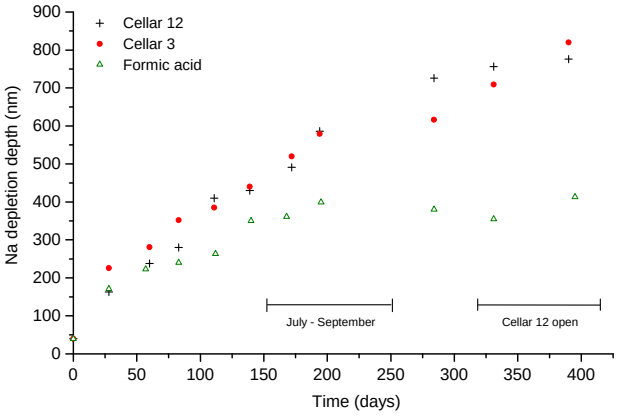

Figure 1. Sodium depletion variation with time over 13 months in N_2, ambient air, formic acid and formaldehyde polluted atmospheres (left) and in cellar 3 and cellar 12 atmospheres (right).

Results

During the exposure time, only alkali ions in the glass were affected by a leaching reaction, causing the formation of hydrated and alkali-depleted layers. The progress of the glass alteration in each atmosphere was followed by plotting the sodium alteration depth as a function of time (Figure 1).

This graph confirmed that the alteration of the glasses is greatly accelerated by the presence of acidic pollutant compared to formaldehyde, ambient air or N_2 atmospheres. The progress of the alteration in formaldehyde atmosphere followed that of the N_2 atmosphere in the first 6 months and then that of the ambient air atmosphere, which was consistent with the visual observations. Thus, contrary to general belief formaldehyde is not the culprit of the alteration of glass exposed to organic polluted atmosphere.

The progress of the alteration (Figure 1) and the chemistry of the altered layer (not shown) of the glasses exposed to the cellars are similar to that in formic acid atmosphere. Acid pollutants not only increase the depth of the alteration, but they also increase the amount of sodium extracted from the altered layer. Therefore, the composition of the glass altered layer formed in acid polluted atmospheres has a sodium concentration ~1 at%, compared to ~5 at% in non-acidic atmospheres. This result is consistent with the composition of the altered layer on the glass objects from the NMS. Moreover, the research indicated that there is competition between the different pollutants possibly due to the difference in their acid-ionisation constants. Thus, in mixed polluted atmospheres, whatever the pollutant proportions, the pollutant with the highest acid-ionisation constant, in this case formic acid, will always predominate in the water film and the crystalline deposits will hence consist mainly of formates. This phenomenon explains the dominance of formates on the NMS glasses in atmospheres where acetic acid predominates.

In addition, the research revealed that the fluctuations in RH and temperature (as recorded in many museum storage or display environments) affected the progress of the alteration, as evidenced by the discontinuities observed in the graph. These fluctuations caused a re-activation of the alkali leaching reaction, which aggravates the glass alteration. Based on the experimental data obtained in this study, it was possible to estimate that a glass with a similar unstable composition would develop an altered layer with a thickness of 30 μm in 40 years if exposed to an organic polluted environment in a museum. These values are consistent with the estimated exposure of the NMS objects to these polluted environments.

The research presents experimental evidence that organic acid pollutants have a dramatic effect on the alteration of unstable soda silicate glasses, and are responsible for the widespread alteration of part of the NMS glass collection. Therefore storage of unstable glasses in wooden cabinets or showcases emitting organic pollutants must be avoided.

Biology of boron isotopes in planktic foraminifers: new understanding based on *in-situ* analysis (SIMS)

D. N. Schmidt[1]

[1]Department of Earth Science, University of Bristol, Bristol UK

Confidential

CO_2 contents of phonolitic melt inclusions from the 472 AD 'Pollena' subplinian eruption of Mt Somma-Vesuvius

J.A. Small & C.J. Hawkesworth

Department of Earth Sciences, University of Bristol, Bristol BS8 1RJ, UK

This one-day project was part of a larger investigation of the role of pre-eruptive dissolved volatile contents in influencing variable explosivity of volcanism at Mt Sommma-Vesuvius. Previously, we measured H_2O concentrations by SIMS in ~ 100 melt inclusions (MI) from two contrasting explosive events in the history of the volcano: the subplinian 'Pollena' eruption of 472 AD and the Plinian 'Avellino' eruption of ~ 3.55 kaBP. The combination of these data with EPMA measurements of Cl, F and S show systematic differences in the pre-eruptive volatile contents of magmas feeding these two eruptions, with Pollena MI having lower maximum H_2O contents and higher Cl contents than their Avellino counterparts. Previous FTIR-based MI studies on Plinian and strombolian-effusive 'interplinian' activities, reported high CO_2 (~ 1500 – 4500 ppm) and S (up to ~ 3000 ppm) contents in relatively mafic MI within olivine and diopside, and concentrations of both routinely below detection limits (< 50 ppm CO_2; < 250 ppm S) in more evolved phonolitic MI in phases such as sanidine, salite, amphibole and leucite. Our study focuses primarily on the most evolved melt compositions in MI from the first erupted basal fall layers, and while previous studies had confirmed low CO_2 contents in similar MI compositions from the Avellino eruption, no such data were published for the Pollena eruption at the time our study was undertaken. In terms of inferring magma storage conditions, it is critical to establish whether the Pollena MI have lower H_2O contents primarily because of a) reduced solubility at shallower storage depths, or b) reduced solubility at similar depth because of the presence of significant CO_2 as a dilutant in the fluid phase. The availability of an improved set of CO_2-standards enabled us to conduct a *preliminary* investigation and measure CO_2 concentrations by SIMS in 17 carefully selected MI from Pollena and one from Avellino.

The CO_2 concentrations in phonolitic Pollena MI, within sanidine, nepheline, leucite and davyne, ranged from ~ 400 – 2600 ppm. The two nepheline-hosted MI have the highest *total* volatile contents (~ 3.6 wt% H_2O, ~ 1800 ppm CO_2), while davyne-hosted MI contained relatively low H_2O (1.7 – 2 wt%) and the highest CO_2 (~ 1000 – 2600 ppm). Sanidine-hosted MI ranged from 2.9 – 3.4 wt% H_2O and 400 – 1100 ppm CO_2. The one Avellino MI (phonolitic, sanidine-hosted) contained significantly lower CO_2 (~ 170 ppm) and higher H_2O (~ 5 wt%) than those from Pollena. These results are somewhat intriguing, since a) the Pollena MI in question have highly evolved phonolitic bulk compositions and low sulphur contents analogous to their Avellino and Pompeii (AD 79) counterparts, which previous studies have shown to contain negligible CO_2, and b) a very recent study [1] reports CO_2 concentrations below the detection limits of FTIR in Pollena MI with more or less identical bulk compositions but generally higher H_2O contents (up to 5.7 wt%) than those we report here. The possibility remains that there may be some systematic discrepancy due to the two very different sample preparation and analytical approaches (SIMS vs FTIR). However, we can rule out some of the most obvious potential problems as being the source of this rather dramatic difference, e.g. high background carbon count rates, and the possibility of contaminated analyses due to residual carbon coat adhering to MI surfaces. Assuming therefore that these CO_2 measurements for Pollena MI are robust, the implications are twofold: 1) $P[H_2O + CO_2]$ *may* be as high as ~ 300 MPa in the case of the most volatile rich nepheline hosted MI, which is significantly higher than the storage pressures of Pollena phonolite melts (~ 100MPa) inferred by Marianelli *et al* and also Scaillet & Pichavant (in prep.) on the basis of experimental phase equilibria; 2) some of these MI and their host crystals may record a secondary 'contaminated' enrichment of CO_2 derived from decarbonation reactions at the magma-host rock interface. These preliminary data are tantalising and certainly require further interpretation, but are insufficient alone to make a

detailed and robust assessment of the role of CO_2 prior to the Pollena eruption. They do, however, suggest that the picture is somewhat different for this anomalous subplinian eruption compared to that for the two Plinian eruptions Avellino and Pompeii.

References

[1] P. Fulignati & P. Marianelli, JVGR. Accepted (2007).

Trace element and volatile compositions of melt inclusions from the 10.5 ka Upper Toluca Pumice, Nevado de Toluca, Mexico: insights into magmatic processes

V.C. Smith[1], J. Blundy[1] & J.L. Arce[2]

[1]Department of Earth Sciences, University of Bristol, Wills Memorial Building, Bristol BS8 1RJ, UK
[2]Instituto de Geologia, UNAM Cd. Universitaria, Coyoacan, Mexico

Introduction

The aim of this study is to establish what magmatic processes triggered the large dacitic 10.5 ka Upper Toluca Pumice (UTP) eruption, and gain more of an understanding of the magmatic systems that feed dacitic volcanoes. We have used the invaluable record provided by the crystals and their trapped melt inclusions (MI) to decipher these magmatic processes. So far, whole-rocks, phenocrysts, matrix glass and MI have been analysed and we have gained information on processes such as crystallisation, degassing, recharge, ascent, and eruption triggering. This understanding of the pre-eruption processes and their timescales is imperative for hazard planning and monitoring of volcanoes.

Approach

Samples were collected from each eruptive unit stratigraphically through a thick sequence of the UTP deposits close to vent. Plagioclase-hosted MI and matrix glasses of each eruptive unit have been analysed using the 4f-ionprobe at the NERC IMF, and the electron microprobe at the University of Bristol. Eighty plagioclase-hosted melt inclusions have been analysed for volatile and light elements (H_2O, CO_2, Li, Be, and B) and 48 of these have also been analysed for a range of heavier trace elements (see Appendix).

Preliminary results

Matrix glass and MI compositions are generally rhyodacitic and range between 71.5-75.5 wt.% SiO_2, 0.9-2.8 wt.% CaO, 3-281 ppm Sr, 27-79 ppm Rb, and 312-765 ppm Ba. However, some of the shards from pumice clasts, mostly in the upper sequence, are more mafic (54.0-66.7 wt.% SiO_2; Fig. 1). The compositional range of these analyses most likely record the mixing of a more mafic melt with the dominant dacitic magma. Further evidence for the mafic input are: (1) the mafic ~60 wt% SiO_2 whole-rock compositions of some pumices in the upper sequence than those erupted earlier (62.6-65.0 SiO_2); (2) calcic rims ($An_{>45}$) of some late erupted plagioclases (cores $An_{<40}$); and (3) slightly higher (~15°C) average Fe-Ti oxide temperatures of late deposits (880°C).

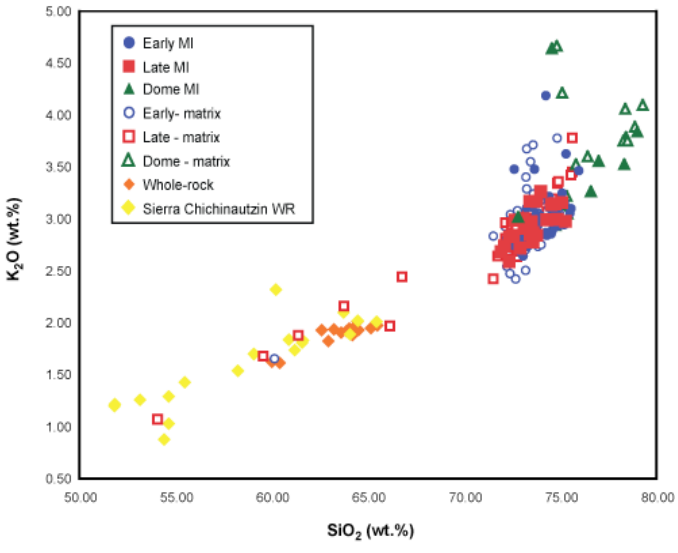

Figure 1. MI, matrix glass, and whole-rock compositions of UTP deposits. Whole rock analyses of the more mafic Sierra Chichinautzin deposits [1], located just to the east of Nevado de Toluca, are also plotted. The least evolved UTP matrix glass compositions plot with the mafic Sierra Chichinautzin samples, suggesting a common source. The most evolved dome compositions correspond to higher crystal contents.

MI data indicate that the magma was extremely H_2O rich, up to 7.5 wt%. Other volatiles were much lower in abundance, CO_2 <1300 ppm, SO_2 <900 ppm, F <4000 ppm, and Cl 200-1600 ppm. Gas saturation pressures of up to 380 MPa were estimated suggesting the magma crystallised over a wide range of depths (≤9 km). Crystallisation appears to be in response to decompression. H_2O and CO_2 concentrations throughout the eruptive sequence are variable (Fig. 2) and do not follow typical open or closed system degassing paths. This considerable variation in XH_2O/XCO_2 is consistent with gas fluxing [2]. We suggest that the analyses with high XCO_2 (~50 mol.%) record the gas influx from a deeper CO_2-rich magma. It is likely that this is volatile transfer from the mafic melt, which mixed with the dacite magma during the eruption.

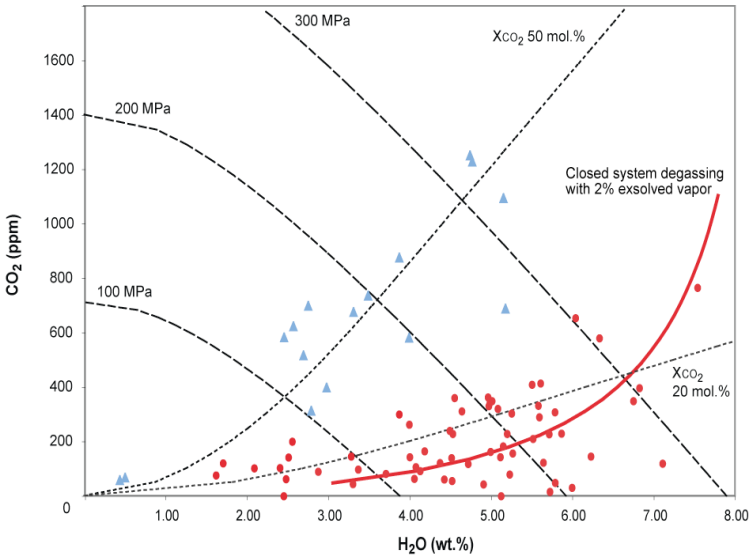

Figure 2. H_2O and CO_2 of MI. Analyses in red (circles) appear to follow a closed system degassing path. Those in blue (triangles) are melt that appears to have been fluxed with CO_2 from a deeper magma prior to being trapped. Isobars, degassing path, and XCO_2 isopleths were calculated using [3].

Although most evidence for a mafic input is late in the eruption sequence there is considerable variation in composition, temperature and pressure throughout the eruption sequence. It suggests that the eruption did not sequentially tap the magma system from the top to the base and the eruption violently evacuated magma from all levels in the system almost simultaneously.

Further work

We plan to do trace-element profiles across zoned phenocrysts on the 4f-ionprobe in late June 2007. We will then fit the profiles to those of diffusion (which will be determined using published diffusion coefficients) to constrain the timing of the mafic influx and obtain rates of magma ascent.

References

[1] A. Marquez & C. De Ignacio, Lithos 62 (2002) 35-62.
[2] P. Wallace, JVGR 140 (2005) 217-240.
[3] S. Newman & J.B. Lowenstern. Computers Geosci. 28 (2002) 597-604.

Li isotope composition of primitive mantle-derived olivine

F.M. Stuart and S. Basu

Isotope Geosciences Unit, Scottish Universities Environmental Research Centre, East Kilbride G75 0QF, UK

Introduction

Olivine phenocrysts from picrites from Baffin Island have the highest magmatic $^{3}He/^{4}He$ recorded [1], supporting an origin in an undegassed mantle reservoir [1]. From initial ion probe data collected in 2005, it was evident that the Li isotope composition of the olivine is highly modified and determining the primordial source composition is not straight forward [2]. In an attempt to determine the cause of the isotope variation and to investigate if the magmatic composition can be retained in the crystal cores, $\delta^{7}Li$ and Li concentration ([Li]) profiles were determined in eight olivine crystals of variable diameters (500 to 3000 μm) and shapes from samples that span the $^{3}He/^{4}He$ compositional range in the region (PI26 (4 crystals), PI25 (2) and DI23 (2)). To check for consistency, three profiles have been taken on a single crystal from PI26 and two on one crystal from PI25.

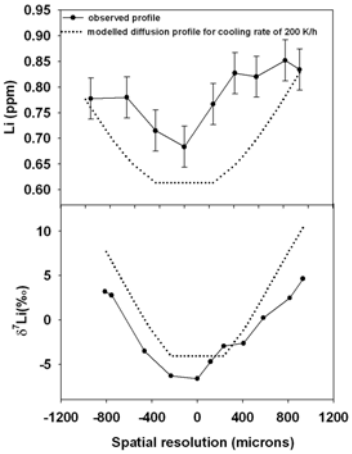

Figure 1. V-shaped Li isotopic profile with increase in [Li] from core to rim. The data can be explained by diffusion at a cooling rate of 200°K/hour

Results

Across-grain $\delta^{7}Li$ profiles vary from flat, to v- and w-shaped, while [Li] profiles are mostly homogeneous, and v-shaped only in 3 case(s) (Figures 1-2). The $\delta^{7}Li$ ranges from -8.33 ± 1.22 to 19.33 ± 2.92 ‰. Even the average $\delta^{7}Li$ for crystals from the same sample show considerable ranges (e.g -0.47 to 12.70 ‰ in PI26). [Li] varies between from 0.68 ± 0.04 to 1.70 ± 0.09 ppm. Within-grain $\delta^{7}Li$ variation is up to 16‰ while for [Li], it is up to 1.7 ppm.

Discussion

All samples have phenocrysts of forsteritic olivine (MgO ≈ 50 %) embedded in a groundmass of pyroxene, plagioclase and Fe-rich olivine. The phenocryst-olivines are typically zoned with Fe- and Ca-rich rims that are depleted Cr and Ni. This indicates late-stage re-equilibration with melt at about 1800°C.

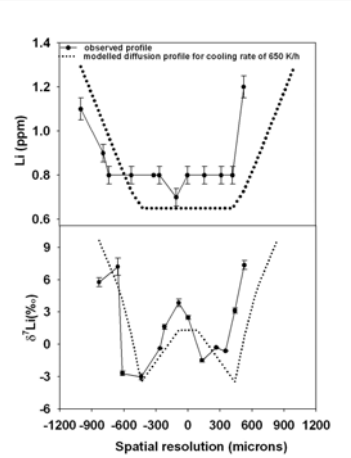

Figure 2. W-shaped Li isotopic profile with increase in [Li] from core to rim. The profiles can be explained by cooling at 650°K/h.

It is important to determine the process that can account for the variation of $\delta^{7}Li$ and [Li]. The absence of correlations between $\delta^{7}Li$ and [Li] (or 1/[Li]), and other elements such as Fe, Mg, Ca, Mn, Ni, Cr, allows us to rule out magmatic processes such as assimilation, fractional crystallization, degassing and post magmatic alteration as a source of the Li isotope variation.

The likeliest source of the observed variation is diffusion. Partition coefficients of Li ($K_D^{Li} = 0.2 - 0.3$) [3], for olivines and pyroxenes indicate that early-formed phenocrysts are embedded in a relatively Li-rich groundmass. As the melt cools below the solidus, and Li becomes less incompatible, it will diffuse into olivine from the groundmass. Because of the relatively large mass difference (15 %) between ^{7}Li and ^{6}Li, they will diffuse in significant different rates. The ratio of their diffusion coefficients $(D_7/D_6) = (m_6/m_7)^{\beta} = 0.9674$ where β is an empirical parameter with value close to 0.215 [4]. As ^{6}Li diffuses in preferentially, $\delta^{7}Li$ progressively becomes more depleted accounting for the v-shaped profile. However, for larger crystals, the core maybe relatively less affected leading to the w profiles.

A similar process has been suggested to explain δ^7Li variation in pyroxene and olivine from meteorites [5,6].

The Li diffusion profiles are strongly governed by the rate of cooling. We have attempted to model the effect of diffusion on both [Li] and δ^7Li with different rates of cooling from the solidus (1200°C) to a final temperature of 600°C. By comparing the modelled and the measured profiles, the rate of cooling can be estimated. Here we illustrate our point with v-shaped (PI26-G5) and w-shaped profiles (DI25-G4) that both show a core-to-rim increase in [Li]. Models were computed by solving the diffusion equation for spherical geometry which approximates the olivine grains:

$$\frac{dC}{dt} = D\left(\frac{d^2C}{dr^2} + \frac{2}{r}\frac{dC}{dr}\right) \quad (1)$$

$$\text{Or } \frac{C_s - C}{C_s - C_0} = \frac{2a}{\pi r}\sin\left(\frac{\pi r}{a}\right)\exp\left(\frac{-\pi^2 Dt}{a^2}\right) \quad (2)$$

Where C_0 is the initial Li concentration, C_s is the Li concentration of the groundmass and C is the concentration at a point whose distance *r* from the centre of a grain size 2*a*, at time *t*. Following [5], we assume that the highest [Li] and δ^7Li measured at the rims reflect the groundmass composition, while the initial conditions correspond to the lowest [Li] and the highest δ^7Li from the core of a w-profile. In the absence of available diffusion coefficient (D) for olivines, we used $D_0 = 0.029$ m^2/s and $E_a = 258$ kJ as in pyroxenes [7]. The Li isotopic composition can be estimated by solving the equation simultaneously for ^{7}Li and ^{6}Li. Preliminary modelling gives fast cooling rates; 200-650°K/h (Figure 1 and 2).

Similarly high cooling rates (650-1000°K/h) have been estimated for high Fo-olivine phenocrysts based on Fe-Mg diffusion in inclusions [8], in agreement with results of modelling the crystallisation of primitive magmas [9]. A better estimate of cooling rate awaits determination of D_0 for Li in olivine, although Li isotope profiles in minerals from mafic magmas and peridotites suggest that diffusion rates in pyroxene and olivine are similar [10].

Obviously the whole-grain Li isotopic composition of olivines is unlikely to represent the true magmatic value. Also, as the groundmass loses Li it evolves to isotopically heavier composition than the original magmatic value. However, such fast cooling rates may leave the δ^7Li of the cores of large olivine grains with w-shaped profile that are close to the initial composition. The range of core δ^7Li from w-profiles values (+2 to +12 ‰) for the Baffin Island picrites spans nearly the range of values measured in oceanic basalts [11,12,13] so does not appear to provide a particularly strong constraint whether the Li originates from a primordial source.

References

[1] F.M. Stuart et al., Nature 424 (2003) 57-59.
[2] Ion Microprobe Facility, annual report (2005).
[3] Zanetti et al Lithos 75 (2004) 39-54.
[4] Richter et al Geochim. Cosmochim. Acta 67(2003) 3905-3923.
[5] P. Beck et al., Geochim. Cosmochim. Acta 70 (2006) 4813-4825.
[6] J.A. Barrat et al., Geochim. Cosmochim. Acta 69 (2005) 5597-5609.
[7] L. A. Coogan et al., Earth Planet. Sci. Lett. 240 (2005) 415-424.
[8] L. V. Danyushevsky et al., J. of Petrology 43 (2002) 1651-1671.
[9] H.E. Huppert & R. S. J. Sparks, Contrib. to Mineralogy and Petrology 75 (1980) 279-289.
[10] A. B. jeffcoate et al., Geochim. Cosmochim. Acta 71 (2007) 202-218.
[11] L. H. Chan et al., Earth Planet. Sci. Lett. 108 (1992) 151-160.
[12] T. Moriguti & E. Nakamura, Earth Planet. Sci. Lett. 163 (1998) 167-174.
[13] P. B. Tomascak & C. H. Langmuir, EOS 80 (1999) F1086-1087.

U and Th zonation in Fish Canyon Tuff zircon: Applicability as a (U-Th)/He standard

F. M. Stuart[1] and K. J. Dobson[1,2],

[1] S.U.E.R.C., Rankine Avenue, Scottish Enterprise Technology Park East Kilbride, G75 0QF, UK
[2]Department of Geographical & Earth Sciences, University of Glasgow, Glasgow G12 8QQ, UK

Introduction

The zircon (U-Th)/He thermochronometer has a closure temperature (T_c) of *c*. 190°C [1], and bridges the gap between the mica $^{40}Ar/^{39}Ar$ (T_c = 350°C) and apatite fission track (T_c = 110°C) thermochronometers. Although the application of zircon thermochronometry is still in its infancy, it is proving a powerful tool for quantifying rock cooling in the mid-upper crust. Published uncertainties in zircon (U-Th)/He ages are usually based on the reproducibility of mineral standards. It is routine practice to assume a homogeneous distribution of U and Th in order to calculated proportion of He that recoils from crystals. However, zonation of U and Th in zircon is common, typically strong and variable. In the most extreme cases, the assumption of homogeneity results in ages that are in error by ± 30% [2]. Characterisation of U and Th zonation in mineral standards is therefore essential. The Fish Canyon Tuff (FCT) zircon has been adopted as a standard by most (U-Th)/He laboratories. Helium ages measured in the three main laboratories [1,3,4] are in good agreement with the U-Pb age of the tuff (28.50 ± 0.07 Ma [5]). However, the reproducibility of all data sets is in excess of ± 10%; significantly higher than typical analytical uncertainties (± 3%). We have investigated the nature of the U and Th zonation in the FCT zircons in order to assess the extent to which the reproducibility accurately reflects the natural variation.

Method

A preliminary cathodoluminescence (CL) study at University of Glasgow revealed that over 98% of all FCT zircons have strong CL zonation. Radiation damage associated with U and Th decay is thought to have some control over the quenching of the CL emission [6], and so the correlation between CL intensity and U and/or Th concentration was investigated to assess whether CL-zonation can be used as a proxy for the U and Th distribution in the FCT zircons. The Cameca IMS 4f ion microprobe was used to measure U and Th concentrations at 15 spots from three FCT zircon crystals. A further 23 sites were analysed during a traverse along the c-axis of a fourth crystal (Figure 1A). These sites were selected from monochromatic SEM cathodoluminescence images to encompass zones exhibiting the full range of CL intensities, and to allow inter-crystalline comparison (Figure 1B).

Results

The ion probe data demonstrate that U and Th concentrations in the FCT zircons are highly variable, and strongly zoned (Figure 1B). Moderate-high CL emission regions typically have 100's ppm U and Th, whereas the low CL emission regions have 1000's ppm U and Th. The correlation between CL emission intensity and U and Th concentration is shown in Figure 1b. There is no apparent correlation between CL intensity and the concentration of any other trace element (e.g. Dy, Yb, Y Ce). Although there are several possible mechanisms for generating and quenching cathodoluminescence in zircons, the observed correlation is consistent with an origin due to the density of lattice defects that result from decay of U and Th (and their daughters).

The U and Th zonation implies that the correction for α-recoil loss for (U-Th)/He age determinations is complicated, and may go some way to explain the poor-reproducibility of the FCT zircon He ages. We calculate that α-recoil corrections made assuming a homogeneous U and Th distribution will generate age variation of ±12%. This is close to the age distribution observed within the (U-Th)/He data set. This study also suggests that the (U-Th)/He age population should contain an average +3.5% age bias. This would change the

mean (U-Th)/He age of the FCT zircon data set (all laboratories) from 28.3 ± 3.1 Ma to 27.5 ± 3.1 Ma. Both are within error of the U-Pb age of the FCT zircon [5].

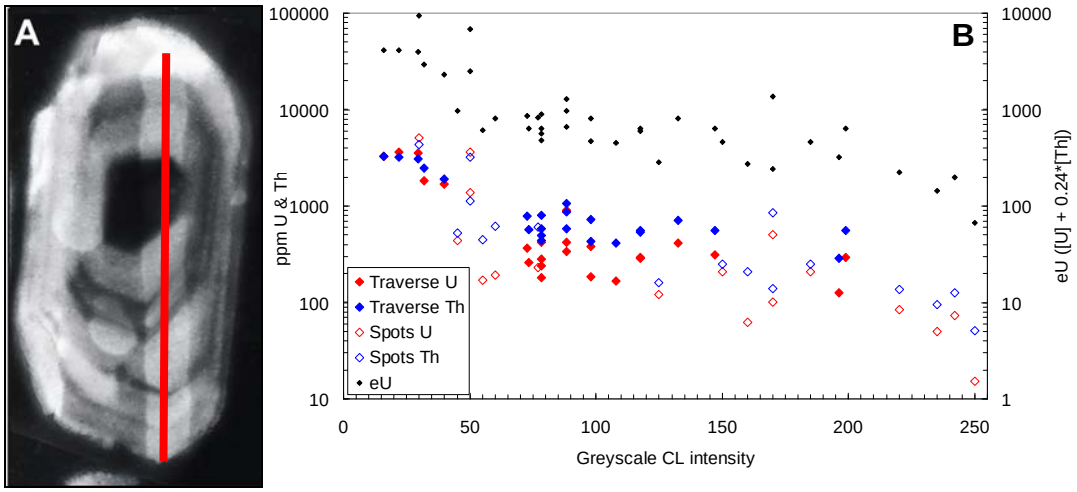

Figure 1. A) CL image of one of the FCT zircons, the image is taken after SIMS analysis and shows the location of the traverse (red). The crystal is ~ 70 µm wide. B) The inter-crystal correlation of CL intensity and U and Th concentration from all 4 crystals (48 sites) analysed.

Although the methodology applied here to assess the impact of U and Th zonation on zircon He ages can only be utilised where large numbers of crystals have been studied, this work highlights the need for careful sample characterisation before zircon He age data can be interpreted. The reproducibility of the FCT zircon He ages reflects the U and Th zonation within the crystal population, and so the established method of using standards to determine age uncertainties on unknown samples must be modified. The existing protocol will tend to over-estimate the age uncertainty associated with unknown samples with simpler, or less extreme concentration profiles. A more accurate determination of the uncertainty of the age of unknowns would be provided by a zircon standard with an approximately homogenous U and Th distribution, or crystals with consistent and extreme zonation that negates the need for the application of the α-recoil correction (e.g. Tardree Rhyolite).

References

[1] P. Reiners, Zircon (U-Th)/He thermochronometry, *in* Thermochronology (2005) Min. Soc. Amer. 151-179

[2] J. Hourigan *et al.* U-Th zonation-dependent alpha-ejection in (U-Th)/He chronometry. Geochim. Cosmochim. Acta (2005) 69 3349-3365

[3] T. Tagami, *et al.* (U-Th)/He geochronology of single zircon grains of known Tertiary eruption age. Earth Planet. Sci. Lett. (2003) 207 57-67

[4] K.J. Dobson, Constraining the post-magmatic evolution of the Hebridean Igneous Province through low temperature thermochronology (2006) PhD Thesis, University of Glasgow.

[5] M. Schmitz, & S. Bowring, U-Pb zircon and titanite systematics of the Fish Canyon Tuff: an assessment of high precision U-Pb geochronology and its application to young volcanic rocks. Geochim. Cosmochim. Acta. (2001) 65 2571-2587.

Distribution of trace elements between zircon, garnet and melt: a key to understanding crustal events and processes

R.J.M. Taylor, S.L. Harley, R.W. Hinton & S. Elphick

[1]School of GeoSciences, University of Edinburgh, Edinburgh EH9 3JW, UK

Background

The interpretation of zircon age data in multiply-deformed and polymetamorphosed high grade terrains presents a significant problem in geochronology because the response of zircon to metamorphism is highly variable even on the microscale. The reliable interpretation of zircon age data must be founded upon detailed textural analysis coupled with in-situ microanalysis that yields independent chemical criteria for constraining the processes that have affected or controlled zircon behaviour. The distribution of REE and other trace elements between zircon and garnet in high-temperature crustal processes is being determined in this project, using both an empirical approach, based on in-situ analysis of zircon, garnet and co-existing phases in natural granulites and migmatites, and high-PT trace element doped experiments that yield zircon-granitic melt, garnet-melt and zircon-garnet-melt products. The distribution data are applied to evaluate the event significance of zircon ages in HT and UHT terranes, the responsiveness of zircon to post-peak mineral-melt reactions, and the relative importance of zircon recrystallisation versus new growth in metamorphism. Examples of such applications are provided in this report, and in a separate but parallel report in this volume (Harley et al.).

Results

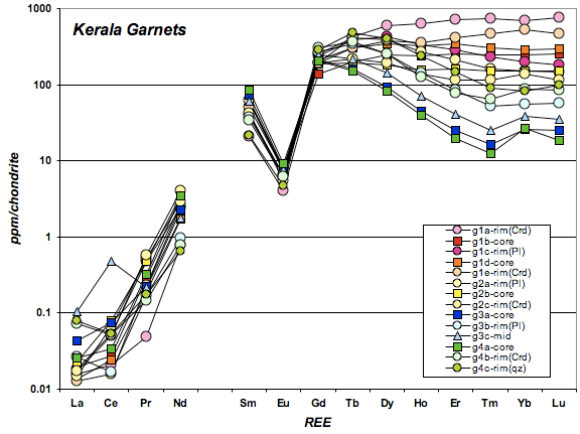

Figure.1. Edinburgh IMS-4f REE data of Kerala garnets. Shows core-rim analyses of four examples.

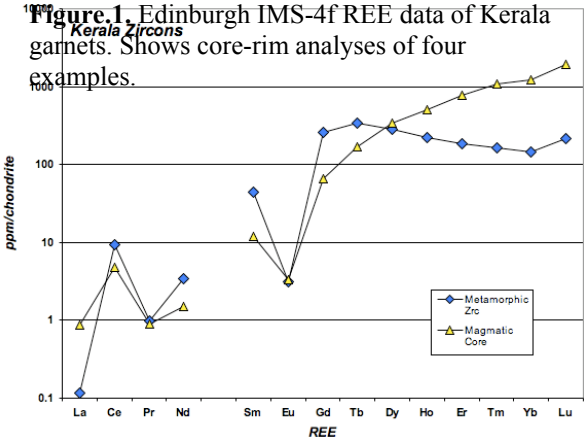

Figure2. Edinburgh IMS-4f REE data for Kerala zircon. Showing average several analyses for metamorphic overgrowths, with example of an inherited core for contrast.

REE distribution patterns for garnet and zircon grains are shown here from the granulite gneisses of the Kerala Khondalite Belt of southern India. The garnet data shows two groups, group 1 having high and flat HREE patterns, and group 2 having a distinct negative slope from MREE to HREE (fig. 1. Shows core-rim analyses of two examples of both types). Zircon data from the same locality shows steep HREE patterns for analyses of magmatic cores and flat or slightly negative HREE patterns for zones interpreted as metamorphic overgrowths (fig.2.).

This highlights the problem of interpreting which of these two garnet types is related to these metamorphic zircon grains and the ages that could be derived from them, or is neither type directly related.

REE partitioning plots between zircon grains and the two groups of garnets show very different patterns (fig. 3.) D_{REE}(zrc/grt) for group 1 garnets shows partitioning for the HREE as being all similar and near unity or slightly less. Whereas the group 2 garnets show a steep $D_{M/HREE}$ (D_{Gd} = 0.73 and D_{Tb} = 6.75)

This matches other data in this volume (Harley et al.) which has consistently shown that D_{HREE}(zrc/grt) patterns of near unity represent equilibrium values for high P-T terrains, and that therefore the group 1 garnets in these Kerala rocks show equilibrium REE partitioning with zircon.

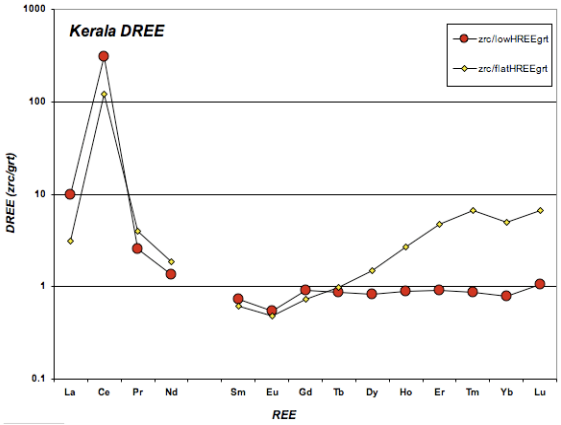

Figure 3. REE partitioning data from the Kerala locality. Two distinct partitioning patterns can be seen. D_{REE}(zrc/grt) data for the zircon overgrowths against group 1 garnets show flat patterns at near unity. Whereas the group 2 garnets show a steeper pattern suggesting preferential incorporation of HREE into zircon.

A further part of the aims of this project is to assess the total REE budget of these high-grade terrains. Fig.4 shows REE data for monazites in the Kerala rocks from which the above zircon/garnet data is derived. Careful study of the zircon and monazite data along with further analysis of other minor phases will help show the controls which the accessory phases found in the gneisses and partial melts of granulite facies rocks have on the total REE distribution in these terrains.

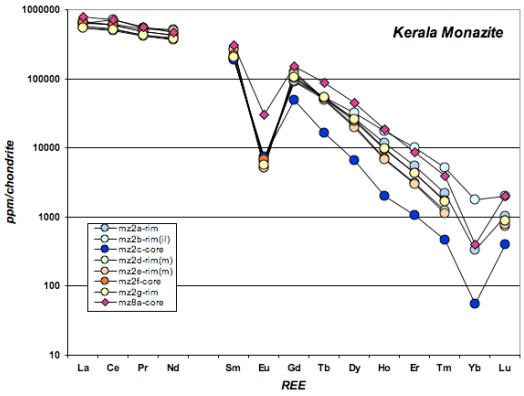

Figure 4. Edinburgh IMS-4f REE data for monazite grains at the Kerala locality.

Significance for Crustal Evolution Studies

The examples briefly described here illustrate the importance of integrating in-situ trace element accessory mineral analysis with both internal microtexture characterisation and petrology in order to interpret zircon U-Pb geochronological data. Care must be taken when matching up the thermobarometric data obtainable from garnet data, to the U-Pb ages

obtainable from zircon grains in the same rock, with detailed REE analysis of both minerals to assess their suitability. This will soon be matched up with experimental data obtained from zircon-garnet-melt experiments in the high P-T facility at Edinburgh.

Mantle $\delta^{18}O$ values in zircons from high pressure granulites

M. Tichomirowa[1] & EIMF[2]

[1]Institute of Mineralogy, TU Bergakademie Freiberg, 09596 Freiberg, Germany
[2]Edinburgh Ion Microprobe Facility, Edinburgh EH9 3JW, UK

Aim of the study

High pressure rocks such as granulites and eclogites are well-known to contain spherical multifaceted zircon grains whose formation has therefore been linked to high pressure metamorphism. There is still a considerable debate about mechanism(s) by which such zircons form under granulite facies metamorphism and hence the interpretation of their U/Pb zircon ages under granulite facies metamorphism. In a former study zircon grains in rocks with obvious granulitic appearance have been shown to suffer complete resetting of the U-Th-Pb system resulting in reproducible $^{207}Pb/^{206}Pb$ ages of 340 Ma [1]. These zircon grains and zircon rims have clearly elevated U and decreased Th contents and have a cathodoluminescence (CL)-dark pattern. We analysed the same zircon crystals with known U-Pb-SHRIMP ages by in situ $\delta^{18}O$ measurements to obtain information on their formation mechanism. Igneous zircons in high temperature equilibrium with mantle magmas are known to have average $\delta^{18}O = 5.3 \pm 0.3‰$ [2]. Significant deviations of $\delta^{18}O$ (zircon) from the mantle value are the direct or indirect result of intra-crustal recycling, i.e. magma interaction with supracrustal materials that ultimately derived their evolved $\delta^{18}O$ from low temperature processes on or near the surface of the Earth where oxygen isotope fractionations are large [3]. Therefore, the oxygen isotope composition of zircon can be used to distinguish between mantle and crustal material and consequently lead to conclusions where zircons have been formed.

Results

79 in situ $\delta^{18}O$ measurements have been performed on 41 zircon grains from four samples analysed previously by in situ U-Pb SHRIMP analyses [1]. The $\delta^{18}O$ values vary mostly between 5 and 9‰. Zircons of the two samples with obvious granulitic high pressure overprint have often cores with brighter CL surrounded by a CL-dark rim. We did not find any clear difference in the $\delta^{18}O$ values comparing core and rim regions of zircon grains from sample ggn 1b, but most of the CL-dark regions of zircons from sample ggn 2 have lower values close to the "mantle zircon average" (Figure 1).

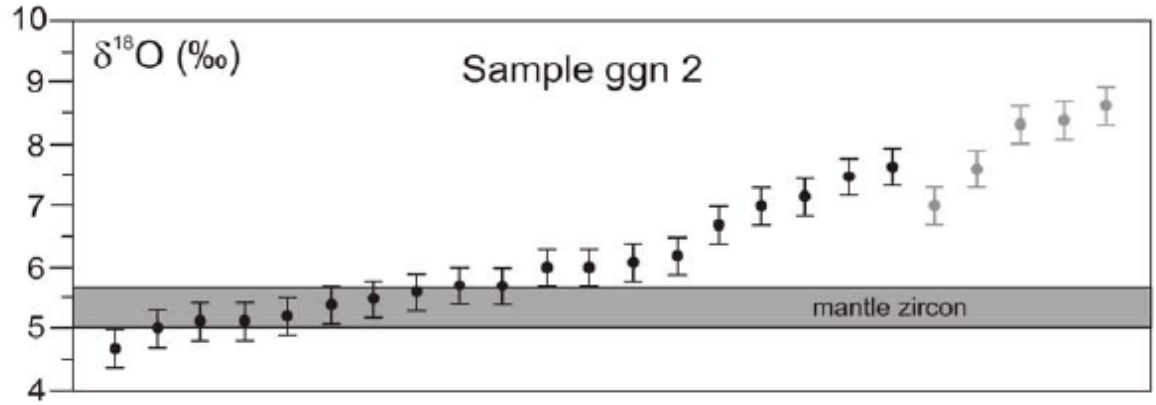

Figure 1. Oxygen isotope composition of in situ analyses of zircons from sample ggn 2. Black symbols indicate regions which are CL-dark, grey symbols indicate CL-brighter cores. Each measurement is given with analytical error of ± 0.3‰.

We observed in several cases a considerable within-grain-variation obviously larger than the analytical error of ± 0.3‰ (Figure 2). Probably, higher $\delta^{18}O$ values occur in zones with a post-metamorphic overprint leading to a change of the CL colour from black to grey (e.g. Figure 2: ggn2-6). Such post-metamorphic zones often form an outer shell on zircon crystals with micro-fractures indicating later shrinkage due to a higher degree of crystallisation. This may be the reason why all zircons from sample ggn 1b have higher than mantle values.

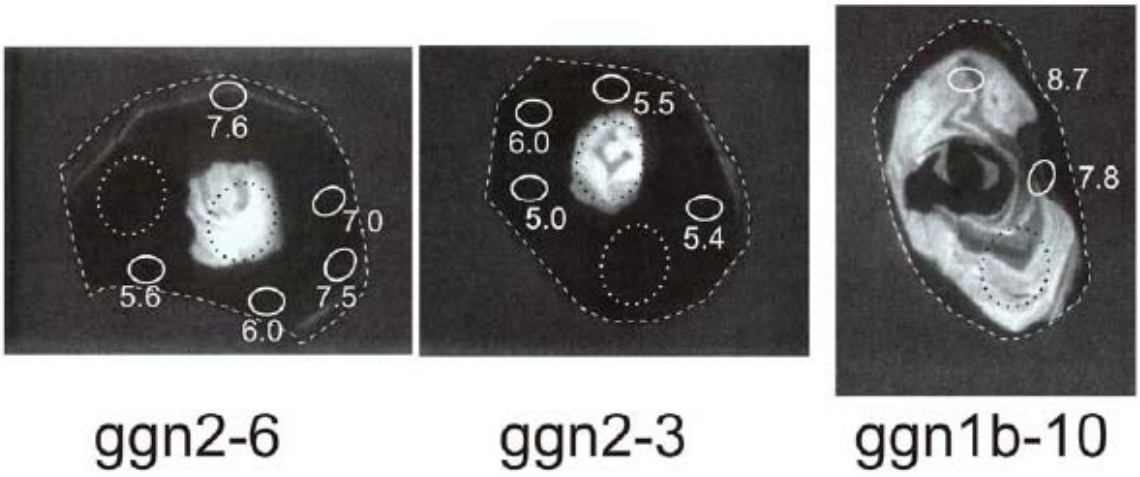

Figure 2. CL-images of three zircon grains showing CL-dark rims and CL-brighter cores. Dashed lines show the zircon grain boundary. Dotted lines show the position of former U/PB SHRIMP analyses. White circles give the position of in situ $\delta^{18}O$ analyses with their isotope values given as numbers in permil.

There is no difference in $\delta^{18}O$ values of grey rims and CL-brighter cores from zircons of the two samples of apparently amphibolite facies rocks where solid state recrystallisation was proposed as the most common process of zircon alteration during metamorphism accompanied by partial resetting of the U-Th-Pb ages.

Conclusions

The observed $\delta^{18}O$ values of many CL-dark zircon rims formed in high pressure rocks was found to be close to the "mantle zircon average". Consequently, such zircons formed under high temperature conditions in equilibrium with mantle melts. That means, that subduction of crustal material (preserved as CL-brighter zircon cores) occurred to very high depths where high temperature mantle melts or fluids interacted with zircon relics and formed new overgrowths and new zircon grains. This finding is in agreement with interpreting the occurrence of micro-diamonds in nearby gneisses as evidence that minimum pressures up to 40 kbar (indicating approximately 120 km subduction depth) were reached [4]. To our knowledge, this is the first evidence of mantle melts/fluids on zircon grains in high pressure crustal metamorphic rocks.

References

[1] M. Tichomirowa, M.J. Whitehouse & L. Nasdala, Lithos 82 (2005) 25-50.
[2] J.W. Valley, P.D. Kinny, D.J. Schulze & M.J. Spicuzza, Contrib. Mineral. Petrol. 133 (1998) 1-11.
[3] J.W. Valley, J.S.Lackey, A.J. Cavosie, C.C. Clechenko, M.J. Spicuzza, M.A.S. Basei, V.P. Ferreira, A.N. Sial, E.M.
King,W.H. Peck, A.K. Sinha & C.S. Wei, Contrib. Mineral. Petrol. 1501 (2005) 561-580.
[4] H.J. Massonne, Proceedings of the 7th International Kimberlite Conference 2 (1999) 533-539.

Rare earth element concentrations in zircons from carbonatites

M. Tichomirowa[1] & EIMF[2]

[1]Institute of Mineralogy, TU Bergakademie Freiberg, 09596 Freiberg, Germany

[2]Edinburgh Ion Microprobe Facility, Edinburgh EH9 3JW, UK

Aim of the study

Zircon grains usually exhibit a typical cathodoluminescence (CL) emission when bombarded with electrons. The CL method has long been applied to detect internal growth or overprint structures of zircon grains. In zircon, there is usually a broad band emission in either blue or yellow regions, or both, upon which sharp peaks of the trivalent rare earth elements (REE) are superimposed. Especially Dy^{3+} was reported to be important for such sharp peaks of the electromagnetic spectrum. The broad band emission in the blue or yellow region of the spectra usually is explained by emission from electron defects localized at SiO_4 groups. Electron defects may also be stabilized by impurities of REE. Therefore, the trivalent rare earth elements (REE) are usually thought to be important for cathodoluminescence emission of zircon grains. We observed complex pattern in CL images of zircon grains from carbonatites and studied therefore their REE concentrations to look for their relation with CL images. The U-Th-Pb system of most of these zircons was disturbed so that mostly younger than formation ages were obtained by U-Pb dating [1].

Results

18 in situ REE measurements have been performed on 11 zircon grains from three samples of the Siilinjärvi carbonatite. Similar zircon crystals from the same samples were analysed previously by CL. In addition to REE, 11 further elements have been determined (Si, P, Ca, Ti, Y, Nb, Zr, Ba, Hf, Th, and U). Some of the analyses show typical REE patterns for igneous zircon crystals with a pronounced positive Ce anomaly and a steep increase of the REE concentrations towards heavy rare earth elements. However, other analyses display only a week positive Ce anomaly and clearly lower HREE concentrations. We could attribute the latter REE patterns to zircon grains or zircon regions which have a turbid whitish appearance whereas clear slightly pinkish zircon grains mostly display the typical REE distribution (Figure 1). There are considerable scatter of concentration even within one zircon grain as shown for grain 2 of sample Siil 10 (Figure 1). We found a decrease of U and Th as well as an increase of Hf and sometimes Ba and Ca in turbid zircon regions.

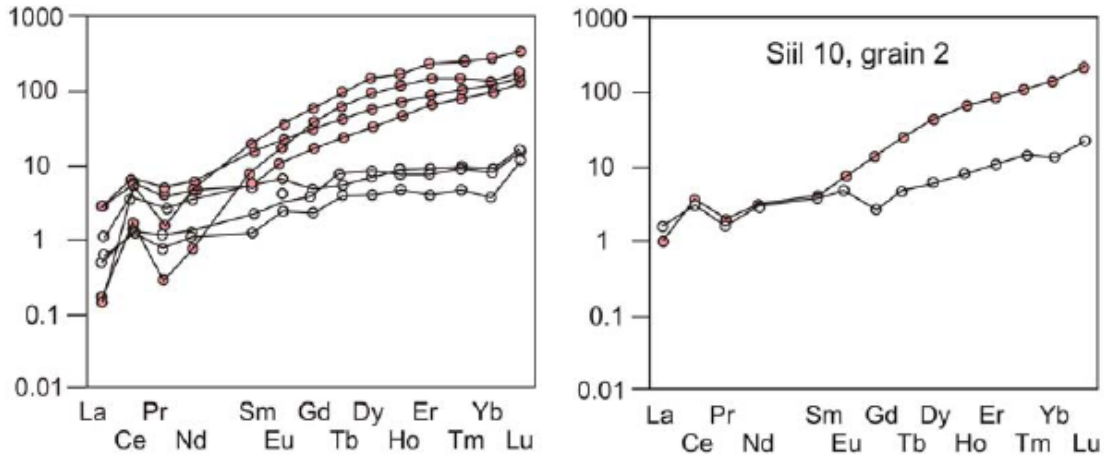

Figure 1. Chondrite-normalized plots of rare earth element concentrations of selected measurements. Clear pinkish regions of zircons are shown by pinkish filled circles, turbid whitish zircon regions by white circles. Further analyses show patterns between pinkish and white filled circles.

The CL images of similar zircons from the same samples show that clear pinkish zircons mostly reveal a blue - dark blue CL, whereas turbid zones give a yellow CL image (Figure 2).

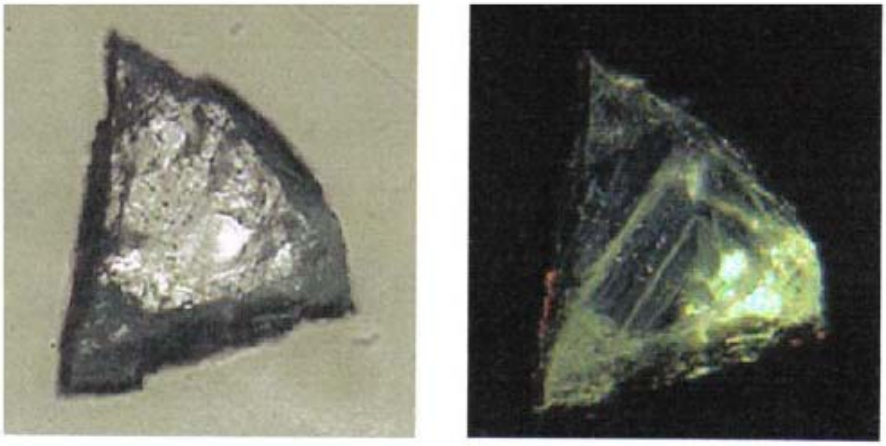

Figure 2. Zircon crystal from sample Siil 9C in transmitted light (left image) and cathodoluminescence (right image). The CL image shows an upper blue emission with growth band and yellow lower regions overprinting the growth structure. The yellow region coincides with a turbid appearance in transmitted light in the right picture. The small red dots on the left and lower side of the crystal in the CL image are carbonate inclusions.

According to our observations in CL images of zircon grains as well in thin sections from carbonatite rocks [1] we attribute the change in CL emission from blue to yellow in zircon crystals to interaction of zircon bearing rocks with carbonatite melts.

Conclusions

The observed complex CL images of zircon grains from the carbonatite Siilinjärvi are correlated with changes in REE concentrations. Zircon regions with dark blue CL emission often reveal relic growth banding and can therefore be related to the formation of zircon crystals. The REE´s of these regions show the usual pattern like many igneous zircons worldwide. However, turbid regions of zircon crystals reveal yellow CL emission and decreased concentration of heavy REE´s. In addition, they have lower U and Th, but higher Hf concentrations. The very low U and Th concentration of carbonatitic zircons do not favour the interpretation that the "yellow" emission center is of radiogenic origin due to radioactive irradiation [2] but may be caused in case of carbonatitic zircons due to interaction of carbonatitic melts with zircons. The decrease of HREE contents in such overprinted zircons makes it unlikely that REE´s are activators of the yellow emission.

References

[1] M. Tichomirowa, G. Grosche, J. Götze, B.V. Belyatski, E.V. Savva, J. Keller & W. Todt, Lithos 91 (2006) 229-249.

[2] L. Nasdala, M. Zhang, U. Kempe, G. Panczer, M. Gaft, M. Andrut & M. Plötze, Reviews in Mineral. 53, (2003) 427-467.

Extinct ^{244}Pu in Hadean zircons

G. Turner[1], J. Gilmour[1], A. Busfield[1] and S. Crowther[1]

[1]School of Earth, Atmospheric and Environmental Sciences, University of Manchester, Manchester M13 9PL, UK

Scientific Report

A one day pilot study was carried out on 2/3/2006 in order to obtain REE data on Hadean zircons which were to be analysed for fissiogenic Xe from spontaneous fission of ^{238}U and (now extinct) ^{244}Pu and neutron fission of ^{235}U. The zircons were subsequently irradiated in the Ascot reactor but have not yet been analysed for xenon (typically 10^5 atoms) due to hydrocarbon background problems following an upgrade (sic) of the channel plate electron multiplier in our resonance ionisation mass spectrometer. Because of the background we have only been able to carry out routine I-Xe dating experiments on meteorites but not the low level searches for Pu xenon in the zircons. A second set of channel plates has been installed and is currently being assessed. Nevertheless the ion probe data has been useful in interpreting the xenon analyses from a previous suite of irradiated zircon, where we have been able to compare Pu/U fractionation with REE/U fractionation (albeit on the two distinct suites of zircons). We concluded that fractionation of Pu^{4+} and U^{4+} relative to the solar system initial value was relatively minor in contrast to the much higher (3 orders of magnitude) fractionation of the $LREE^{3+}$ and U^{4+}. Aspects of that work have been presented at two conferences [1] [2], and it is currently being submitted to Earth and Planetary Science Letters [3]. An abstract of the work is reproduced below.

The presence of xenon isotopes from in-situ spontaneous fission of short-lived ^{244}Pu has been confirmed in a suite of 16 Hadean detrital zircons from Western Australia. In order to investigate the effects of xenon loss on estimates of the inferred Pu/U ratio we have irradiated the zircons with thermal neutrons to generate Xe from ^{235}U neutron fission. ^{131}Xe/^{134}Xe and ^{132}Xe/^{134}Xe ratios have been used to calculate the relative contributions from spontaneous fission of ^{244}Pu and ^{238}U and neutron fission of ^{235}U and hence compare nominal Pu/U ratios and xenon retention ages. U-Xe ages are typically lower than the Pb-Pb ages, indicating that xenon loss is common. We show how the ternary mixing diagram can be used to place constraints on the timing and extent of this loss and to generate a corresponding Pu-U-Xe isochron. Although the zircons investigated in this study were extracted from the same metasedimentary unit, the timing of xenon loss is variable. This suggests that the loss may be the result of variable degres of metamictization from grain to grain. Inferred $(Pu/U)_o$ ratios show a general decrease with the discordancy between Pb-Pb and U-Xe ages. For the least discordant samples we infer $(Pu/U)_o \sim 0.007$ which is close to the published chondritic value. While we cannot completely exclude the effects of Pu/U fractionation in magmatic and other processes between formation of the Earth and crystallisation of the zircons we conclude that they have been relatively small (<factor 2?) and reflect the compatible behaviour of Pu and U in the 4+ valence state.

Subsequent to the zircon work we submitted a proposal for combined REE and xenon analyses of individual chondritic phosphates. Combined REE and Xe analyses are central to establishing a better value for the solar system Pu/U ratio in that apatite is the main carrier of U and I, while merrilite is the main carrier for Pu and REE. Our proposal was accepted but the work has been delayed on account of the hydrocarbon problem referred to above. When that is fixed we hope to carry out the proposed meteorite studies.

References

[1] A. Busfield, S. Crowther, G. Turner and J.D. Gilmour, (2006) Constraining the Pu/U ratio of the early Solar system, Meteoritics and Planetary Science, 41 A34, Suppl.

[2] S.A. Crowther, G. Turner, A. Busfield and J.D. Gilmour, (2006) Plutonium-244 in the early Earth, GCA Supplement 70, 120

[3] G. Turner, A. Busfield, S. Crowther, T.M. Harrison, S.J. Mozjsis and J.D. Gilmour, (2007) Pu-Xe, U-Xe, U-Pb chronology and isotope systematics of ancient zircons from Western Australia. Submitted to Earth Planet. Sci. Lett.

Partitioning of trace elements among Mg-perovskite, Majorite-garnet, and silicate melt

M. J. Walter

Department of Earth Sciences, University of Bristol, BS8 1RJ, UK

Abstract

Mineral/melt partition coefficients for a suite of trace elements were obtained in a one-day (July 27, 2005) project using the Cameca ims-4f ion probe. The purpose of this short study was to measure a suite of trace elements in experimental run products containing Mg-perovskite, Majorite-garnet, and melt [1]. The goal was to compare results for trace elements measured on a different SIMS instrument, as well as to fill in gaps for trace elements not previously analysed. Of special importance was analysis of Sc, which was not measured previously, and Ce for which previous measurements were suspect, in order to more fully develop lattice strain based partitioning models for trivalent cations. The probe session was entirely successful in obtaining the desired data. For those elements of overlap with previous measurements, reproducibility was excellent. Lattice strain models are dependent on the fitting procedure. Best fit results indicate similar mineral/melt partitioning behaviour of trivalent cations for perovskite and majorite, with Young's modulii of ~ 400 GPa. Data are used to constrain models for differentiation of an Hadean magma ocean.

Results

Experiment 249 of [1] was selected for analysis because of the large melt pool and large crystals (~ 50 μm) available for analysis. The ion beam spot size was approximately 20 μm in diameter. We analyzed five spots on the melt phase, two majorite grains, and seven perovskite grains over the course of the one-day project. Results are given in Table 1.

Table 1. Mineral/melt partition coefficients

	Pv/mt new	previous	maj/mt new	previous
Li	0.037	-	0.048	-
Sc	2.631	-	0.855	-
Ti	0.855	0.96	0.113	0.08
V	0.961	-	0.642	-
Ga	0.385	-	0.566	-
Rb	0.267	-	0.070	-
Sr	0.013	0.016	0.014	0.017
Y	0.314	0.25	0.323	0.33
Zr	1.263	1.36	0.098	0.15
Nb	0.221	-	0.017	-
Cs	0.206	-	0.093	-
Ba	0.020	0.04	0.011	0.017
Ce	0.020	0.04	0.009	0.017
Th	0.235	-	-	-
U	0.064	-	0.034	-

The new results provide data for Sc that are pivotal for anchoring the lattice strain model [2] for trivalent cations. Also, Ce (and Ba) D's in previous analyses appeared unusually high, and the new data reduce D's by about a factor of 2. Our previous model [1] predicted a D^{Sc} for perovskite of ~ 1 – 2, and the measured result is just somewhat greater than predicted. In contrast, D^{Sc} for majorite was nearly identical to that predicted from previous models.

Examples of fitted lattice strain models for trivalent cations are given in Fig. 1, with new data used in the fit shown in red. We were also able to obtain important new data for partitioning of Rb, U and Th, which are the parent nuclides of Sr and Pb isotopic daughter species.

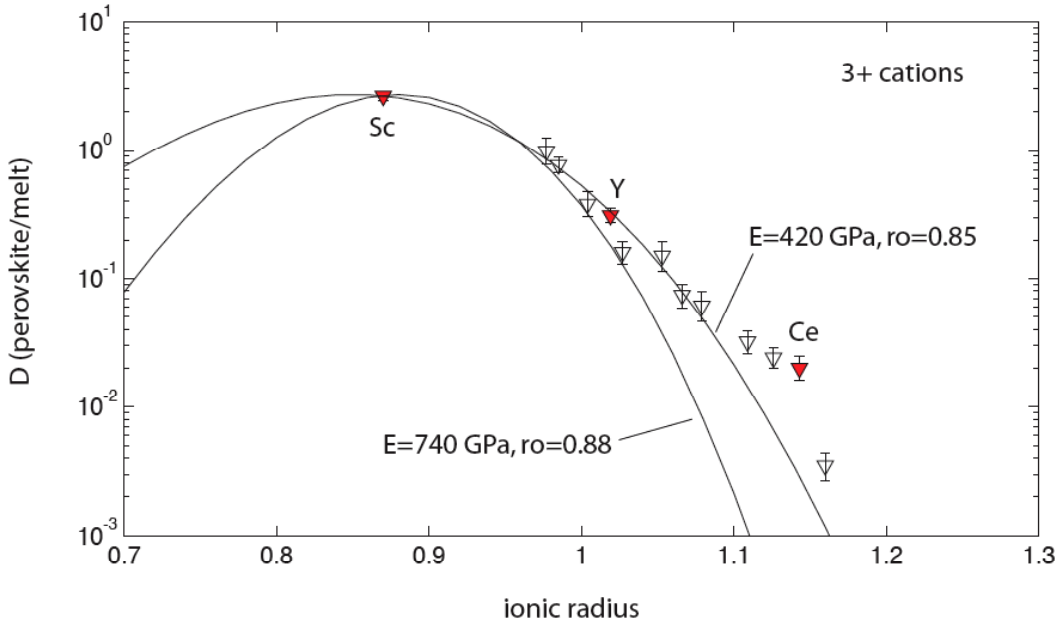

Figure 1. $D^{pv/melt}$ vs. ionic radius ($Å^3$) for trivalent cations. Lattice strain models using r_o as a free parameter yield a Youngs modulus (E) of 740 ± 220 GPa and r_o of 0.88. When r_o is fixed at 0.85, a much better fit is obtained with an E of 420 ± 20 GPa.

These new data are now being incorporated into a new set of trace element models for crystallization differentiation in a magma ocean. Provisional models indicate that maximum amount of perovskite (93%) + ferropericlase (4%) + Ca-perovskite (3%) fractionation from a chondritic magma ocean, based on the refractory lithophile element of the upper mantle, is about 12%. The melt residue and crystal pile may have Rb/Sr and U/Pb ratios similar to EMI and HiMu reservoirs, respectively. Results were presented at the 2006 Goldschmidt Conference.

References

[1] M. Walter, E. Nakamurs, R. Tronnes, & D. Frost, GCA, 68 (2004) 4267-4284.
[2] J. Blundy and B. Wood, Nature 372 (1994) 452-454.

Trace element abundances in Majorite-garnet and Ca,Ti- perovskite inclusions in natural diamond

M. J. Walter & G. Bulanova

Department of Earth Sciences, University of Bristol, BS8 1RJ, UK

Abstract

We used the Cameca ims-4f ion probe in a one-day project (May 25, 2006) to analyse a suite of trace elements in a rare set of mineral inclusions in natural diamonds from the Collier 4 kimberlite pipe, Juina, Brazil. The analysed inclusions have mineral stoichiometries that include majoritic garnet, Ca-silicate perovskite and CaTi-silicate perovskite. The perovskite phases are likely to be exsolved from a single phase CaTi-perovskite solid solution. The SIMS analyses revealed extreme incompatible element enrichments in all phases, with LREE at the 10^2 and 10^4 times chondrite in majorite and perovskite, respectively. The observed elemental enrichments and relative abundances in perovskite may reflect equilibration with a primitive carbonate liquid.

Results

The analysed majorite grain located near the out rim of the diamond is approximately 30 μm in diameter and the ion beam spot size was approximately 20 μm in diameter. Replicate analyses gave reproducible results (Fig. 1). The overall lithophile element enrichment is greater than in any previously anlysed majorite inclusion. Although the major element chemistry indicates an eclogitic precursor, the REE pattern is not traditionally eclogitic but probably reflects equilibration with the host melt/fluid. The Cr-Al systematics of this grain indicate equilibration at 200-250 km depth. Modeling indicates that the REE pattern could be derived from a kimberlitic melt at relatively low temperatures (e.g. 1500 K).

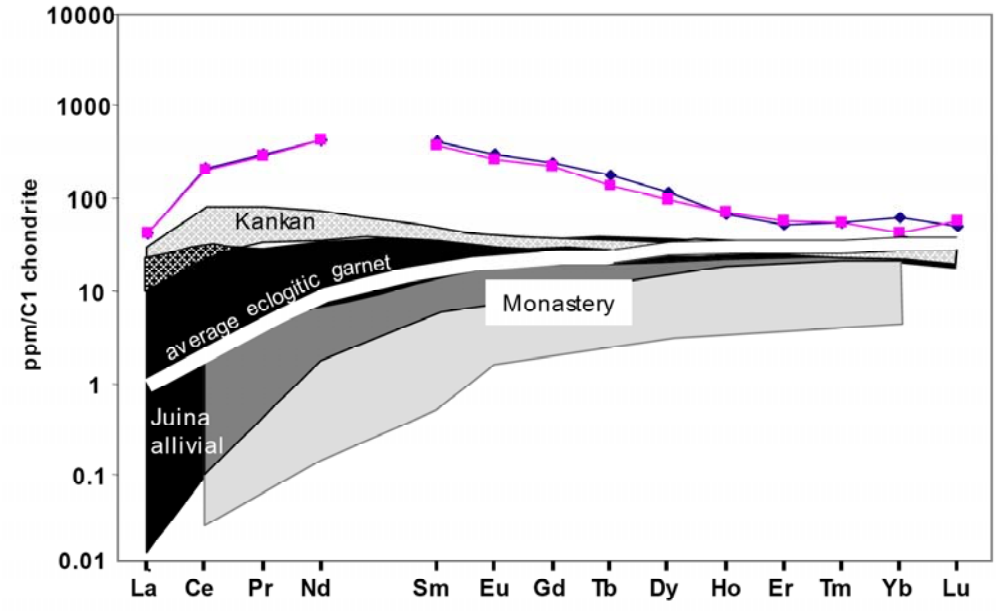

Figure 1. Chondrite normalized REE in Collier-4 majorite diamond inclusion and compositional fields of world-wide majorites from diamonds.

The perovskite inclusion was in the interior of the diamond. The Ca- and Ti-rich exsolutions were less than the diameter of the beamsize. This meant that the measured elemental abundances represent a mixture of the two phases. We analysed two areas of the inclusion,

with each analysis overlapping one phase more than the other. Results are shown in Figure 2. Lithophile element enrichments are at least an order of magnitude greater than previously observed for Ca-rich perovskite inclusions in diamond, although REE patterns are very similar. In contrast REE patterns are unlike those for CaTi perovskite that crystallise from kimberlitic host magmas at low pressures. Preliminary modelling indicates that the REE pattern observed in the Ca-perovskite could reflect equilibration with a primitive carbonate-rich liquid at transition zone conditions. If the diamond crystallised from a carbonate melt in the transition zone it may have encapsulated a near liquidus perovskite phase, and the measured element abundances may reflect the primitive melt from which the phases were derived.

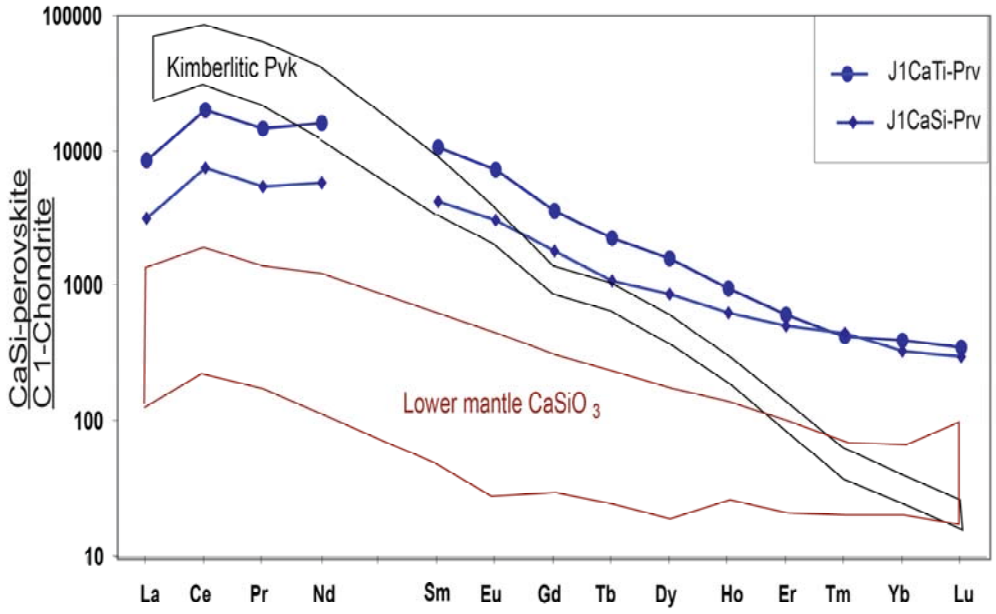

Figure 2. Chondrite normalised REE in CaSi- perovskite diamond inclusions and compositional fields of world-wide majorites from diamonds.

Investigating diffusive fractionation of Li in olivine phenocrysts

H. Wickens[1,2] & T. Elliott[1]

[1]Department of Earth Sciences, University of Bristol, Bristol BS8 IRJ, UK
[2]Now at: Shell UK, Aberdeen

Overview

Mid-ocean ridge basalts show significant Li isotopic variations that are potentially a valuable tracer of recycled material, but there remains the shadow of the possible influence of near surface contamination. The ability to measure Li in early forming olivine phenocrysts would allow us to see through any possible contamination and usefully, Li is hosted in sufficient quantities for SIMS analysis to make this tractable. Unfortunately, our in-situ Li isotopic work has illustrated that diffusive fractionation of Li isotopes also occur and that in response to chemical gradients imposed by changing temperature, the crustal magmatic history of a sample can influence the Li isotope ratios of its phenocrysts. In order to assess the significance of this process more rigorously, we undertook a detailed study on a single sample.

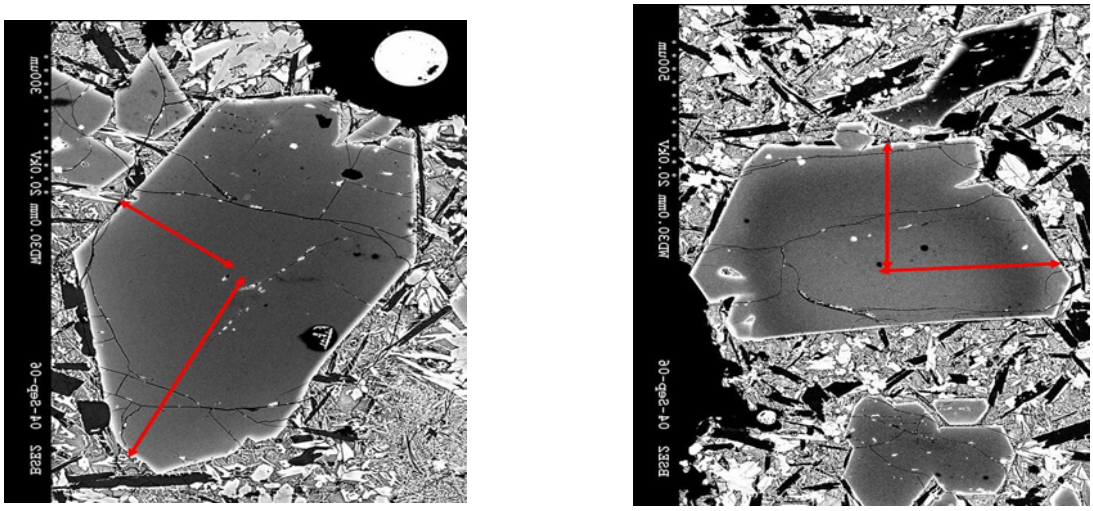

Figure 1. Two phenocrysts analysed for Li isotope profiles, that show modest normal and zoning respectively. Both have lower Fo outermost rims.

Background

We chose a mafic flow we had already extensively studied petrographically and for which we had analysed various different splits of olivine phenocrysts by MC-ICP-MS. Phenocryst cores range from Fo87-82, indicating their derivation from rather primitive magmas. Some phenocrysts have a complex history with phases of reverse and normal zoning, but all are rimmed by a thin layer of ~Fo76 (Fig. 1). We were interested to see how signatures of the cores compared to bulk MC-ICP-MS analyses that yielded d7Li of ~4-6‰. The heterogeneity of different splits analysed by MC-ICP-MS suggested some isotopic zoning was likely present. We selected a sample with relative coarse groundmass, rather than a rapidly quenched flow, to be able to compare the influence of cooling on eruption relative to pre-existing zoning in the phenocrysts (xenocrysts?).

Results

In a 5 day session in October 2007, 55 points in profiles across 5 different crystals were measured for both Li isotopic composition and concentration. The phenocryst cores yielded a range of isotopic compositions from ~17-8‰. These values are all higher than the MC-ICPMS measurements and clearly very variable. A striking aspect of the variation is that the

heaviest values were found in the least Fo rich cores. For example the core of Fig. 1a, with a composition of Fo87 was 8‰ whereas Fig. 1b with a core of Fo82 was 15‰. The phenocryst in Fig. 1a has no obvious isotopic variation from core to rim. In contrast the olivine crystal in Fig. 1b has a complex isotopic profile (Fig. 2). Despite some striking fluctuations in the Li concentrations there is no clear increase in Li towards the edge of the crystal that has previously been observed to accompany isotopic lightening of the crystal rims by diffusion [1,2]. The isotopic profile, in fact seems to correspond more closely to changes in Fo content, with heavy values in the Fo 82 core, lighter values in the Fo 86 ring and then heavier values again as the crystal zones normally back to Fo 82 (we did analyse the less Fo rich outmost rim, which is too narrow). Another interesting feature is that the peak Li concentration is associated with a P concentration a factor of three higher than the rest of the crystal. We measured P concentrations as possible charge balancing complement to Li in olivine (H. O'Neill, pers comm.)

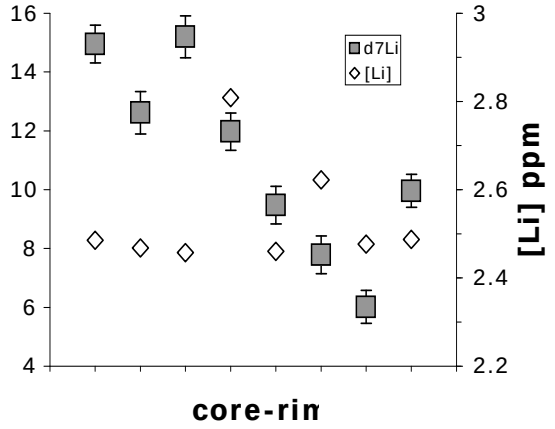

Figure 2. Li isotopic and concentration profiles (W-E) across the olivine shown in Fig. 1b.

Discussion

Despite purposely picking a flow with coarsely crystallised groundmass, to enhance the influence of diffusive fractionation on cooling, the lightening of Li isotope compositions to crystal rims seems far less obvious than in previous work of our own and others [1,2]. Instead a further control appears to be at work, namely a matrix influence on the Li isotope composition. All SIMS measurements appear to be heavier than bulk olivine measurements, as has been previously suggested [1]. The heaviest values are seen in the relatively Fe rich cores. Likewise in the single crystal Li isotope ratios become lighter in zones of higher Fo that appear unrelated to a general diffusive zoning across the crystal (Fig. 2). These effects appear to be quite large (~8‰ for 4 units Fo). In a normally zoned crystal, any diffusive lightening towards the rim would be counter-balanced by the matrix influence from decreasing Fo. Thus the crystal in Fig. 1a, might in fact be diffusively influenced, but without more accurate calibration of the olivine matrix effect this is difficult to conclusively demonstrate. Interestingly, there were apparent differences in olivine compositions measured by SIMS and MC-ICPMS in our studies of peridotites (see report of Elliott, Wickens and Regelous), but in this case the divergence of the techniques **increased** with increasing Fo (albeit the olivines spanned a different compositional range, from Fo 86-90). It remains unclear why such apparent matrix influences were less manifest in our earlier work [1] and in calibration of glass standards [3]. Speculatively, it may be related to increasing beam intensity and opening the contrast aperture to obtain more precise analyses. This requires more work, although accurate calibration of mineral phases is difficult because of likely diffusive isotopic zoning, making comparison of bulk and *in situ* techniques problematic.

References

[1] A.B. Jeffcoate, T. Elliott, S.A. Kasemann, D. Ionov, K. Cooper & R. Brooker, Geochim. Cosmochim. Acta 71(2007)
202-218.
[2] I. Parkinson, S. Hammond, R. James & N. Rogers Earth Planet. Sci (in press)
[3] S.A. Kasemann, A.B. Jeffcoate & T. Elliott Anal. Chem. 77 (2005) 5251-5257